CHALMERS
UNIVERSITY OF TECHNOLOGY

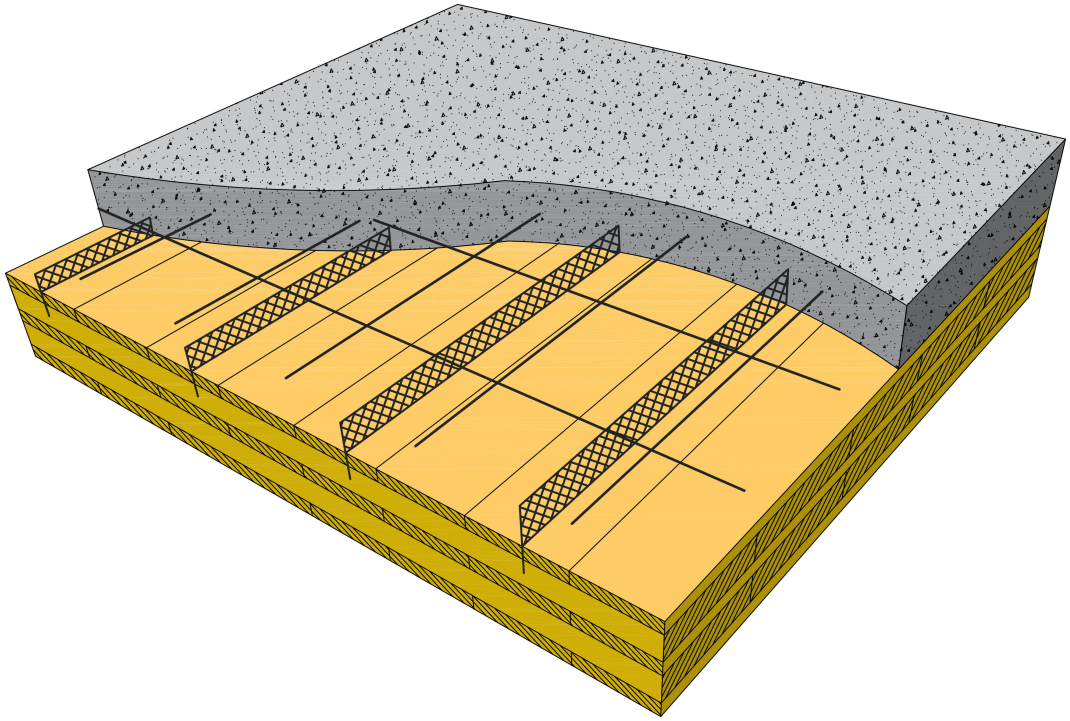

Moisture Safety Evaluation of CLT-Concrete Composite Slab

Master's thesis in Structural Engineering and Building Technology

ZARÉH BAGHDASARIAN SETRAGIAN
CHRISTIANTO CHANDRA KUSUMA

Department of Architecture and Civil Engineering
Division of Building Technology
Sustainable Building
CHALMERS UNIVERSITY OF TECHNOLOGY
Gothenburg, Sweden 2018
Master's thesis ACEX30-18-46

Master's thesis ACEX30-18-46

Moisture Safety Evaluation of CLT-Concrete Composite Slab

Master's thesis in Structural Engineering and Building Technology

ZARÉH BAGHDASARIAN SETRAGIAN
CHRISTIANTO CHANDRA KUSUMA

CHALMERS
UNIVERSITY OF TECHNOLOGY

Department of Architecture and Civil Engineering
Division of Building Technology
Sustainable Building
Chalmers University of Technology
Gothenburg, Sweden 2018

ZARÉH BAGHDASARIAN SETRAGIAN
CHRISTIANTO CHANDRA KUSUMA

Supervisor:
Yutaka Goto, Chalmers, Department of Architecture and Civil Engineering
Elin Hiller and Jens Erik Jörgensen, Skanska Sverige AB

Examiner:
Holger Wallbaum, Chalmers, Department of Architecture and Civil Engineering

Master's thesis ACEX30-18-46
Department of Architecture and Civil Engineering
Division of Building Technology
Sustainable Building
Chalmers University of Technology
SE-412 96 Gothenburg
Telephone: +46 (0)31-772 1000

Cover: An illustration of CLT-Concrete composite slab.

Typeset in LaTeX
Chalmers Reproservice
Gothenburg, Sweden 2018

Moisture Safety Evaluation of CLT-Concrete Composite Slab
Master's thesis in Structural Engineering and Building Technology
ZARÉH BAGHDASARIAN SETRAGIAN and CHRISTIANTO CHANDRA KUSUMA
Department of Architecture and Civil Engineering
Division of Building Technology
Sustainable Building
Chalmers University of Technology

Abstract

Timber-concrete composite structures are used with the intention of providing greater capabilities than regular structures composed of a singular material. With its benefits, the combination of the two materials comes with challenges that have to be overcome. Moisture damage is one of the possible risks in combining these materials and it has to be check thoroughly to ensure minimum risk of mould growth. Risk of mould growth is either regulated by specifying the limit of humidity allowed for a certain material, or by growth prediction through numerical modelling. Although both are used in the construction industry, modelling is considered to be a more detailed numerical approach as a means for assessing mould growth.

The composite structure focused in this study was a floor section with the combination of CLT and cast-in-situ concrete. The general aim was to identify possible moisture damages on the CLT when exposed to the properties of fresh concrete through transient heat and moisture simulation, and evaluated with a mould growth model. The obtained results were used to evaluate moisture safety by observing the possible levels of mould growth in the construction.

Several types of concrete were used as the moisture source: fresh concrete with 0.38 and 0.6 water-cement ratios, and hardened concrete with 0.5 water-cement ratio for a comparison. The vapour diffusion resistance of the fresh concrete materials had to be modified based on the findings of previous studies. This was done to overcome one of the limitations of the program, in which it was not capable to model fresh concrete. Different parameters were tested for the simulations, which were the curing and drying conditions, regional climates, initial concrete condition, addition of vapour retarder and influence of building envelope. No possible moisture damages were observed in the CLT for the case with fresh concrete materials under all the simulated variables. For hardened concrete, at fully saturated condition, it did not achieve moisture safety requirements under all the defined parameters. However, lowering the initial relative humidity of the concrete to 95% was enough for the construction to obtain satisfactory moisture performance.

Although the simulation results of fresh concrete showed that it was below the mould growth safety limit under the simulated variables, in reality it could be higher. This was due to the limitation of the program mentioned previously in regards to modelling fresh concrete. Furthermore, the program did not take gravity force into account, and it did not able to model non-porous material such as steel. However,

these two factors were assumed not to impact the results by a large margin. Based on these limitations, this study can be further improved by conducting experiments to validate the results.

Keywords: CLT, concrete, composite slab, Mould Growth Index, transient, heat, moisture.

Acknowledgements

The "Moisture Safety Evaluation of CLT-Concrete Composite Slab" report was the result of a master thesis done by two students in the master program of Structural Engineering and Building Technology (120 credits) within the Department of Architecture and Civil Engineering at Chalmers University of Technology. This master thesis was 30 credits and carried out from January until June 2018. It was a collaborative effort between the building department of Skanska Teknik in Malmö and Chalmers University of Technology.

First of all, we would like to express our deep gratitude to Dr. Yutaka Goto and Prof. Holger Wallbaum, who agreed to be our supervisor and examiner on such a short notice. We are really appreciative of our supervisor, Dr. Yutaka Goto, who provided us with useful knowledge, academic guidelines and availability, even through his busy schedule.

We would also like to thank Skanska Teknik for giving us the opportunity to make this research possible. Particularly to our supervisor at Skanska, Elin Hiller, who came up with the idea of this master thesis and to the manager of Skanska Teknik's building department in Malmö, Jens Erik Jörgensen. Both had provided us with useful feedback and support during the thesis work. Additionally, thanks to Mikael Afflekt from the building physics department in Skanska Teknik Gothenburg, who helped us with the practical issues.

We would like to express our appreciation to all the teachers at Chalmers University of Technology, especially Angela Sasic Kalagasidis and Pär Johansson for their assistance during the research project and previous helpful courses related to this study. We would also like to thank each student who was with us in the Master's Studio for their companion through the good and bad times of the whole journey.

Finally, we are truly thankful for our families and friends for the support, encouragement and inspiration that made us who we are today.

Gothenburg, June 2018

Zaréh Baghdasarian Setragian
Christianto Chandra Kusuma

Contents

List of Figures

List of Tables

1
Introduction

This chapter presents the background of timber-concrete composite slab, aim, scope and methods as well as the limitations of this research.

1.1 Background

Composite structure systems which consist of timber and concrete have been used as building structures since the second quarter of the 20th century. The usage of timber-concrete composite structures began because of a limited availability of steel due to high demand during the period between first and second world war. This steel shortage forced society to find another form of building structures and therefore the composite timber-concrete structures came to life (Raquel de Sousa Monteiro, 2015). In 1943, One of the first projects that used timber-concrete composite structure was accomplished in USA, in which they investigated the capability to develop cost-effective highway bridges with shorter span (Lukaszewska, 2009).

The purpose of using timber-concrete composite varies depending on continent or country. For example, timber-concrete composite floors are mostly used for historical building in Europe to replace the old timber floor with a new floor that gives a better mechanical behavior. In New Zealand, timber-concrete composite is used in multi-storey buildings as it is considered to be a more sustainable choice compared with traditional building materials, such as concrete or steel, because wood has the ability to regrow and reproduce which eventually reduces carbon footprint by storing CO_2 during its lifespan (Yeoh, 2010). Timber-concrete composite slab consists of a timber at the bottom and a concrete on the top. Shear connectors are used to connect timber and concrete together as they increase the interaction rate of the composite member (Svenskt Trä, 2017a). The timber segment can either be glued laminated (Glulam), solid timber, laminated veneer lumber (LVL) or cross-laminated timber (CLT). Concrete can either be prefabricated or cast-in-situ (Yeoh, 2010).

For this research, the focus was on composite slabs that consist of CLT and cast-in-situ concrete. Combining CLT and concrete provides greater benefits compared to slabs with CLT solely. Some of these benefits are higher flexural rigidity, which allows for longer spans and a better dynamic behavior than the traditional timber slabs due to higher damping ratio for the composite slabs, which make it less sensitive to vibration and have a better acoustic behavior (Svenskt Trä, 2017a). An illustration of this type of composite slab is shown in Figure 1.1.

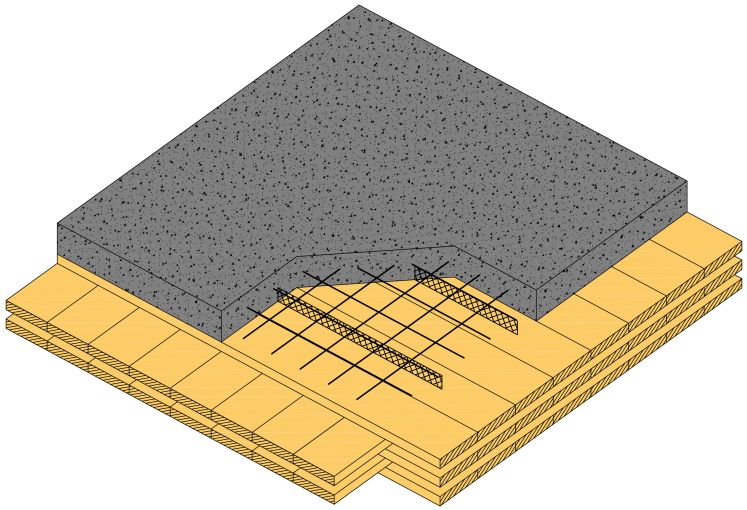

Figure 1.1: Timber-concrete composite slab illustration

Previous studies in the field of timber-concrete composite slabs focused more on the structural behavior of the slab such as deflections, connections between timber and concrete, dynamics and vibrations properties of the composite slab. Some studies were done on the hygrothermal properties of CLT, such as the research of (Alsayegh, 2012) in *Hygrothermal Properties of Cross Laminated Timber and Moisture Response of Wood at High Relative Humidity*, but none of the previous research found explicitly concentrated on the possible moisture-related problems regarding the combination of CLT and concrete.

1.2 Aim and Scope

The purpose of this master thesis was to investigate and determine the possible risks in CLT when it is used in combination with concrete to make a timber-concrete composite slab. More specifically, the following aims were pursued:

- To identify possible damages on CLT when it is subjected to the moisture, heat and alkalinity of the drying process of fresh concrete.
- To investigate possible damages on various CLT-concrete floor details, properties and conditions.

1.3 Method

The methods used for this research were literature review and numerical simulation. In the literature review, existing research and findings regarding concrete, CLT and the hygrothermal behaviour of CLT were discussed and used as the base of this research. Afterwards, different types of model were simulated using transient heat and moisture transfer simulation software. The simulation results were evaluated with a mould growth model to assess the impact of moisture source from drying concrete on the potential moisture risks on CLT.

1.4 Limitation

This study focused on moisture evaluation of the CLT-concrete composite slab and therefore there were several limitations. The moisture evaluation of concrete in the composite slab was not taken into account as it is only used to simulate a moisture source to the CLT. Due to the limited time and unavailability of equipment at the time of writing this master thesis, the results of the simulations could not be compared with lab experiments in order to validate the simulation results. Furthermore, the mechanical properties of the composite slab such as deflection, shear capacity and moment capacity were not discussed in this research. However, some mechanical properties such as noise insulation, vibration and fire resistance were taken into consideration in designing the analyzed floor detail.

2
Literature Review

In this chapter, literature studies are presented from several research, books, articles and other sources. Different properties of wood, in general, are given and critical elements which affect vapour permeability of wood during the drying process of the concrete are discussed. Furthermore, various factors that contribute or prevent growth of microorganisms are described and the threshold for mould growth from various regulations and guidelines are presented.

2.1 Heat-Air-Moisture Properties of Wood

2.1.1 Moisture Storage

Wood is a hygroscopic material, which means it can gain or lose moisture from or to the surrounding air. The amount of moisture gain or moisture loss depends on moisture condition of the wood and its surrounding air. Air always contain a certain amount of moisture in form of water vapour. The maximum amount of water vapour in the air depends on the air temperature and pressure, and the higher the air temperature is, the more moisture it can uptake. Relative humidity (RH) measures the amount of water vapour the air contains and it can be calculated by dividing the vapour content by the saturation vapour content in a certain temperature (Burström, 2007).

$$RH = \frac{v}{v_s} \cdot (100) \tag{2.1}$$

Where, RH is relative humidity ($\%$), v is the vapour content of the air (g/m^3) and v_s is the saturated vapour content of the air in a certain temperature (g/m^3). A relative humidity of 100% means that the air is fully saturated with vapour.

Moisture ratio (μ) measures the amount of moisture (water) in a material and it is determined by taking the ratio between water weight of the moist material and dry weight of the material (Forest Products Laboratory, 2010). Moisture content (w) measures also the amount of moisture in a material but per cubic meter and it is calculated by multiplying density of the material by its moisture ratio (Hagentoft, 2001).

$$\mu = \frac{m - m_d}{m_d} \cdot (100) \tag{2.2}$$

$$w = \rho \cdot \mu \tag{2.3}$$

Where, μ is the moisture ratio (%), m is the weight of the moist material (kg), m_d is the dry weight of the material (kg), w is the moisture content (kg/m^3) and ρ is the density (kg/m^3).

Moisture in wood can be categorized into two, hygroscopic moisture (bound moisture), which is adsorbed moisture on the surface of wood cells, and capillary water (free water), which is moisture in the form of liquid water inside the wood. The range of relative humidity for hygroscopic moisture starts when the wood is completely dry, i.e. at 0% RH, until the point where the moisture begins to condensate (likely around 98% RH), with the assumption that no external moisture source such as water leakage is present. Capillary water range starts after the condensation point of the vapour until relative humidity reaches 100% (Alsayegh, 2012). Figure 2.1 shows the relation between moisture content and relative humidity and it illustrates the two different regions for moisture storage in wood. It can also be seen that the hygroscopic region starts at 0% RH until very high relative humidity (nearly 98%) and continues with capillary water. In capillary water region, the moisture content of wood increases greatly with increasing relative humidity.

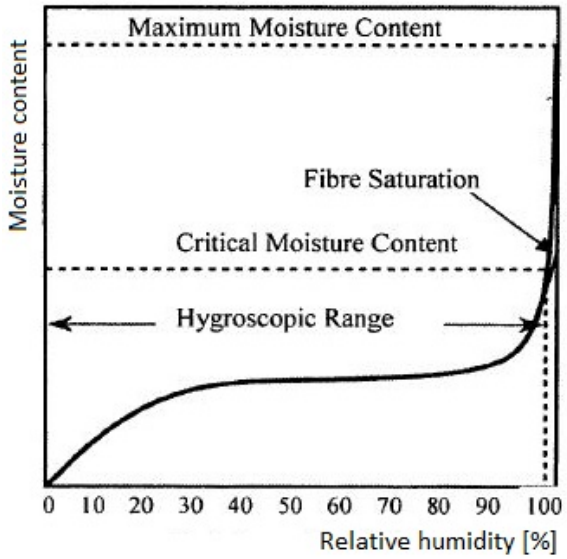

Figure 2.1: Equilibrium moisture content profile of wood (Kumaran, 1996).

Fibre saturation point (FSP) is the moisture condition of wood in which the cell walls are totally saturated with bound water but the cell lumina are not filled with liquid water. fibre saturation point of wood is approximately at 28% moisture ratio but it can vary by some few percentages depending on the species of wood (Forest Products Laboratory, 2010).

Materials in general including wood, are always adjusting to become in equilibrium with its surrounding when it is stored in a certain climate, where the temperature and the vapour content are constant. Equilibrium moisture content (EMC) is the condition in which the wood is no longer gaining nor losing moisture. The relation between equilibrium moisture content and relative humidity of the surrounding air

at a certain temperature is typically shown in a sorption isotherm. Adsorption is the process when the material gain or adsorb moisture from the surrounding, i.e. the initial condition of the wood is dryer than the surrounding air, while desorption is the process where the material lose or desorb moisture into the surrounding, i.e. the initial condition of the wood is wetter than the surrounding (Burström, 2007). Figure 2.2 shows the desorption and adsorption isotherms at a temperature of 20°C. As it can be seen in the figure that the adsorption curve is always located below desorption curve and the moisture ratio of the wood varies between the two curves at a certain relative humidity. The ratio between the adsorption curve and desorption curve is approximately 0.85:1 at relative humidity between 80% and 90%. Such relations in which different curves are given for the adsorption and desorption of a material is known as hysteresis (Alsayegh, 2012).

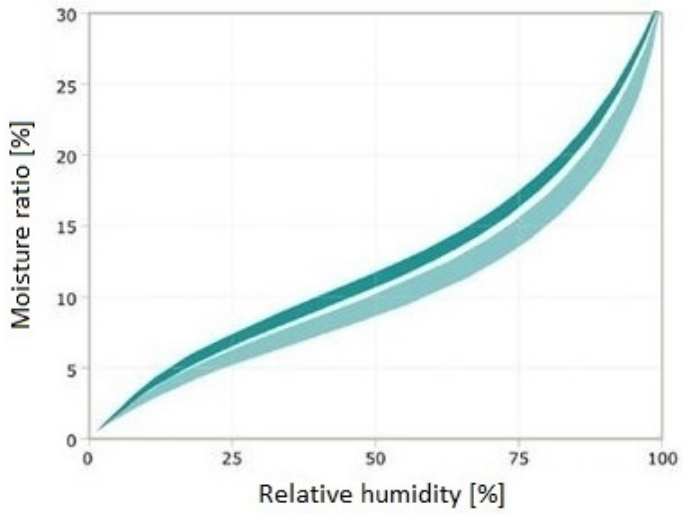

Figure 2.2: Desorption (upper curve) and adsorption (lower curve) at temperature of 20°C (Svenskt Trä, 2017b).

2.1.2 Moisture Transport

Transport of moisture through wood results from different types of transport mechanisms and it can either occur as vapour or liquid. Diffusion and convection are the main moisture transport mechanisms in vapour phase, while capillary suction is the main transport mechanism in liquid phase. Moisture transport rate can vary remarkably depending on the transport mechanism. Although different types of moisture transport are often occurring simultaneously, one mechanism always dominates (Sandin, 1997).

2.1.2.1 Vapour Transport

Vapour transport occurs at moisture ratio below the fibre saturation point (FSP), when the relative humidity is at hygroscopic sorption region. The two main mechanisms for vapour transport in wood are diffusion and convection (Burström, 2007).

Moisture diffusion is the movement of water vapour from high vapour concentration towards low concentration region aiming to become in equilibrium with the surrounding area. Water vapour can penetrate through the material at different rates depending on the porosity of the material. The more porous the material is, the faster water vapour penetrates. Vapour permeability (δ_v) describes moisture diffusion penetration rate in a material and it depends on many factors, such as moisture ratio, temperature and density of the material. Figure 2.3 describes the variation of vapour permeability of wood as a function of relative humidity and it can be seen that vapour permeability increases as relative humidity increases (Burström, 2007) (Sandin, 1997).

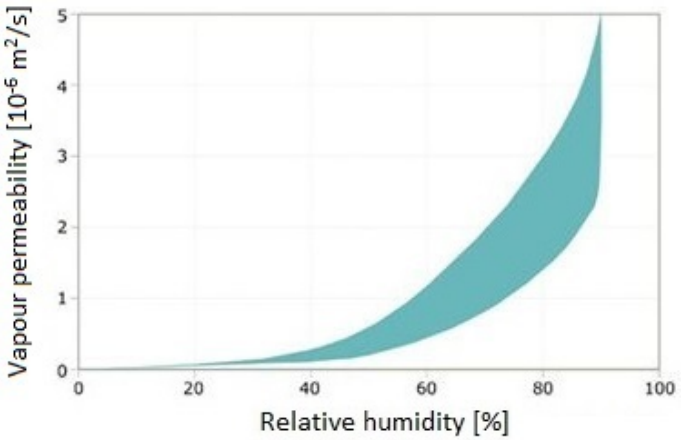

Figure 2.3: Vapour permeability of pine and spruce as a function of relative humidity (Svenskt Trä, 2017c).

Table 2.1 below presents the amount of water for cases of adsorption (W_{ads}) and desorption (W_{des}) for different relative humidity. It also gives values of vapour permeability for the given relative humidity.

Table 2.1: Moisture content and vapour permeability for spruce in tangential direction at a given relative humidity (Hagentoft, 2001).

RH [%]	$\mathbf{W_{des}}$ **[kg/m^3]**	$\mathbf{W_{ads}}$ **[kg/m^3]**	δ_v **[10^{-6} m^2/s]**
35	40	35	0.3
50	50	45	0.3
70	70	60	0.6
80	80	75	1.0
90	105	95	1.6
95	120	115	2.1
100	145	135	≈ 3.5

If the thickness of a material is known, it is possible to define moisture diffusion by vapour resistance instead of vapour permeability. Vapour resistance describes the

ability of a material to hinder moisture transport and it can be determined as the ratio of material thickness and vapour permeability (Burström, 2007).

$$Z = \frac{d}{\delta_{\mathrm{v}}} \tag{2.4}$$

Where, Z is vapour resistance (s/m), d is the thickness of material (m) and δ_v is the vapour permeability (m^2/s).

Moisture convection is the transport of water vapour through air movement. Temperature differences, drafts and ventilation are the main influences to create pressure differences in buildings, which makes it possible for water vapour to transport with the air movement into different parts of the construction. The rate of water vapour transport depends on the pressure difference, water vapour of air and air permeability of the construction (Burström, 2007).

2.1.2.2 Liquid Transport

As the relative humidity inside the wood increases and transforms from hygroscopic sorption region to capillary water region, the moisture transport mechanism also changes. Moisture transport in liquid phase occurs at very high relative humidity, at moisture content above the fibre saturation point (FSP) (Burström, 2007). The main mechanism for liquid transport in wood is capillary suction. Capillary suction is the movement of moisture in the form of liquid from areas with high moisture content to areas with lower moisture content, in special cases where the material is in direct contact with liquid water. Driving force for capillary suction is capillary forces which cause capillary pressure differences between the two areas (Burström, 2007). Moisture transport rate in capillary suction depends on pore size and pore structure of the material. Water sorption coefficient is an indication of the rate and amount of water that a material is capable to uptake when it is placed in contact with liquid (Sandin, 1997). The amount of absorbed water per square meter, m_s (kg/m^2), is calculated by Equation 2.5 shown below, where A is water sorption coefficient ($kg/m^2\sqrt{s}$) and t is time (s).

$$m_{\mathrm{s}} = A\sqrt{t} \tag{2.5}$$

Wood is an anisotropic material which means it has different properties in different directions. The water sorption coefficient of wood varies depending on its direction to the grain. Table 2.2 gives water sorption coefficient for wood in both parallel and perpendicular to the grain direction.

Table 2.2: Water sorption coefficient for wood with grain directions (Hagentoft, 2001).

Direction	**A** $[\mathbf{kg/m^2\sqrt{s}}]$
Wood parallel to grain	$20 \cdot 10^{-3}$
Wood perpendicular to grain	$4 \cdot 10^{-3}$

Beside capillary suction, liquid can be transported by gravity and wind force. Gravity causes water to flow downwards in a construction, while wind force can transport liquid in lateral and vertical directions.

2.1.3 Thermal Properties

Wood is considered to have good insulation properties because of its high porosity. As an anisotropic material, wood has different thermal conductivity values depending on heat flow direction with respect to the grains. Thermal conductivity of timber is around 0.14 W/(m.k) in the direction perpendicular to the grains, and it increases by 2.5 times when the heat flow direction is parallel to the grains. Beside the heat flow direction, thermal conductivity of wood also depends on the moisture content, density and temperature of the wood. Thermal conductivity increases linearly with increasing moisture content and density. As for temperature, it has a minor impact on thermal conductivity. It increases thermal conductivity by approximately 2% to 3% for every 10°C of increasing temperature (Burström, 2007).

Unlike thermal conductivity, heat capacity does not depend on wood's density, but temperature and moisture content has a big impact on it. Heat capacity increases with increasing moisture content and temperature (Forest Products Laboratory, 2010). Generally, heat capacity of wood varies between 1500-1700 J/(kgK), which considered to be relatively high compared with other building materials such as concrete (Svenskt Trä, 2003).

2.1.4 Air Permeability

Permeability can be defined as a porous material's ability in fluid migration from influence of pressure differences (Perré, 2007). Liquid and air permeability of wood highly affect its ability in being processed, such as from impregnation of wood preservatives or pulping agents, or through diffusion from drying or fumigation. The level of permeability impacts the time needed, the quality, and ultimately the cost of processing wood (Cŏté, 1963). Other than that, air transport is considered to be an important factor in environmental control, because air movement carries both heat and moisture through the material. Air leakages through the building envelope cause heat loss, and the use of wind/weather barrier is customary to prevent this. Polyethylene sheets are commonly used to control air leakage, that could also function as a vapour barrier (Bomberg, 1993).

Air permeability of wood is greatly influenced by the species itself and the grain direction of air flow. It is highly anisotropic, as longitudinal permeability is typically the highest compared to radial and tangential direction. Whether it is normal wood or reaction wood (compression or tension) has some effect on permeability as well. Research of air permeability on beech and spruce by (Tarmian, 2009), gives the result shown in Figure 2.4.

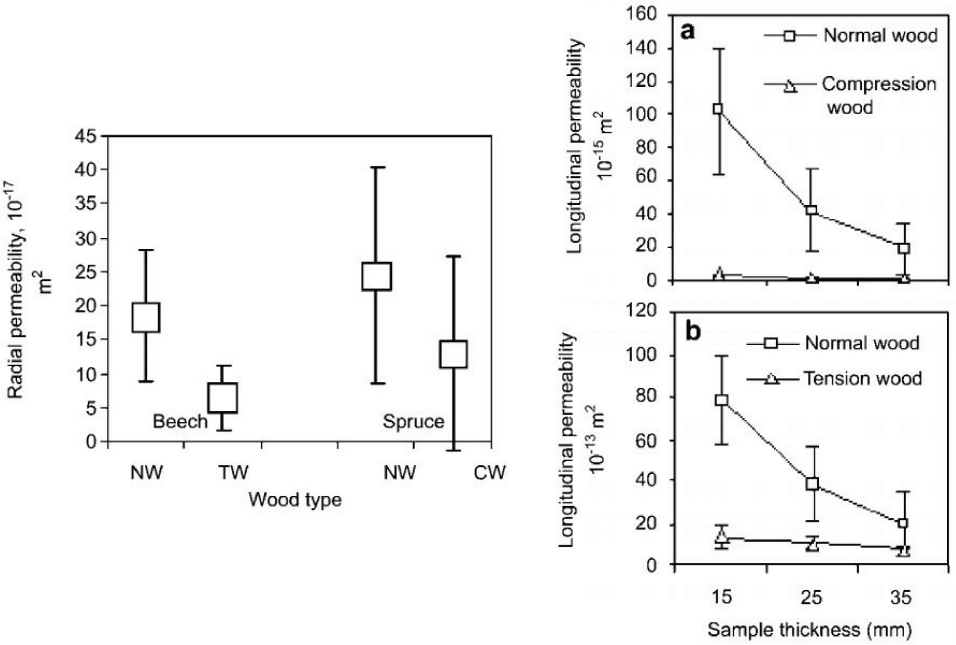

Figure 2.4: Radial and longitudinal air permeability for spruce (**a**) and beech (**b**). NW, normal wood; TW, tension wood; CW, compression wood (Tarmian, 2009).

Normal wood tends to have higher permeability for both radial and longitudinal direction than reaction wood for both beech and spruce. The thickness of the sample has a significant effect on the permeability as well, with lower permeability on thicker specimens. It can be observed that longitudinal permeability is always higher than radial, with a ratio of around 400 times bigger for the case of spruce normal wood ($105 \cdot 10^{-15}$ m^2 compared to $25 \cdot 10^{-17}$ m^2). This value for air permeability of spruce perpendicular to the grain is similar to the value found on the *Introduction to Building Physics* book by (Hagentoft, 2001), which is $20 \cdot 10^{-17}$ m^2.

A different research using Japanese cedar sapwood by (Tanaka, 2015) shows a similar anisotopic behaviour regarding grain directions. Longitudinal permeability is the highest with $2.4 \cdot 10^{-12}$ m^2, tangential permeability is the second highest with $37 \cdot 10^{-17}$ m^2 and radial permeability is the lowest with $3 \cdot 10^{-17}$ m^2.

2.2 Cross-Laminated Timber

Cross-laminated timber (CLT) is a relatively new timber product that has been used for different types of structures. CLT was developed in the beginning of 1990s in central Europe, in Austria and Germany, and it began to be used as a construction material by the end of the 1990s and the early 2000s (FPInnovations, 2013). CLT is manufactured with odd numbers of layers such as 3, 5, 7 or more, with the same or varying thickness of the different layers (Svenskt trä, 2016). These several layers of lumber boards are oriented perpendicularly on each other and glued together (FPInnovations, 2013). There are several types of adhesives used for glueing CLT layers together but the two standard adhesives that are commonly used in Europe are, Polyurethane Reactive (PUR) and Melamine Urea Formaldehyde (MUF). The thickness of the adhesive layer that is applied between CLT panels varies between 0.1 mm and 0.3 mm, which can make up to 1% of the total mass of the timber

(Alsayegh, 2012). However, there are alternative methods to attach the different layers of lumber together beside glueing and these are with nails or wooden dowels, but they are less common (FPInnovations, 2013). The size of CLT panels can be as large as 500 mm thick, 3000 mm wide and with a length of up to 24 m. Furthermore, CLT is a flexible material and it can be used alone as a building material or in combination with other building materials (Svenskt trä, 2016).

The demand for wood-based material in general is currently growing because of the positive impact on the environment regarding carbon footprint. Figure 2.5 shows the carbon footprint for traditional building materials during production. It can be seen that timber stores a large amount of CO_2 and the emissions during the production of it are very minimal in comparison to concrete, steel or masonry (Scalet, 2015).

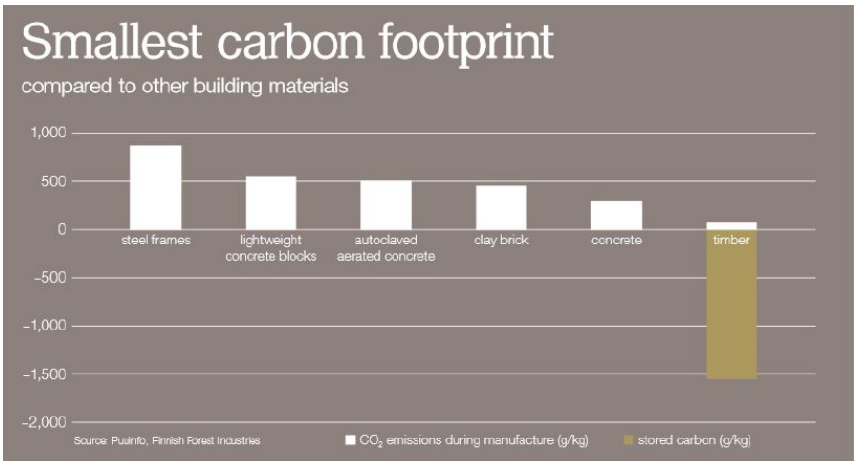

Figure 2.5: The carbon footprint of materials during production (Scalet, 2015).

The production of the CLT panels are nearly emission-free and consume very minimal fossil fuel. The maximum emission of CLT panels during its production is 0.44% from the limited emission value. However, the sustainability of CLT becomes questionable when the glue is taken into consideration. The production of glue for CLT is based on synthetic material, which is not environmentally friendly and causes health problems. Although there are new ecological types of adhesive in the market, they are not used in CLT productions because they don't meet the bonding requirements. Despite this, the production of CLT in general still requires less energy, water, fossil fuel than other building materials and it has a negative carbon footprint since the wood in CLT can store CO_2 under its lifespan. Recycling CLT waste is possible in small scale in laboratories by separating the CLT layers from the glue and recycle the layers individually. It is currently not possible to recycle the CLT in large scale due to unavailability of recycling machines that can handle a big amount of waste. As a result, reusing CLT waste is the most common solution and it is done by chopping the CLT into small pieces and used for manufacturing of wood composite panels such as chipboard, wood bonded panel and wood fibre insulation panels. Disposal of the CLT waste by incineration or landfill disposal are also another option, however, these two alternatives are considered less sustainable due to emissions of greenhouse gases as a result of burning or landfilling (Scalet, 2015).

Wood-based materials can only be considered as sustainable if it comes from a sustainably managed forests, where wood is grown and harvested responsibly. Excessive use of wooden materials may result in deforestation which makes the use of wood no longer sustainable. Deforestation permanently damages the harvested area, unless they are carefully treated. Some parts of the world had given effort on the importance of conserving wood. For example, in Europe, it is currently under a reforestation phase, where there are more trees growing than they are cut. Other than the source of wood, the durability of the wood-based product such as CLT is another aspect to consider. The lifespan of CLT buildings are approximately 50 years and any cause that shorten the lifespan, e.g. moisture damages, will affect the sustainability aspect of the CLT. A CLT building component that is torn down before its lifespan is burned or disposed of in landfills, which results in the release of CO_2 that is stored in the wood during its lifetime and it needs more energy to regrow the wood to replace it (Scalet, 2015).

2.3 Heat-Air-Moisture Properties of CLT

The hygrothermal properties of CLT described in this section are mainly based on the research of (Alsayegh, 2012). European spruce CLT was tested among several other CLT specimens in the research. The dry density of the specimen was 340 $\pm$ 12.7 kg/m^3.

2.3.1 Moisture Storage

The specimen used to find the equilibrium moisture content (EMC) in the experiment from Alsayegh was plain spruce. This was based on the acknowledgment of the contributed overall weight of glue on a CLT specimen is less than 1%. As it was treated as plain wood, it had similar equilibrium moisture content as other plain wood specimens from previous research. Figure 2.6 shows the adsorption isotherm result for the specimen.

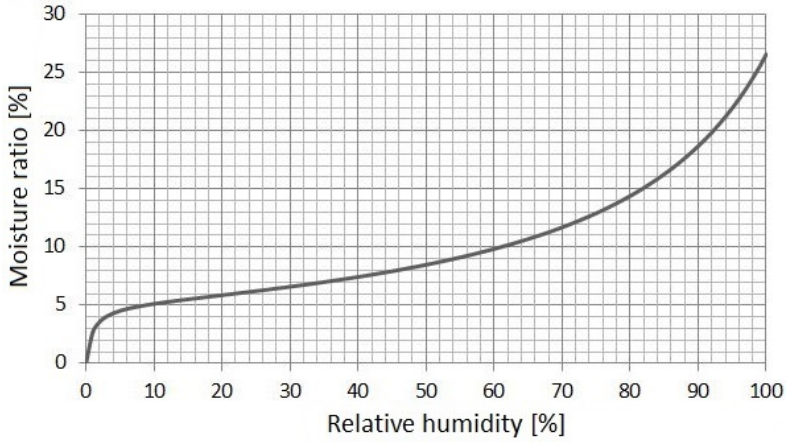

Figure 2.6: Adsorption isotherm of european spruce (Alsayegh, 2012).

2.3.2 Vapour Transport

Water vapour transport (WVT) of CLT shows similarities to plain wood. The specimens are tested using the dry and wet cup method as specified in ASTM E96 (2010). Cups are filled either to represent low RH (0%) or high RH (100%) with the specimen sealed to the mouth of the cup. The surrounding RH environment is set to either 50%, 70% or 90%. This causes the water vapour to move between the higher RH to lower RH condition. The RH within the specimen can be assumed as the average between the RH inside the cup and the surrounding environment, e.g., when the cup has 0% RH and the surrounding is 70% RH, the material is considered to have 35% RH. Table 2.3 shows the result of the WVT of European spruce CLT from (Alsayegh, 2012) and a comparison to spruce wood stud from (Wu, 2007).

Table 2.3: Water vapour transport comparison between european spruce CLT (Alsayegh, 2012) and spruce wood stud (Wu, 2007).

CLT WVT	**RH of specimen**	**Spruce wood stud WVT**
kg/m.Pa.s	%	kg/m.Pa.s
-	10	$2.92 \cdot 10^{-13}$
-	20	$5.05 \cdot 10^{-13}$
$(7.59 \pm 0.82) \cdot 10^{-13}$	25	-
-	30	$8.02 \cdot 10^{-13}$
$(12.7 \pm 1.46) \cdot 10^{-13}$	35	-
-	40	$12.6 \cdot 10^{-13}$
$(25.2 \pm 3.68) \cdot 10^{-13}$	45	-
-	50	$20.0 \cdot 10^{-13}$
-	60	$32.3 \cdot 10^{-13}$
-	70	$53.2 \cdot 10^{-13}$
$(60.3 \pm 11.9) \cdot 10^{-13}$	75	-
-	80	$90.0 \cdot 10^{-13}$
$(83.4 \pm 18.6) \cdot 10^{-13}$	85	-
-	90	$156 \cdot 10^{-13}$
$(110 \pm 25.7) \cdot 10^{-13}$	95	-
-	100	$281 \cdot 10^{-13}$

2.3.3 Liquid Transport

The presence of glue between the wood layers has made some difference regarding the behaviour of liquid water transport between CLT and plain wood. The glue limits the movement of liquid which lowered the liquid transport coefficients of CLT. The transport coefficient taken from the test for CLT in perpendicular (radial and tangential) direction is $1.63 \cdot 10^{-3}$ kg/m$^2\sqrt{s}$. As for plain spruce, the transport coefficient is $12 \cdot 10^{-3}$ kg/m$^2\sqrt{s}$ (WU, 2007), which is about seven times larger.

2.3.4 Thermal Properties

Thermal conductivity of CLT is similar to plain wood specimens. Its performance is not affected by the presence of glue between the layers. It is mostly affected by the density of each specimen and the moisture content. Table 2.4 shows a thermal conductivity comparison between CLT and plain wood tested at 12% moisture ratio.

Table 2.4: Thermal conductivity comparison between CLT (Alsayegh, 2012) and plain wood (Forest Products Laboratory, 2010).

Specimen	**Density (kg/m^3)**	**Thermal Conductivity (W/(mK))**
CLT test 1	340	0.103
CLT test 2	340	0.104
Pine (Eastern white, Sugar)	370	0.110
Spruce (Engelmann, White)	370	0.110
Spruce (Red, Stika)	420	0.120
Pine (Lodgepole, Ponderosa)	400-430	0.130

2.3.5 Air Permeability

Air permeability of CLT depends on the glue discontinuity within the specimen. Some specimen has been found to be permeable and others to be impermeable. Definition of impermeable from the research of (Alsayegh, 2012) is that the air flow resistant cannot be measured by the equipment used for the experiment because it is very low. All three European spruce CLT tested were impermeable.

Research from (Raji, 2009) showed similar results. The air permeability was tested for both solid pinewood and laminated pinewood, and the laminated specimen gave a lower air permeability. The average permeability in perpendicular direction to the grain of solid pinewood was $5.8 \cdot 10^{-17}$ m^2 and $0.78 \cdot 10^{-17}$ m^2 for laminated pinewood. Although the presence of adhesive seal had a significant impact on air permeability, it was concluded that it does not have a big influence on thick wood specimens as it has low permeability to begin with.

2.4 Drying Process of Fresh Concrete

The properties of fresh concrete were considered to be the possible source of moisture on CLT layer of the composite slab. Several important properties of the drying process were studied, as it might affect in either stimulating or preventing moisture damages with regards to mould growth.

2.4.1 Curing Condition

Curing of concrete is defined as providing proper conditions for concrete in terms of moisture and temperature in order to achieve the desired concrete quality. Duration of curing can vary depending on specific demands but mainly it lasts between 3-14 days. During the curing period, the relative humidity of air inside the concrete has to exceed 80% and the temperature of concrete has to be higher than 10°C. The most important benefit of curing is to increase the strength of concrete and it increases as the curing duration increases which can be seen in Figure 2.7. The strength of concrete increases greatly during the first few days and after a period of 7 days, a cured concrete has 50% higher strength than uncured concrete. Another benefit of curing is to reduce cracking of concrete, in which it decreases permeability (Kosmatka, 2008).

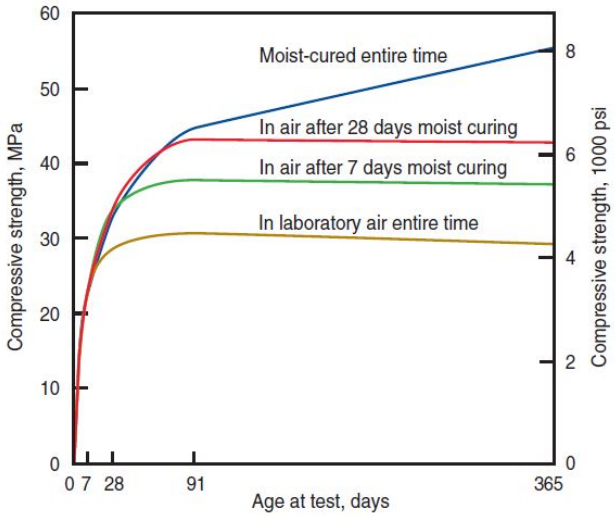

Figure 2.7: Concrete strength increases with increasing curing duration (Kosmatka, 2008).

Curing period of concrete depends on many factors, such as the type of concrete, ambient temperature and moisture condition, desired strength and eventual exposure condition. Curing temperature for concrete varies between 10-50°C depending on the desired early and final strength of concrete. Higher early strength can be provided by increasing the curing temperature, but the 28-day strength decreases as a consequence. Figure 2.8 describes the development of concrete strength at different curing temperatures. The recommended curing temperature for concrete according to (Powerblanket, 2017) is approximately 13°C as shown in Figure 2.9.

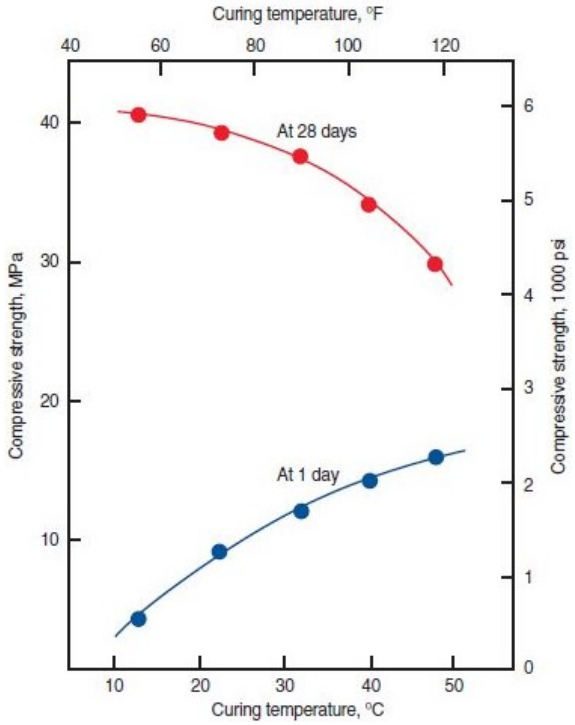

Figure 2.8: Concrete strength at 1 and 28 days at varying temperatures (Kosmatka, 2008).

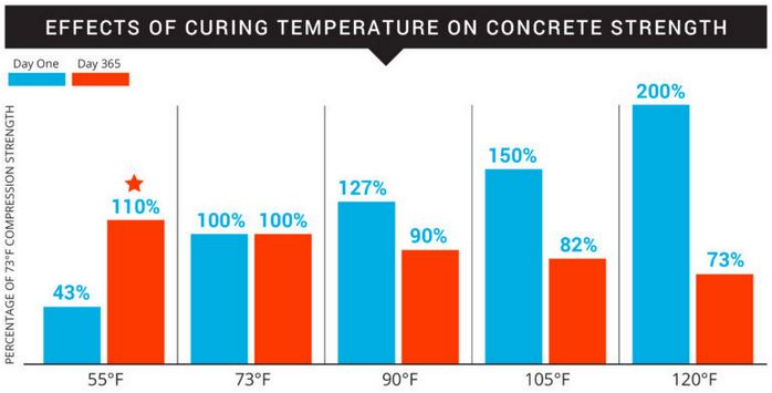

Figure 2.9: Strength test of concrete cured at temperatures of 55°F (13°C), 73°F (23°C), 90°F (33°C), 105°F (41°C) and 120°F (49°C) (Powerblanket, 2017).

2.4.2 Drying Condition

Drying of concrete describes as providing suitable conditions for concrete to dry and reaches the desirable moisture condition in order to decrease the possibility of damages due to high moisture content. Drying is a critical aspect for concrete floors due to the fact that flooring materials are commonly sensitive to high moisture content. The rate of drying depends primarily on shape and thickness of concrete elements and elements with a large surface area, such as concrete slabs, dries relatively faster than elements with a smaller surface area. Beside the shape and thickness of con-

crete element, there are other factors affecting the drying rate of concrete, such as water to cement ratio (w/c), drying temperature, curing conditions, one sided or two sided drying, cement type and relative humidity of the surrounding air (Kosmatka, 2008). The most significant factor among them in most cases is the w/c ratio. The drying time for concrete with 0.5-0.7 w/c ratio to reach 90% relative humidity is anywhere in between 3 to 9 months. For concrete with a w/c ratio of 0.38-0.5, it could take around 2 to 3 months for it to reach 90% relative humidity with adequate drying conditions (Laticrete International Inc., 2017).

Svenska Byggbranschens Utvecklingsfond (SBUF) (Development Fund of the Swedish Construction Industry) describes the expected time for concrete slabs with different w/c ratio to dry to the desired relative humidity (either 90% or 85%) and it can be seen in Table 2.5. The values in Table 2.5 are preliminary and it can be adjusted by using correction factors. The correction factors can increase or decrease the time needed for drying and they are depended on the thickness of the slab, ambient temperature and relative humidity, one side or two sides drying and curing conditions.

Table 2.5: Standard drying time (SBUF, 1995).

RH [%]	**w/c =0.4**	**w/c =0.5**	**w/c =0.6**	**w/c =0.7**
85	50 days	90 days	135 days	180 days
90	20 days	45 days	65 days	95 days

Table 2.6 gives the correction factors for common thicknesses for the concrete slab with different w/c ratio. The correction factor increases as the thickness of concrete slab increases.

Table 2.6: Correction factor for different slab thickness (SBUF, 1995).

Thickness	**w/c =0.4**	**w/c =0.5**	**w/c =0.6**	**w/c =0.7**
100	0.4	0.4	0.4	0.4
150	0.8	0.8	0.8	0.7
180	1.0	1.0	1.0	1.0
200	1.1	1.1	1.1	1.2
250	1.3	1.4	1.5	1.8

The drying time decreases as the temperature increases and it increases as the relative humidity increases. Table 2.7 shows the correction factors for temperature and relative humidity.

Table 2.7: Correction factor for temperature and relative humidity (SBUF, 1995).

RH [%]	10°C	18°C	25°C	30°C
35	1.2	0.8	0.7	0.6
50	1.2	0.9	0.7	0.6
60	1.3	1.0	0.8	0.7
70	1.4	1.1	0.8	0.7
80	1.7	1.2	1.0	0.9

One- or two-sided drying have a big impact on drying time. One-sided drying requires longer time to dry than two-sided drying as can be seen in Table 2.8.

Table 2.8: Correction factors for one- or two-sided drying (SBUF, 1995).

Drying condition	w/c =0.4	w/c =0.5	w/c =0.6	w/c =0.7
One-sided	2.0	2.3	2.6	3.2
Two-sided	1.0	1.0	1.0	1.0

The time needed for drying is affected also by curing conditions and Table 2.9 takes this factor into consideration.

Table 2.9: Correction factors for variations in curing conditions (SBUF, 1995).

Curing Condition (drying to 90% RH)	w/c =0.5	w/c =0.6	w/c =0.7
Dry	0.5	0.5	0.7
4 weeks of high moisture (tight cover)	0.5	0.7	0.8
4 weeks of rain	1.0	1.3	1.3

Another factor that can be taken into consideration to speed up the drying process is adding silica fume into the concrete mix. This reduces the drying time of concrete by almost 50%. The required amount of silica fume is 10% for w/c ratio higher than 0.5 and 5% for w/c ratio less than 0.5. The actual time needed for drying of a concrete slab is difficult to determined theoretically but an estimation of it can be made by multiplying all the different factors that are described above with the preliminary approximated drying time.

The drying time for a concrete slab can also be estimated with software aided computation such as TorkaS. It was developed by a collaboration of Lund University, with SBUF, Tyréns, Swerock AB and Cementha AB. This program is under constant development and continuously updated. It works by simulating the process of drying concrete with time steps and dividing the slab into calculation cells. All properties of drying concrete such as hydration and moisture transport are calculated in each time step interval (Hassan, 2017).

In another research done by (Mjörnell, 2003), the drying time for self-compacting concrete and ordinary Portland concrete from build-in moisture were studied, with different w/c ratios and different climate conditions. The specimens used were cylindrical shaped with diameter of 200 mm and height of 100 mm. The climate condition for drying of concrete was a constant temperature of 20 °C with relative humidity of 50%, water storage in 28 days and afterwards drying in a constant temperature of 20 °C and relative humidity of 50%, and self-drying by sealing all surfaces after casting of concrete. The duration of the three experiments setup were one year (365 days) in which the relative humidity was measured for each specimen after 7, 14, 28, 90, 180 and 365 days of casting.

Figure 2.10 shows the resulting relative humidity for the different type of specimen for one experiment case. It was measured at 40 mm from the drying surface under one-sided drying condition of 20 °C and 50% relative humidity. Curve 1 is self-compacting concrete with w/c ratio of 0.38 and curves 2, 3, 4 and 5 are also self-compacting concrete but with w/c ratio of 0.6 and different types of fillers. However, the curves that were of interest are curve 6 with w/c ratio of 0.38 and curve 7 with w/c ratio of 0.6 because the type of cement used for the mixture was ordinary Portland cement without any fillers. It can be seen in the figure that the time needed for curve 6 to reach relative humidity of 90%, 85% and 75% is 15, 61 and 365 days, respectively. Curve 7 needed 75 and 175 days to reach a relative humidity of 90% and 85%, respectively.

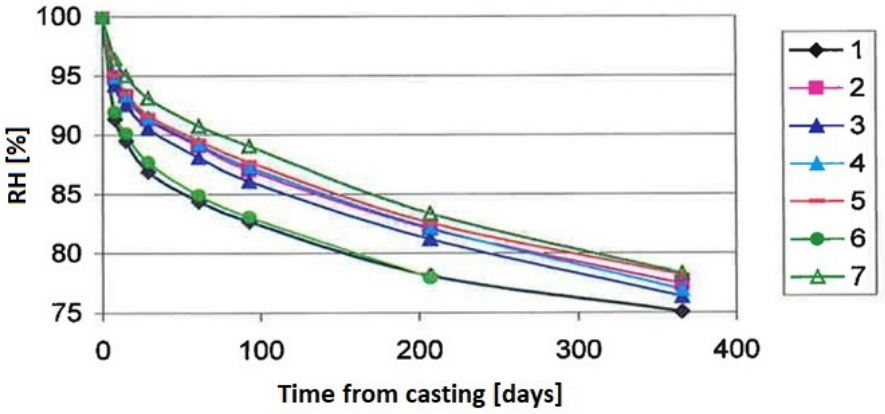

Figure 2.10: Drying time for different types of concrete with accuracy ± 1.5% RH (Mjörnell, 2003).

Mjörnell also compared the experiment results with the results from the SBUF method and TorkaS program as can be seen in Table 2.10. The comparison shows that the estimated time for drying in SBUF method is significantly shorter than the measured results. TorkaS gave relatively closer results to the experiment measurements compared to SBUF method.

Table 2.10: Estimated drying time (days) to reach 90% and 85% RH for concrete specimen 6 and 7 (Mjörnell, 2003).

Concrete	RH = 90%			RH = 85%		
	Experiment	SBUF	TorkaS	Experiment	SBUF	TorkaS
6 (w/c=0.38)	15	14	15	61	34	93
7 (w/c=0.6)	75	29	61	175	60	207

2.4.3 Moisture

Moisture transportation in concrete can be in the form of liquid water or water vapour. For concrete that is fully saturated, the driving force for movement is either capillary action or evaporation from exposure to the surrounding air. When concrete is no longer in a state of full saturation, the difference of relative humidity on either side of the surface is the driving force for moisture movement (Kosmatka, 2008).

One cubic meter of concrete with 0.5 w/c ratio commonly holds 125 kg of water, in which half of it is used in the hydration process of cement, and the other half is free water that has to be dried out until the concrete has an acceptable relative humidity level. This drying process of concrete starts with evaporation of liquid water on the surface into the air. As the moisture in the surface evaporates, water from within the concrete moves outwards to replace it. This in turn causes shrinkage development in the absence of water. After all the liquid water have evaporated, the surface is no longer covered with water and the concrete stops shrinking. Then the drying process continues by evaporation and vapour diffusion from moisture within the body to the surrounding air (Laticrete International Inc., 2017). This causes variation of relative humidity along the depth of concrete and Figure 2.11 gives an illustration for the distribution of relative humidity in different depth and shrinkage value for a 150 × 300 mm cylinder specimen. The specimen is moist cured for 7 days and dried afterwards at a temperature of 23°C.

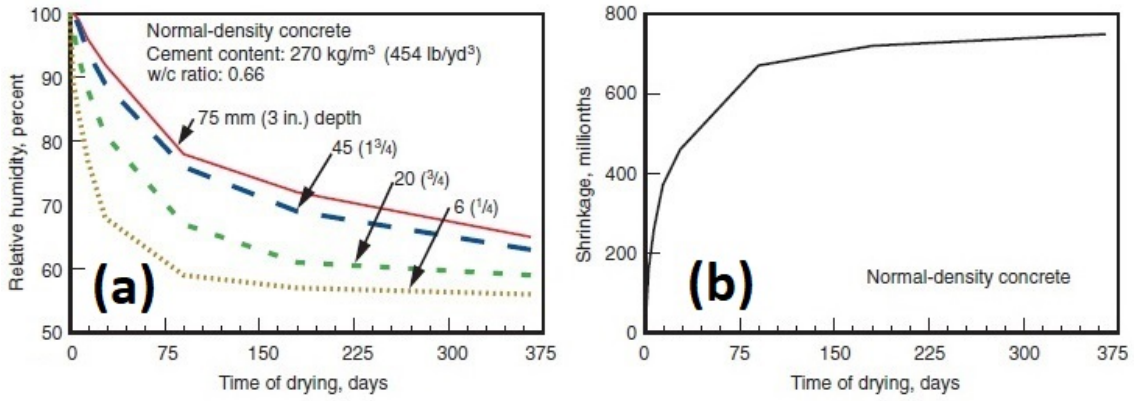

Figure 2.11: Distribution of relative humidity in various depth (**a**) and shrinkage of concrete (**b**) in one year period (Kosmatka, 2008).

2.4.4 Temperature

Mixtures of water and cement form a chemical reaction that produces heat discharge, which is called heat of hydration (HOH). This increases the temperature of concrete during the drying period. There are many factors affecting the amount of heat that is emitted to the surrounding, such as volume of concrete, cement composition, water to cement ratio (w/c) and size of cement particles. High temperature causes concrete to expand, and the temperature difference causes nonuniform cooling in concrete that might cause cracks to develop. The general rule to prevent this is to control the temperature within the concrete so that the difference between the inner layer and the outer layer does not exceed 20°C (Portland Cement Association, 1997).

In a typical construction, the temperature change is not considerable as the heat of the concrete is easily released to the surrounding environment, whether it is air or soil. For thicker concrete construction such as foundation, the internal heat takes a longer time to be dissipated and the temperature inside the concrete remains high. Some of the impacts of concrete thickness on temperature can be seen on Figure 2.12.

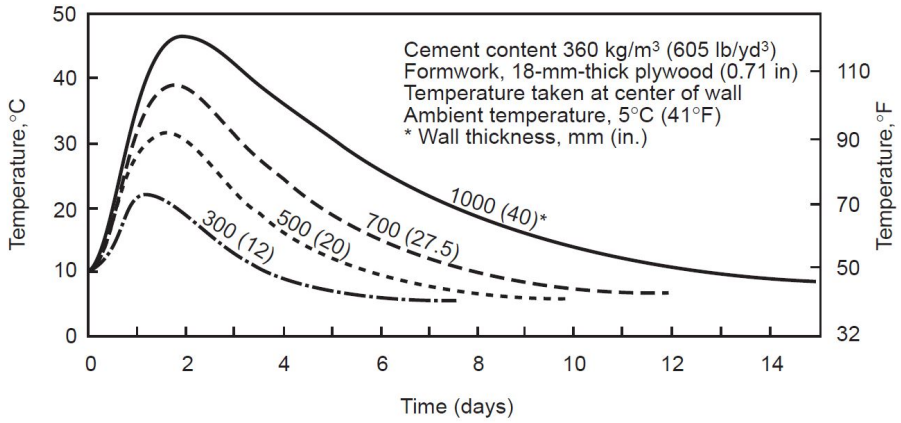

Figure 2.12: Influence of thickness on concrete temperature (Portland Cement Association, 1997).

Cement composition is another important aspect to consider that contributes to heat generation during the hydration process of cement paste. Cement properties is influenced by the formation of clinker in which it depends on oxide composition of the cement. The main clinker components are tricalcium silicate (C_3S), dicalcium silicate (C_2S), tricalcium aluminate (C_3A) and tetracalcium alumino-ferrite (C_4AF). The clinker components are responsible for heat generation during hydration process and they determine the cement type. The more of C_3S is in cement, the faster the cement hydrates and greater heat is generated, and the opposite applies when the cement contains more of C_2S (Sedaghat, 2016).

Sedeghat also discusses in his research the influence of w/c ratio on heat generation. The heat released during hydration in seven days increases by increasing w/c. Sedeghat further addresses the effect of cement fineness on HOH and the finer the

cement particles are, the higher the surface area for cement is to react with water, which results in generating greater heat.

Sedeghat investigated the amount of heat generated from typical Portland cement paste by conducting experiments on several cement types, in which he calculated total heat and heat flow for a period of 7 days. One of the specimen which is called Cement A, had 57% C_3S, 14% C_2S, 7% C_3A, 12% C_4AF and a Blaine fineness of 417 m^2/kg. The experiment on the specimen has the properties stated in Table 2.11.

Table 2.11: Experimental specimen properties (Sedeghat, 2016).

Properties	**Internal Mixing A.1 and A.2**	**External Mixing A.1**	**External Mixing A.2**
Cement (g)	3.3	9.81	3.38
Water (g)	1.65	4.9	1.69
w/c ratio	0.5	0.5	0.5
Ambient temperature (°C)	23	23	23
Test duration (h)	168	168	168

The mixing of the cement followed the methods stated in ASTM C1702, for internal mixing and external mixing. The detailed procedure of the two methods was not discussed in detail in this research, but it was noted that both methods yielded similar results regarding the generated heat. The results of the experiment are given in Figure 2.13 and 2.14. Total average generated heat during the hydration process of the Portland cement in a period of seven days is 350 J/g for internal mixing and 358 J/g for external mixing. Most of this hydration heat is generated during the beginning of hydration process, in the first 48 hours. It could be seen that the curve in Figure 2.14 has an initial drop at the beginning, which may be caused by the speed of internal mixing with the chosen mixing tools of the experiment.

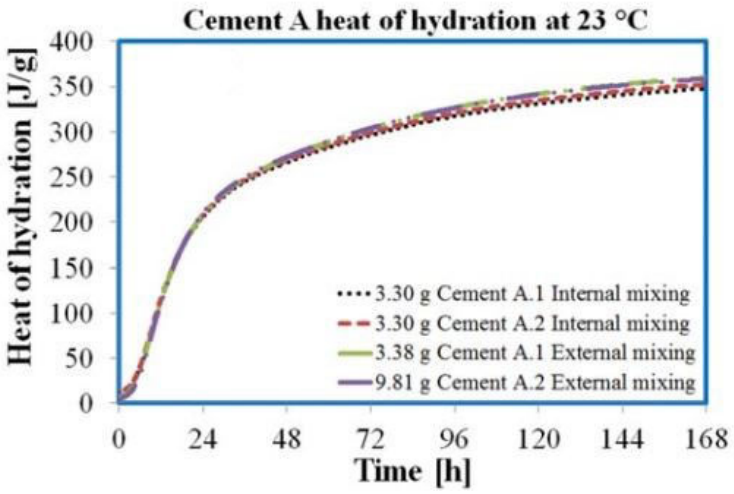

Figure 2.13: Heat of hydration of cement paste (Sedeghat, 2016).

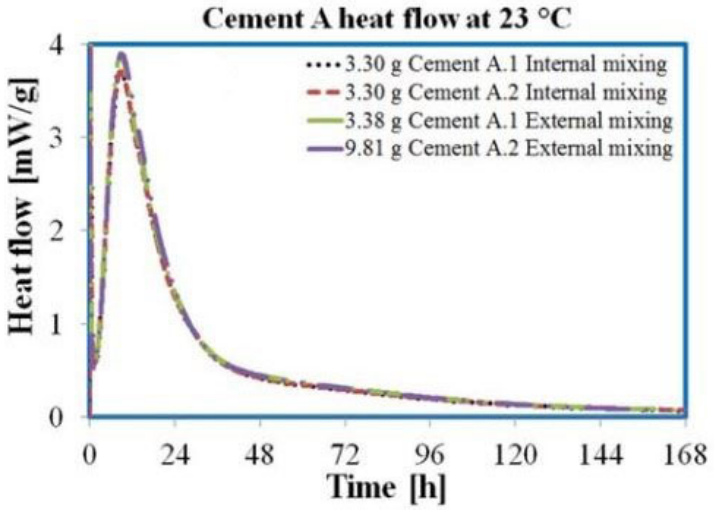

Figure 2.14: Heat flow of cement paste (Sedeghat, 2016).

2.4.5 Alkalinity

Concrete is well-known to be a highly alkaline material. The pH value of a typical fresh concrete is usually around 13, but it also depends on the cement type used. This value decreases until it reaches about 8.5 throughout the drying period, due to reactions from the surrounding carbon dioxide to the exposed concrete surface. This carbonation process also gradually affects concrete underneath the surface layer. The whole concrete section ends up having the same overall pH value in the final stage of drying (Grubb, 2007).

The depth of carbonation is of interest in the construction industry for several reasons. The exposure to carbonated concrete can potentially cause corrosion, even though the alkaline state of concrete is favourable to prevent the steel reinforcement from being corroded (Grubb, 2007). High pH value of the concrete surface also negatively affects adhesives in floor installations. The mixture of substrates with pH value of greater than 9 can compromise the adhesive and its bonding system (Moisture Meter, 2015).

2.5 Bio-deterioration Risk of Timber

A proper knowledge of the different types of microorganisms is important to understand their mechanism and their effect on timber, as well as the ideal environments and factors that could make them grow.

2.5.1 Wood Fungi

There are different types of fungi that grow on and in wood. The main two types of fungi are mould fungi which cause wood discoloration, and decay fungi which cause degrading of the wood (Ewing, 2003).

Mould fungi are the common name for different types of fast-growing fungi. Mould can grow on the surface of a material and often cause discoloration, as black or greenish-brown marks. Beside discoloration, mould fungi can form spores which have a negative effect on people's well-being and eventually causes allergies and health problems. Mould fungi do not cause any change in mechanical properties of timber and it can be removed by wiping it out with a mixture of water and bleach. It can also be removed by peeling the affected surface. Treating of mould fungi helps to eliminate or reduce the negative effect of mould (Zabel, 1992).

Decay fungi are any type of fungi that cause degrading of wood and there are up to 200 different types of decay fungi. They form inside of the wood which becomes difficult to detect them in the early stages, but there are some indicators that refer to the decay fungi existence in wood even if they are not visible. Some of these indicators are moisture stains, unpleasant smell and even cracks in the wood in later stages. Another indicator can be the presence of insects and spiders (Ewing, 2003). High content of moisture, above fibre saturation point (FSP), is needed in order for decay fungi to colonize in wood, but after they have been colonized they can continue to grow in lower moisture content (Zabel, 1992). Wood decay fungi can be divided into three major types according to the way they attack the cell of the wood. These are brown-, white- and soft-rot fungi (Ewing, 2003).

Brown-rot fungi attack cellulose part of the wood and they cause decaying of wood which gives a brownish colour that refers to the name of the fungi. Brown-rot cause cracks in wood and they affect the mechanical properties in the early stages. On the other hand, white-rot fungi attack both cellulose and lignin of wood and break them down which cause deterioration of the mechanical capacity of the wood. However, soft-rot fungi belong to mould fungi, but they act as rot-fungi in terms of degrading of the wood. After soft-rot fungi attack, the wood becomes soft on the outside and hard from the inside which cause deterioration of load carrying capacity of the wood (Ewing, 2003).

In addition to mold fungi and decay fungi, there are other types of bacteria that attack wood and change the properties of the wood. Examples of these bacteria are erosion and tumbling bacteria which attack the moist wood in the early stages and cause increasing of wood permeability (Hansson, 2010).

2.5.2 Growth Factor of Wood Fungi

There are many physical and chemical factors affecting on formation and development of wood fungi. These factors are relative humidity, temperature, time, oxygen, the substrate (the wood itself), pH condition and UV light. Some of these factors are presented and described in more detail in this section.

2.5.2.1 Relative Humidity, Temperature and Time

Relative humidity and temperature have the biggest impact on the growth and development of wood fungi. They are also depended on each other in terms of fungi

growth, and the critical value of one depends on the other.

According to a previous study by (Viitanen, 1996), it is stated that the growth of mould fungi takes several weeks for a temperature range of 5-50°C if the relative humidity is kept at 80%. The growth of mould fungi can become very slow at the same relative humidity if the temperature is lowered to 0-5°C. However, growth of mould fungi becomes much faster if the relative humidity becomes above 95% even though the temperature is low. The time needed for the appearance of mould fungi in very high relative humidity (above 95%) is relatively short, a few days if the temperature is between 25-40°C, and 1-2 months when the temperature is between 10-20°C (Viitanen, 1996).

In 1991, Viitanen and Ritschkoff came to a conclusion in their study that the risk for mould growth would not exist if the relative humidity kept under 75% under normal temperature variations, 0-40°C. Figure 2.15 shows the relation between relative humidity, temperature and time needed for initial mould growth.

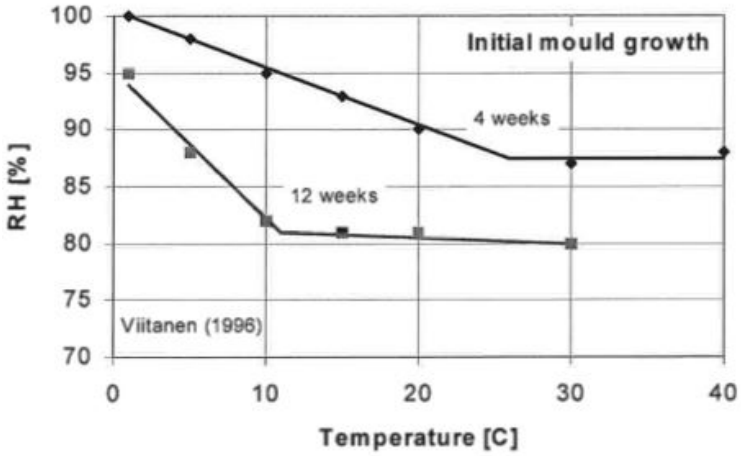

Figure 2.15: Minimum relative humidity required for initial mould growth in wood at different temperatures (Viitanen, 1996).

As stated previously, the mould fungi require moderately low relative humidity to grow, but in order to produce spore they need higher relative humidity (Grant, 1989). Mould growth does not become visible to the naked eye unless they start to produce spore, which determines a critical relative humidity for mould growth to become visible (Nilsson, 2004). (Viitanen, 1996), in his research, claims that a relative humidity of minimum 85% and a temperature above 20°C in a period of three months is required for mould growth to become visible. Increasing relative humidity or temperature results in producing spores in a shorter period of time (Nilsson, 2004). Figure 2.16 shows the relation between relative humidity, temperature and time needed for the visual appearance of mould growth.

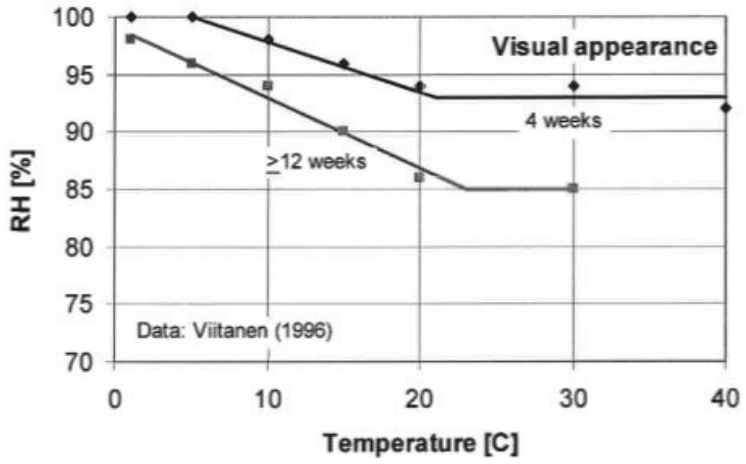

Figure 2.16: Minimum relative humidity required for visible appearance of mould in wood at different temperatures (Viitanen, 1996).

On the other hand, decay fungi need significantly higher relative humidity to grow. In order for the decay fungi to establish, the moisture ratio in the wood must be above FSP, approximately 26% for CLT (FPInnovations, 2013). The relative humidity has to increase to nearly 100% so the moisture ratio in the wood becomes above FSP. The ideal moisture ratio for brown-rot fungi is between 30-70% (Viitanen, 1994). However, once the rot-fungi have established in the wood, they have the possibility to grow even though the moisture ratio decreases to 20% (Alsayegh, 2012), partly due to their ability to provide water from other sources than the material that they grow on (Nilsson, 2004). The critical relative humidity for different microorganisms can be seen in Table 2.12.

Table 2.12: Critical relative humidity for different types of microorganisms (Hocking, 1993).

Microorganisms	**Critical RH** [%]
Aspergillus versicolor	90-97
Cladosporium sphaerospermum	96
Penicillium brevicompactum	95
Penicillium chrysogenum	75
Ulocladium consortiale	62-83
Stachybotrys atra	61-72

2.5.2.2 pH

Fungi build-up is most effective in a slightly to strongly acidic environment with a pH value of 3 to 6. Each type of wood decay fungi has their own ideal pH condition for optimal growth, and their own top and bottom pH limit where growth stops. Wood-stain fungi are very dependent on the pH. They are rendered inactive if exposed to pH of more than 5. Other fungi such as brown-rot grow best at a pH of

around 3 (Zabel, 1992).

Extreme levels of acidity and alkalinity hinders the growth of fungi. Different species of fungi have different tolerance to extreme pH conditions. Some species of *Aspergillus* still showed some growth in pH range of 2 to 10.5 with the ideal temperature of 30°C, although with very poor activity compared to in optimum pH range. Species of *Fusarium* and *Penicillium* does not show any growth at above 10 pH (Wheeler, 1990). These findings correlate to a common method of removing mould fungi, and that is by applying water mixture solution with either baking soda, detergent or bleach. These household products are highly alkaline, with bleach having the highest alkalinity out of them with a pH value of around 12. Dozens of mould removal commercial products that are currently available are highly alkaline. As mentioned in Section 2.4.5, concrete is also highly alkaline, which could affect mould growth activities in its surroundings.

2.5.2.3 UV Light

Ultraviolet (UV) light is widely known to have the ability to kill or stop the growth of microorganisms. This property of UV light has made it useful to be used for decontamination of microbial activity in hospitals, food products or building materials. The type of UV light that is usually used is UVC which has a basis wavelength of 200-280 nm. Microorganisms such as mould- and decay-fungi are harmfully affected if exposed to UV radiation within the 250-260 nm wavelength. One study shows that UVC light was very effective in disabling the activity of several spore genera, including *P.corylophilum*, a type of fungi that appear in damp buildings (Begum, 2009). The analyzed area for mould growth in this study was the CLT located under the concrete layer. The drying conditions were assumed to be weather protected as well, which gave no exposure to UV light. With this dark and damp surroundings, gave suitable conditions for potential mould growth.

2.6 Mould Growth Threshold

Certain conditions have to be met for any building material to be considered as moisture safe. The regulations/guidelines mentioned in this subsection were selected as the threshold for the analyses.

2.6.1 BBR

(Nilsson, 2015) in his handbook, states that the *Boverkets byggregler* (BBR) (Swedish Building Regulations), recommends the relative humidity for wood or wood-based materials should not exceed 75% over a long period of time. The critical value of 75% for timber products is considered to be valid at room temperature. Nilsson mentions also that a higher relative humidity than the critical relative humidity is acceptable only if the exposure time is relatively short. On the other hand, if wood is exposed to moisture conditions higher than its critical value, consequences are present in terms of changing of thermal, mechanical and moisture properties of the

wood. High moisture value also affects on growth of mould and bacteria. However, the growth of mould and decay fungi does not just depend on relative humidity but as well on the temperature, exposure time and many other factors as it described previously (Nilsson, 2015).

2.6.2 ASHRAE Standard 160 - 2009

Conditions that stimulate mould growth depends on various factors that have been mentioned in Section 2.5.2. However, standards tend to simplify in determining the criteria for the construction industry to follow (TenWolde, 2011). In accordance with ASHRAE standards, performance criteria for mould growth depend on the temperature and humidity conditions of the building material's surface. These conditions must be followed to negate any mould growth activity:

1. 30-day running average surface RH $< 80\%$ with temperature between 5°C and 40°C (41°F and 104°F).
2. 7-day running average surface RH $< 98\%$ with temperature between 5°C and 40°C (41°F and 104°F).
3. 24-hour running average surface RH $< 100\%$ with temperature between 5°C and 40°C (41°F and 104°F).

There might potentially be further simplifications of these criteria in the future revised version, where only criterion (1) is stated, and criteria (2) and (3) are to be removed. The simple nature of the standard could be improved with more detailed performance criteria for the materials, but as moisture performance of building materials are rather difficult to acquire, it would be quite demanding to fulfill if the standard is specified in more detail (TenWolde, 2011).

2.6.3 Mould Growth Index

Based on the research of (Viitanen, 1991), a mould growth model for pine and spruce is currently available. The model is well fitted for these analyses as a large scope of North-European timber were used in the making of the model. The mould growth model takes into account relative humidity, temperature and exposure time to simulate the growth of mould in a certain material with their respective properties. The bare minimum and maximum condition of the aforementioned factors need to be known for the simulation of mould growth. The model is evaluated using the Mould Growth Index (MGI) from the same research, which can be seen in Table 2.13.

Anything above 1 can be considered as a risk of mould, because mould already exists beyond that point, even though at an MGI of 1 or 2 it is only possible to be seen with a microscope. An MGI of 1 or 2 is usually considered to be safe in most construction, but in some cases it is a possible health risk for a person who is very sensitive towards allergens. A typical construction should have an MGI of below 3 to be considered as moisture safe, because above that point mould can already be seen by the naked eyes.

Table 2.13: Mould growth index (Viitanen, 1991).

Index	Growth Rate	Description
0	No growth	Spores not activated
1	Small amounts of mold on surface (microscope)	Initial stages of growth
2	<10% coverage of mold on surface (microscope)	-
3	10%–30% coverage of mold on surface (visual)	New spores produced
4	30%–70% coverage of mold on surface (visual)	Moderate growth
5	>70% coverage of mold on surface (visual)	Plenty of growth
6	Very heavy and tight growth	Coverage around 100%

The model suggests that the overall condition needed for mould growth can be presented in a purely mathematical model, in Figure 2.17. The relative humidity curve for possible mould risk is a function of temperature, described in the following function:

$$RH_{crit} = \begin{cases} -0.00267T^3 + 0.160T^2 - 3.13T + 100.0 & \text{when } T \leq 20 \\ 80\% & \text{when } T > 20 \end{cases} \tag{2.6}$$

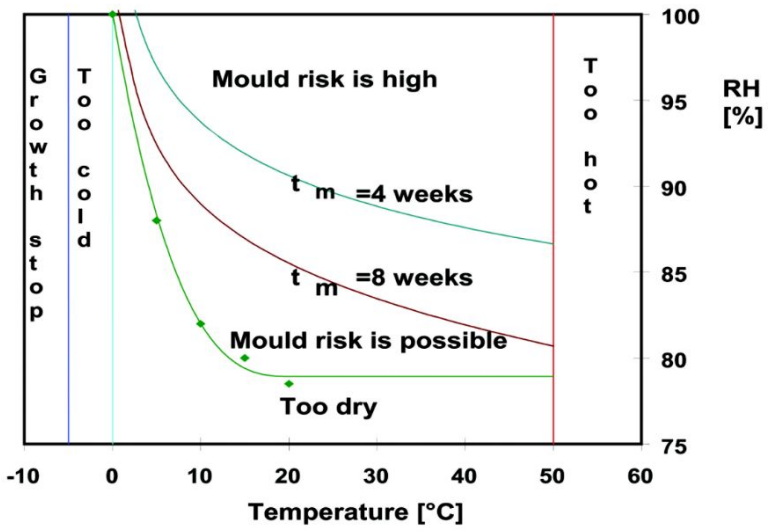

Figure 2.17: Conditions favourable for initiation of mould growth on wooden materials (Hukka, 1999).

In the model, possible mould risk could be defined as 1 in the MGI. t_m represents the time needed for the MGI to reach 1 in constant RH and temperature conditions. It is found with Equation 2.7, where W is the wood species (0 = pine, 1 = spruce) and SQ is the surface quality (0 = resawn, 1 = original kiln-dried).

$$t_m = exp(-0.68lnT - 13.9lnRH + 0.14W - 0.33SQ + 66.02) \tag{2.7}$$

Equation 2.7 is no longer valid when the mold growth passed the M = 1 threshold, therefore it is further developed by the assumption that the mould index increases linearly with time, resulting in Equation 2.8 :

$$\frac{dM}{dt} = \frac{1}{7exp(-0.68lnT - 13.9lnRH + 0.14W - 0.33SQ + 66.02)} k_1 k_2 \tag{2.8}$$

$$k_1 = \begin{cases} 1 & \text{when } M < 1 \\ \dfrac{2}{t_v/t_m - 1} & \text{when } M > 1 \end{cases} \tag{2.9}$$

$$t_v = exp(-0.74lnT - 12.72lnRH + 0.06W + 61.5) \tag{2.10}$$

$$k_2 = max(1 - exp[2.3(M + M_{max})], 0] \tag{2.11}$$

$$M_{max} = 1 + 7\frac{RH_{crit} - RH}{RH_{crit} - 100} - 2\left(\frac{RH_{crit} - RH}{RH_{crit} - 100}\right)^2 \tag{2.12}$$

Relative humidity is not always a constant value. As it fluctuates, conditions for mould growth may go through cycles of favourable and unfavourable condition. This deceleration of growth from exposure to unfavourable conditions can be described using the time of the dry period (t - t_1):

$$\frac{dM}{dt} = \begin{cases} -0.032 & \text{when } t - t_1 \leq 6h \\ 0 & \text{when } 6h \leq t - t_1 \leq 24h \\ -0.016 & \text{when } t - t_1 > 24h \end{cases} \tag{2.13}$$

As the result is purely numerical, it can be interpreted as a risk of possible growth or activity of various mould fungi on the surface of the material (Hukka, 1999).

In a more recent study by (Viitanen, 2007), it discusses the possibility to improve the model to be used for other types of building material, in addition to timber. The method used is to apply material data from other studies to the same equation. Experiments are done with specimens of various building materials, that are exposed to a certain temperature and relative humidity condition. The materials used include spruce plywood and a pine sapwood model for reference. The results of the experiments can be seen in Figure 2.18.

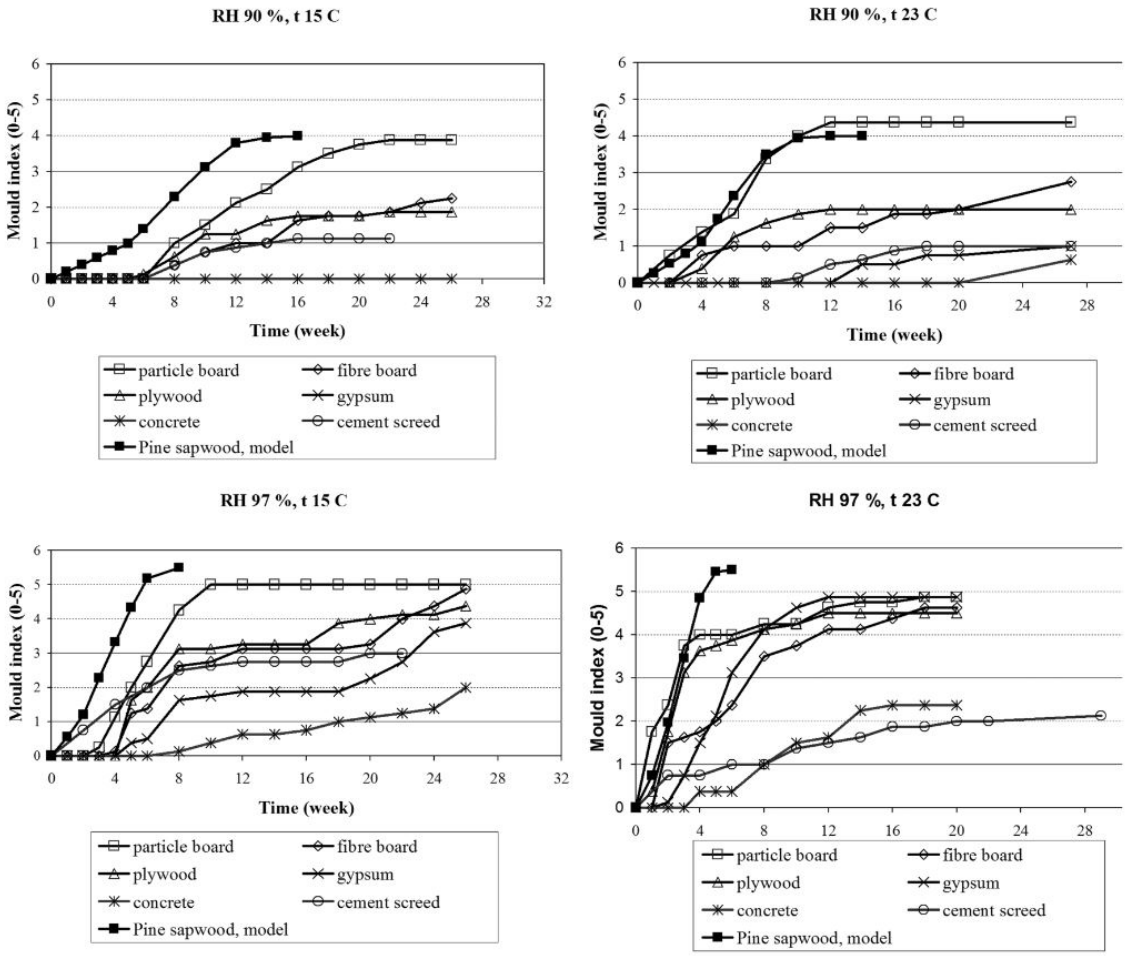

Figure 2.18: The growth of mould on building materials at constant humidity and temperature conditions. 90% RH, 15°C; 90% RH, 23°C; 97% RH, 15°C; 97% RH, 23°C (Viitanen, 2007).

At RH 90% and temperature 23°C, it takes around 7 weeks for pine sapwood to reach an MGI of above 3 with a maximum of 4, while the spruce plywood stays at maximum MGI of 2 even after 28 weeks. At RH 97% with the same temperature, pine sapwood reaches above 3 in the 3rd week and continues until more than MGI of 5 on the 5th. The spruce plywood reaches above 3 at approximately the same time as pine with a maximum MGI of just below 5 after the 12th week. The results mentioned are with conditions of constant RH and temperature throughout the duration of the experiment, which is not always the case in reality.

2.6.4 Regulations/Guidelines for The Study

From the three regulations/guidelines stated above, the mould growth index was chosen as the threshold for measuring potential moisture risks. Regulations from BBR and ASHRAE have relatively simple but strict guidelines that are meant to prevent any risk of mould activity by explicitly limiting the allowed relative humidity level in the construction in cases where mould growth risk are not assessed. The

mould growth index is a more detailed numerical approach in determining potential mould activity by taking into account relative humidity, temperature and exposure time of the material. It also allows some level of mould growth as long as it is below the safety level. The study involved materials with high levels of humidity that does not fulfill requirements from BBR and ASHRAE, but the construction can still be considered as moisture safe if it can be proved with a more detailed approach.

3
Cross Section Design

In this Chapter, a design for the CLT-concrete composite slab was made in order to define a proper cross section of the floor. The floor details were determined by building usage specification according to Eurocode, as well as fire protection and noise insulation requirements from the *Boverkets byggregler* (BBR) (Swedish Building Regulations). The final cross-section detail was determined by the market availability of CLT-concrete composite slab from manufacturers that fulfill all requirements. A proper exterior wall design in joint connection with the floor was also determined and presented.

3.1 Design Requirements

Dimensioning in timber construction is typically governed by noise insulation, fire resistance performance and vibration requirements. In the case of CLT-concrete composite slab, the presence of concrete helps to add mass which can contribute to the performance of the floor section regarding those three criteria. Load bearing requirements is an important aspect as well in sizing of floor section, but it is usually not the determining factor for timber construction.

The floor section was designed for a multi-storey office building with a minimum clear span of 6 m. However, the final floor span depended on the market availability of the product. In order to do the simulations of the CLT-concrete composite slab, a floor had to be modelled in which it would fulfills regulations.

3.1.1 Träguiden Preliminary Design

CLT-concrete composite slabs can be constructed with a span between 6-12 m with a total height depending on the span length. The total height of the slab increases as the span of the slab increases and it can be preliminarily calculated by dividing the span length with 25 ($l_{span}/25$). The total height of the span consists of CLT slab thickness and concrete slab thickness and an appropriate distribution of the total height can be 60% for the CLT slab and 40% for the concrete slab (Svenskt Trä, 2017a).

In order for the CLT and concrete to have a sufficient interaction, shear connectors have to be applied in between the two composites. These shear connectors make

the CLT and concrete behave as close as possible to a single building material instead of two separate materials. Shear connectors must have enough rigidity to transform the force between CLT and concrete without any sliding between the two layers, they also have to be easy to install without taking a long time. There are different types of shear connectors with varying efficiency and cost (Svenskt Trä, 2017a). The presentation of *Timber-Concrete Composite floor system (TCC)* by (Merz, 2018) showed the most common types of shear connectors in CLT-concrete composite slab, which are described in Figure 3.1.

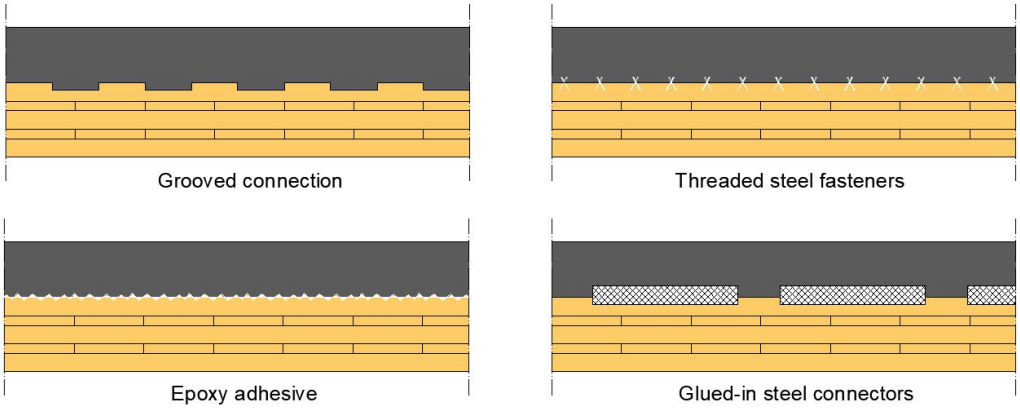

Figure 3.1: Types of shear connectors.

Träguiden further specifies that these types of connection have their own interaction rate between the concrete and CLT layer. The glued-in steel connector has approximately 85% interaction rate and the threaded steel fastener has 70%. This means that a composite section with glued-in steel connectors has 85% effective bending stiffness capacity, compared to the same floor section with assumed full interaction.

3.1.2 Eurocode Regulations

The cross-section was designed to withstand the floor loading requirements of an office building with a minimum span of 6 m. According to Chapter 6.3 in Eurocode 1 (EN 1991-1-1), office building is considered to be building category B with characteristic load of 2.0 to 3.0 kN/m^2 for general distributed load (q_k) and 1.5 to 4.5 kN for local concentrated load (Q_k). Vibrations of the floor slab must also be taken into consideration while designing the cross-section of the floor. Regulations regarding vibrations are mentioned in Chapter 7.3 in Eurocode 5 (EN 1995-1-1).

3.1.3 BBR

The designed CLT-concrete composite slab has to fulfill BBR regarding fire safety and noise insulation.

3.1.3.1 Fire Safety

BBR sets requirements regarding fire safety that every building has to fulfill in order to minimize the risk of loss of lives in the event of fire. According to BBR, buildings

or areas inside the building such as rooms are divided into different activity classes depending on various factors which are the following (Fallqvist, 2016).

- If a person has a good knowledge of the building and evacuation route.
- If a person is capable to evacuate without any help.
- If a person is awake

Beside the activity classes, buildings are divided into different building classes depending on the area of the building, number of floors, number of people, protection requirements and activity class (Fallqvist, 2016).

The building in this research was considered to be a multi-storey office building in which it met activity class 1 (VK1). The number of floors in the building was assumed to be more than three floors and less than sixteen floors, which falls into building class 1 (BR1). Fire resistance classification for an intermediate floor, which was studied in this research, was R60 (Fallqvist, 2007). The CLT-concrete composite slab must resist fire without losing its stability in a minimum of 60 minutes in ordinary fire development aspect. In cases for architectural design which desires exposed timber, additional timber thickness have to be considered as a sacrificial layer in the event of fire.

3.1.3.2 Noise Insulation

It is appropriate to have further understandings regarding airborne and impact noise experience for a person under different activities, to better understand the regulations. The noise level typically produced from human activities can be seen in Figure 3.2. Dark blue boxes mean that the noise is easily heard. Light blue boxes mean the noise can also be heard but does not interfere under normal circumstances, while white boxes mean the noise is not heard (Boverket, 2008).

Airborne noise							
R'_w/D_{ntw} [dB]	Hum	Normal conversation, Office machinery in calm environment	Normal conversation, Office machinery	Loud conversation	Shout	Moderate sound level from speaker	Sound from disco
35							
40							
44							
48							
52							
60							

Impact noise							
$L'_{n,w}$ $L'_{nT,w}$ [dB]	Quiet walk with soft shoes	Quiet walk with heels shoes	Fast walk/run with soft shoes	Fast walk/run with heels shoes	Normal jump	Moderate jump	Gymnastics/ Powerful jump
64							
60							
56							
52							
48							
44							
40							

Figure 3.2: The practical experience for different airborne and impact noises (Boverket, 2008).

R'_w is the airborne noise insulation level and $L'_{nT,w}$ is the impact noise insulation level. A difference of 3 dB is considered to be an audible change in noise level, and a difference of 8 to 10 dB would feel as a 100% increase or decrease in sound level (Hagberg, 2007).

Just as fire safety requirements, BBR has specific demands regarding noise insulation. The need for noise insulation varies depending on the noise sources and the required noise insulation in the room or in the building. These regulations are divided into four different category or classes. Class C is the minimum demand according to BBR and every building has to fulfill this requirement. Class B has generally 50% better noise insulation than class C, while class A is the most strict class and it provides the best acoustic conditions, and it has approximately 100% better noise insulation than class C. Class A is the most desirable class to achieve, but the typical aim for most construction is to achieve class B or C. The last category is class D which applies only if class C can not be achieved such as in older buildings, and it has about 50% lower noise insulation than class C (Hagberg, 2007). Each and every building type have these four different regulation classes but the value of the noise insulation in each class varies depending on the usage or type of the building, i.e. residential building, commercial building and etc (Swedish Standard Institute, 2007).

As it was mentioned in the design requirements, Section 3.1, this research addresses multi-storey office building. The critical factors for noise insulation in an intermediate floor slab were airborne and impact noise insulation. Tables 3.1 and 3.2 show the impact and airborne noise index for different types of spaces and classifications. The floor section for the chosen sound class must have a higher value than the airborne noise insulation index (R'_w) and must be lower than the impact noise insulation index ($L'_{nT,w}$).

Table 3.1: Highest impact noise insulation index, $L'_{nT,w}$, for office space (Svensk Standard SS 25268:2007).

No	Type of room/space	**From space with low step noise load** $L'_{nT,w}$ (dB)				**From space with high step noise load** $L'_{nT,w}$ (dB)			
		Sound class				Sound class			
		A	B	C	D	A	B	C	D
21a	Conference room for more than 20 person	52	60	60	-	48	56	56	64
21b	Private work space or conversation space	68	-	-	-	64	64	68	-
21c	Space with requirements for freedom of movement	64	-	-	-	60	60	64	-
21d	From other occupation	64[a]	64[a]	68[a]	-	60[a]	60[a]	68[a]	-
[a] The requirement relates to normalized step noise level, $L'_{nT,w}$									

Table 3.2: Lowest airborne noise insulation index, R'_w, for office space (Svensk Standard SS 25268:2007).

No	Type of room/space	**Between rooms** R'_w (dB)				**From corridor** R'_w (dB)			
		Sound class				Sound class			
		A	B	C	D	A	B	C	D
20a	Private work space or conversation space	40	35	35	-	35	30	30	-
20b	with moderate privacy	48	44	44	40	40[a]	35[a]	35[a]	30
20c	with high privacy	52	52	48	48	44	44	40	40
20d	Space for socializing such as break room or dining room	48	44	44	40	-	-	-	-
20e	Hygienic area or restroom	48	44	44	40	35	30	30	-
20f	Between hygienic area	35	35	-	-	-	-	-	-
20g	Space with other tenant	52	52	48	44	52	52	48	44
20h	Common stairwell/corridor with other tenant	52	48	44	35	35	35	30	-

[a] For construction with a large glass portion that gives a good amount of outside view, 5 dB lower values are accepted.

In Table 3.1, whether it is low or high step noise load is determined by the frequency of activity inside the room/space. Normalized step refers to adjusting the measured sound level differences from similar dwellings that use different sound absorbing material using the Sabine Equation, which was not discussed in this research. This research was performed without any specific demands regarding noise insulation, thus the minimum requirement for the noise insulation (class C) was considered to be sufficient for the CLT-concrete composite slab to achieve.

3.2 Market Availability

A market research was done to gather information and different alternative for CLT-concrete composite slab. Most of the information regarding the composite slab was found from either Austrian or German manufacturer, in which CLT production started from. It can be presumed that it is a big market there as there were several CLT-concrete composite slab manufacturers as well as shear connector manufacturers available. However, the product data obtained were fairly limited due to the unavailability of the detailed specifications of the floor product from some manufacturers. Table 3.3 shows the properties of the floor section found from the available market which fulfills the criteria mentioned in previous sections. The floor properties were taken from Xlam Concrete product, from Austrian based production company called MMK Holz-Beton-Fertigteile GmbH, and HBV-Balkendecke product from a German based company called TiComTec GmbH.

Table 3.3: Properties of CLT-concrete composite floor.

Properties	Product name				Units
	Xlam Concrete		HBV-Balkendecke		
Total height	240	280	240	250	mm
Concrete quality	C35/45	C35/45	C30/37	C30/37	-
Concrete thickness	100	120	80	110	mm
CLT quality	C24	C24	GL24h	GL24h	-
CLT thickness	140	160	160	140	mm
Maximum span	6.6	7.45	7.00	8.00	m
Variable load capacity	3.5	3.5	2.7	2.7	kN/m^2
Floor const. load capacity	1.0	1.0	1.5	1.5	kN/m^2
Self-weight	300	360	280	345	kg/m^2
Airborne noise insulation R'_w	-	64	56	58	dB
Impact noise insulation L'_{nw}	-	47	46	43	dB
Fundamental frequency f_1	-	-	7.05	7.00	Hz
Fire resistance	R60	R60	-	-	-

According to (TiComTec GmbH, 2017), glued-in steel connectors are commonly used for their timber-concrete composite system with a height of either 90, 105 or 120 mm and a length up to 1000 mm. Due to the limited scope of this research, the given products in Table 3.3 was assumed to also fulfill the vibration requirements that are mentioned in Section 3.1.2.

3.3 Floor Section Design

Based on the design requirements and product specifications found in the market, the chosen CLT-concrete composite floor section was Xlam Concrete with the height of 240 mm. The reason behind it was, it fulfilled all the criteria mentioned previously and considered to be the more economical option since less material is used. It can be seen in Table 3.3 that this product does not have the data for noise insulation properties, but it can be assumed that it is likely to have similar properties as the BHV-Balkendecke product with the same height. Furthermore, the Xlam Concrete has higher concrete thickness than the BHV-Balkendecke product which means it possibly has better noise insulation properties.

The thickness of concrete layer was 100 mm and CLT was 140 mm. According to CLT handbooks, a thickness of 140 mm can be produced with either three or five layers with many different arrangements of the panel thickness. In this research, five layers were used in accordance with the product drawings from Xlam Concrete, with the panel thickness of 20 mm and 40 mm for odd and even panels, respectively (Svenskt trä, 2017a). Glued-in steel connectors were used for the designed floor section with a height of 90 mm, in which 40 mm was glued inside the CLT and

50 mm was left to interlock with concrete when it was cured. The length of shear connectors was 1000 mm and they extended through the length of the slab. (Bathon, 2005) suggests that a span of 320 mm between shear connectors would be sufficient. The glued-in steel connectors would not hinder moisture transport in horizontal direction due to their mesh-shaped profile. Figure 3.3, 3.4, 3.5 gives the drawing of the designed floor section.

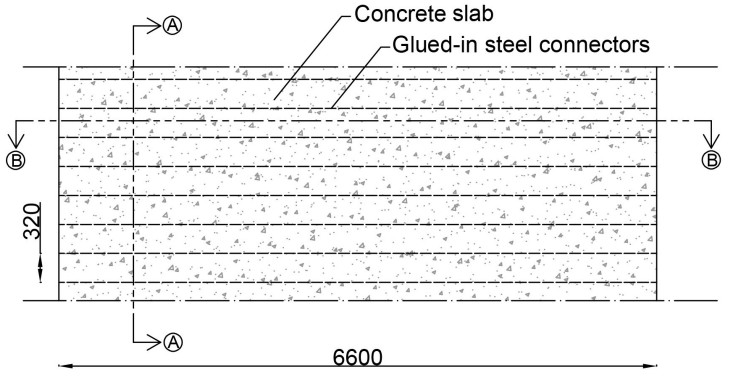

Figure 3.3: Top view of designed floor section (mm).

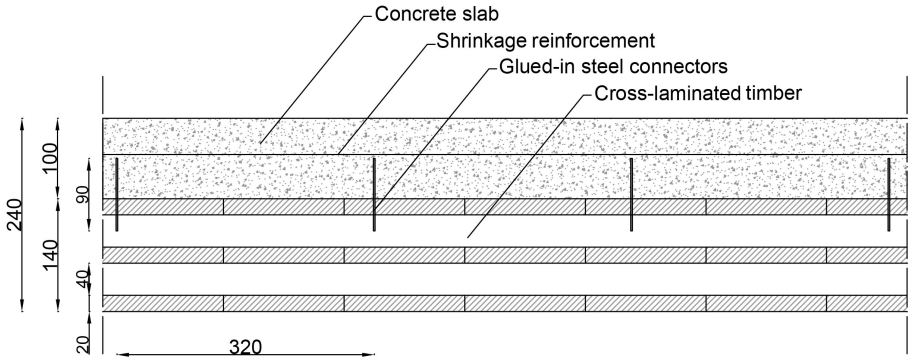

Figure 3.4: Cross section A-A of designed floor (mm).

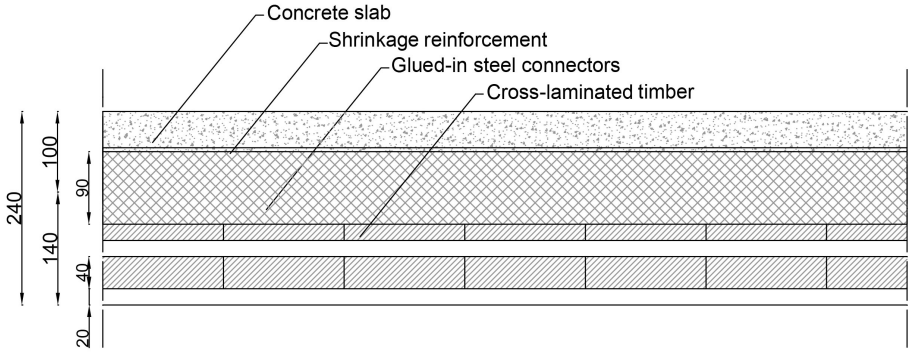

Figure 3.5: Cross section B-B of designed floor (mm).

3.4 Building Envelope Design

The building envelope was designed for the purpose of simulations in which the floor was at a joint connection with the exterior wall. The impact of outdoor conditions on the moisture behaviour of the floor was of interest to investigate. The aim is to have a typical wall design with thermal performance that fulfills Swedish standards. BBR 25 recommends U-value for a wall to be less than 0.18 W/m^{2}K. Due to the limited scope of this research, the wall design that fulfills BBR was taken from Träguidens proposal of exterior walls.

Figure 3.6 and Figure 3.7 below describes the cross-section of the exterior wall in connection with the designed floor. The total thickness of the exterior wall was 409 mm and it had a U-value of 0.15 W/m^{2}K, 41 dB sound insulation, and REI60 fire resistance classification (Svenskt Trä, 2017a). The chosen exterior wall met the regulation from BBR regarding the thermal performance.

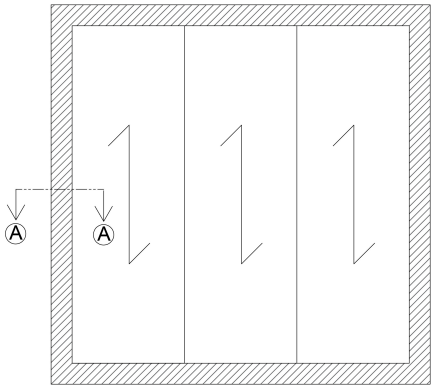

Figure 3.6: Top view of floor-wall section.

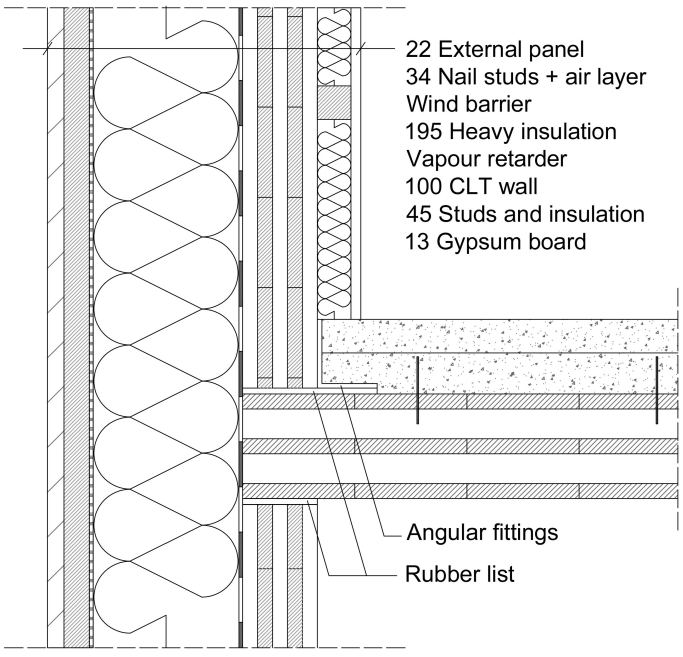

Figure 3.7: Cross section A-A of designed exterior wall (Svenskt Trä, 2017a).

4

Modelling and Methodology

4.1 Method

The simulation method used in this thesis was to model the hygrothermal behaviour between concrete and CLT with commercial software, WUFI 2D. The inner workings of the program is described in the report of (Künzel, 1995). The calculated temperature and relative humidity variations were studied, evaluated and compared between the variables. The results were further evaluated for risk of mould growth using the Finnish mould growth model. This section explains about the model framework of WUFI 2D and the Finnish mould growth model.

4.1.1 WUFI 2D

WUFI (Wärme- und Feuchtetransport Instationär) is a commercial program for transient heat and moisture transport calculations in constructions and building components. Transient calculation takes into consideration the temperature and moisture variation over time which gives a more realistic result, compared to steady state calculation which does not account for dynamic temperature and moisture change. WUFI was developed in Fraunhofer Institute for Building Physics in Germany. It includes a material database which was developed in cooperation with Lund University, Sweden, and other institutions. The program includes many different software versions, such as WUFI Pro, 2D, Plus and Passive. The software version used for this research was WUFI 2D version 3.3 and it gave the possibility to model the designed floor in two-dimension and calculate the moisture and temperature transfer for the building component. The following section explains the simulation steps through the different inputs in the software.

4.1.1.1 Geometry

This menu gives the possibility to draw the desired geometry of the building component in X and Y coordinates, as shown in Figure 4.1. The building component is limited to be drawn in shape of square or rectangle.

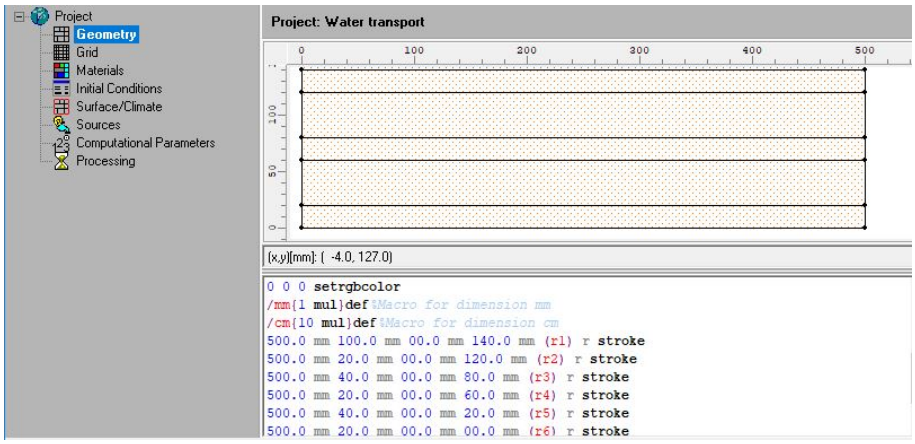

Figure 4.1: Geometry in WUFI 2D.

4.1.1.2 Grid

The grid density of the building component can be changed from the grid menu. The drawn components have different grid element size depending on the position of the element, as it can be seen in Figure 4.2. Elements near to the boundary layer have a smaller grid size than the ones in the middle. The program can automatically choose the grid size, but it is also possible to change the grid density in three different levels, which are fine, medium and coarse. Finer grid level gives more accuracy during the simulation with longer simulation time. If the required grid is different than the program's default options, it is possible to set the grid size manually in X and Y coordinates.

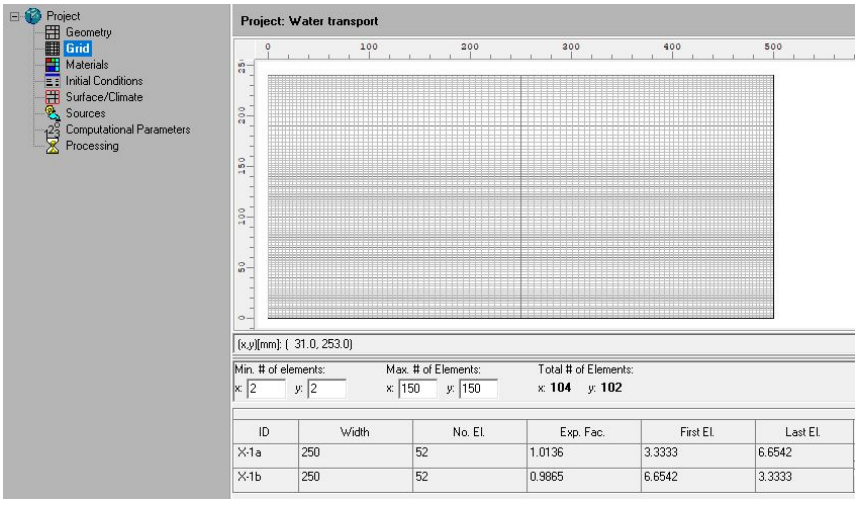

Figure 4.2: Grid size in WUFI 2D.

4.1.1.3 Material

The choice of materials can be done in this menu, see Figure 4.3. The program has different database sources with the largest from Fraunhofer-IBP. A Swedish material database from Lund University is also available in the program. It is also possible to manually define a database if the properties of the material are known.

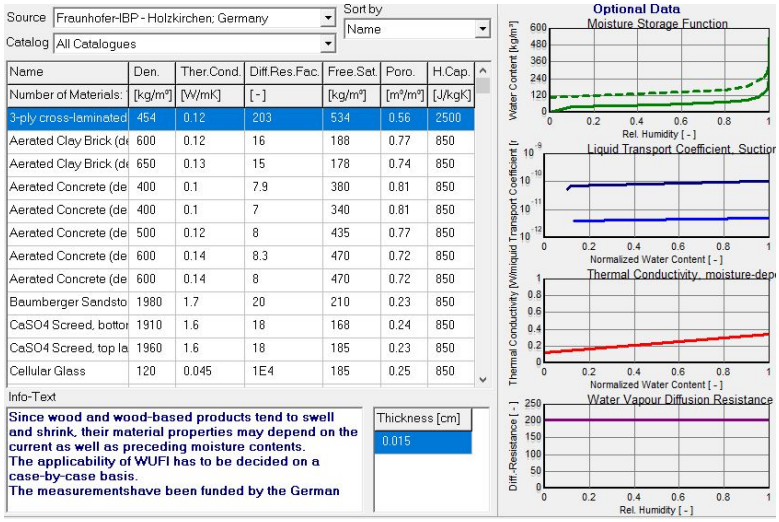

Figure 4.3: Materials in WUFI 2D.

4.1.1.4 Initial Condition

The simulation in the program begins with the initial condition for the materials regarding temperature and moisture content. The moisture content (W) increases as the RH increases, and RH of 1 indicates that the material is fully saturated. These conditions can be defined in this menu, see Figure 4.4.

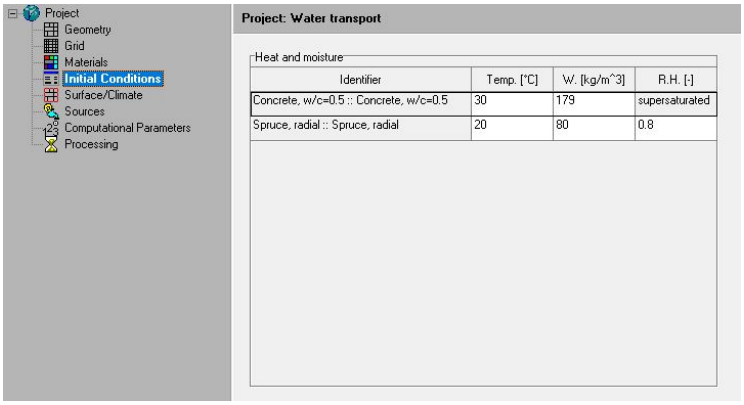

Figure 4.4: Initial condition in WUFI 2D.

4.1.1.5 Climate

With the help of this menu, the temperature and relative humidity of the boundary is defined for the material. It can either be set as outdoor or indoor climate, for example, Figure 4.5 shows the temperature and relative humidity of Gothenburg for a period of one year. The program has climate data for different cities in Europe and the climate data for the cities in Sweden are developed in cooperation with Lund University. For indoor climate, the temperature can be set with the moisture content derived from the current outdoor condition. Further in this dialogue box, the surface inclination and the exposure orientation can be defined so the program takes rain and solar radiation into consideration, as it can be seen in Figure 4.6.

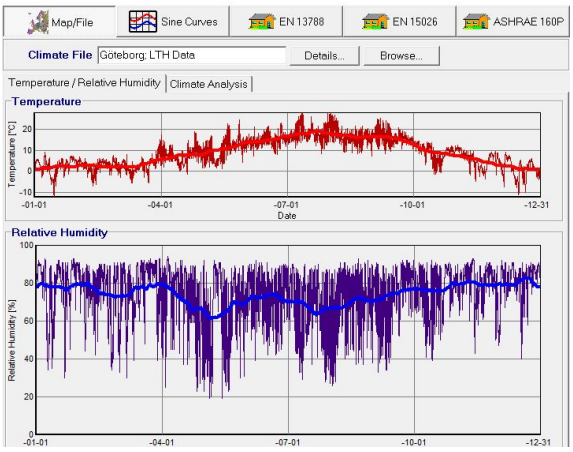

Figure 4.5: Gothenburg temperature and relative humidity in WUFI 2D.

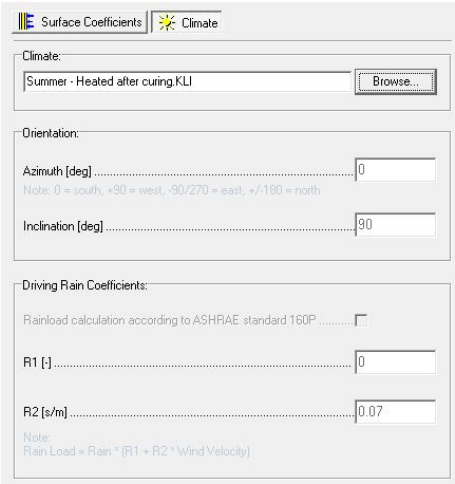

Figure 4.6: Climate menu in WUFI 2D.

4.1.1.6 Sources

In the sources menu, moisture, heat and air exchange source can be added to the material to simulate cases such as leakage, solar radiation or air gap circulation. Figure 4.7 shows an example for a heat source that is imported from a text file.

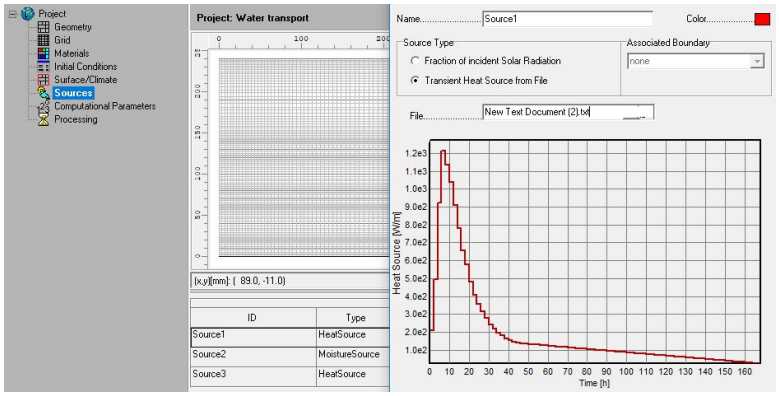

Figure 4.7: Heat source in WUFI 2D.

4.1.1.7 Computational Parameters

The start date, time and duration of the simulation are defined in this menu, shown in Figure 4.8. The default time step for the simulation in the program is one hour but this can be changed to the desired time step and interval. It is also possible to decide which result to show after the simulation. This information can be either water content, relative humidity, temperature, capillary transport, diffusion transport, vapour pressure or heat flux. If more information is desired to get along with a smaller time step, more time is required to do the simulation.

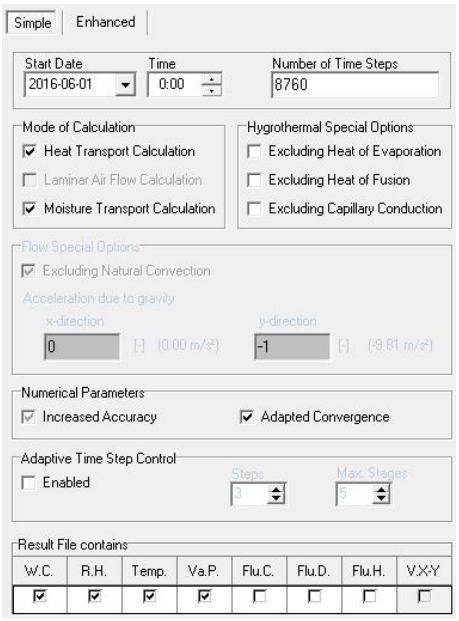

Figure 4.8: Computational parameters menu in WUFI 2D.

4.1.1.8 Limitation of WUFI 2D

Like many other programs, WUFI 2D could not simulate the given model perfectly as in reality. One of the factors for this research that the program has difficulties in is simulating fresh concrete. The program is fully capable to model hardened concrete, but not fresh concrete with regards to the hydration process that goes through it. Fresh concrete consume approximately half of its water during the hydration process, and the other half is dried out. However, the program neglects this water consumption during the hydration process and only simulate drying through moisture transport. This in turn, prolonged the drying process than in reality, which is why it was necessary to change the moisture transport properties of the concrete material to have a similar drying time as fresh concrete.

Another factor that the program does not take into account in its simulation is gravity force. This factor was relevant to the research as the wet concrete layer was located on top of the CLT layer. There was a potential liquid transport due to gravity as fresh concrete contains free water, and this water would gather on the lower part of concrete, causing a higher risk for moisture problem in the CLT.

However, this factor was considered to be less important to the research, as capillary suction is the dominant mechanism for liquid transport in wooden materials, with the assumption that there are no cracks in wood and no gaps between wood lamellas.

Lastly, the program lacks the capability in modelling non-porous materials such as steel. The program assumes that any given material is porous. Materials such as steel can still be modelled in the program by giving it a very low porosity and a very high vapour diffusion resistance, but it gives unreliable results in its simulation. Although, in the studied floor section, the steel shear connector does not play a significant role in the heat and moisture transport due to their mesh-shaped profile and small size percentage to the overall floor section. This had made the steel unnecessary to be modelled and this limitation of the program did not have an impact on the simulation.

4.1.2 Finnish Mould Growth Model

The Finnish mould growth model was developed by VTT Technical Research Centre of Finland and Tampere University of Technology (TUT). It is based on the original mould growth model, which is mentioned in Section 2.6.3. The collaboration between VTT and TUT resulted in a spreadsheet and a MATLAB script that can evaluate the risk for mould growth in a material from the hourly change of temperature and relative humidity for the investigated material. The model takes into consideration the different types of material, surface type, surface coating and their sensitivity towards mould, by defining mould sensitivity class and mould decline factor of the material in the model. The mould sensitivity class is divided into four categories, which are very sensitive, sensitive, medium resistant and resistant. The mould decline factor also consists of four classes, which are strong decline, significant decline, moderate decline and almost no decline. After determining the previous factors along with the temperature and relative humidity, the model calculates the mould index which varies between 0 to 6, explained in detail on Table 2.13. For a typical construction, an MGI of below 3 is considered as moisture safe.

4.2 Variables

The variables which were taken into consideration during the simulation process of the model are described in this section.

4.2.1 Water-Cement Ratio of Concrete

Higher water to cement (w/c) ratio results in a longer drying period. One of the most common w/c ratio used for a slab section is 0.4 as it has a relatively fast drying time with sufficient workability. Due to unavailability of a detailed research on the drying behavior of fresh concrete with 0.4 w/c ratio, the nearest w/c ratio were considered as an adequate substitute. The research found on concrete with

w/c ratio closest to 0.4 was from (Mjörnell, 2003), where the drying behavior of a 0.38 w/c ratio concrete was studied as mention in Section 2.4.2. The research also conducted experiment with 0.6 w/c ratio concrete, which was also used as a comparison between low and high w/c ratio in this study.

The material properties that were taken from the research of (Mjörnell, 2003) for both w/c ratios included the density, porosity, moisture storage function and vapour diffusion resistance factor. In order to get the moisture storage function, the moisture ratio curve from Mjörnell's research for the both materials were multiplied with their density. The vapour diffusion resistance factors were modified through trial and error, to simulate the drying performance of concrete with 0.38 and 0.6 w/c ratios used in the experiment mentioned in Section 2.4.2. This was done due to the limitation of the program in modelling fresh concrete stated in Section 4.1.1.8. All other material properties needed for the simulation were taken from the provided Fraunhofer-IBP material properties for concrete with w/c ratio of 0.5 in the program. The two experiment-based materials were also compared to the original 0.5 w/c ratio from Fraunhofer-IBP for a better understanding of the drying behaviour. The properties of these materials are shown in the following Table 4.1 and Figures 4.9 to 4.12. W38 and W60 are the experiment-based concrete with w/c ratio of 0.38 and 0.6, respectively. H50 is the concrete based on Fraunhofer-IBP with 0.5 w/c ratio.

Table 4.1: Concrete material properties used for the simulations.

Properties	**W38**	**W60**	**H50**	**Units**
Bulk density	2380	2323	2300	kg/m^3
Porosity	0.128	0.172	0.18	m^3/m^3
Specific heat capacity, dry	850	850	850	J/kgK

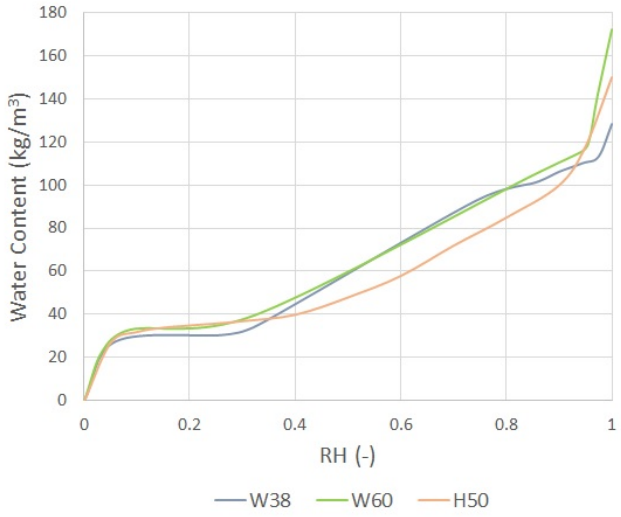

Figure 4.9: Moisture storage function of W38, W60 and H50 concrete.

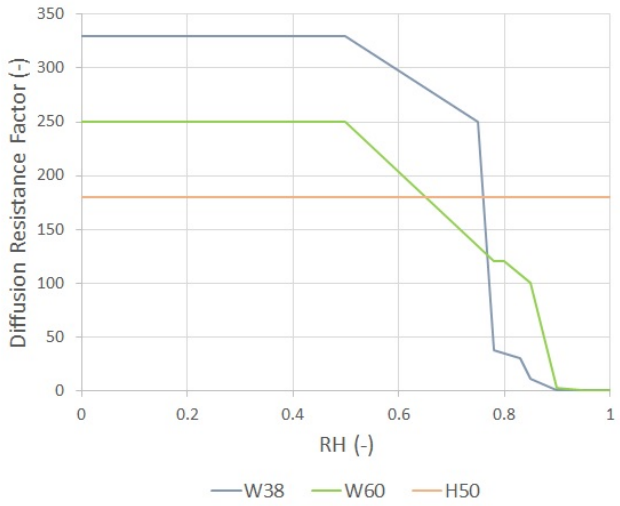

Figure 4.10: Vapour diffusion factor of W38, W60 and H50 concrete.

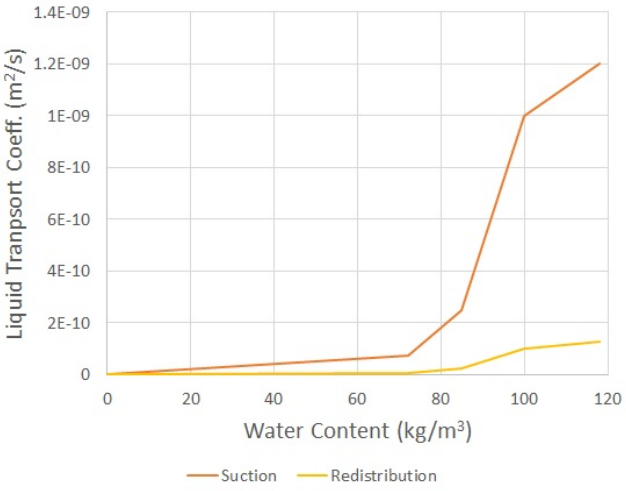

Figure 4.11: Liquid transport coefficient for W38, W60 and H50 concrete.

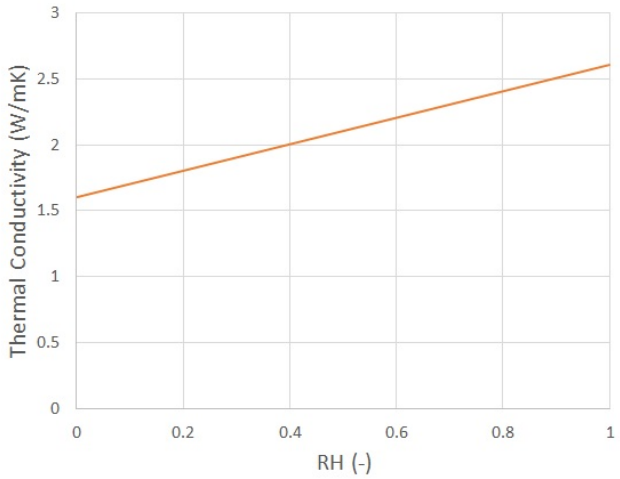

Figure 4.12: Thermal conductivity for W38, W60 and H50 concrete.

The drying performance comparison between the material used in this study and the material from Mjörnell's research can be seen in Figure 4.13. The drying climate condition and dimensions for the experiment-based materials were the same as in Mjörnell's research. It can be seen in the figure that curve W38 corresponded to curve 6 and curve W60 corresponded to curve 7. This verified the drying behavior of experiment-based materials with the behavior of fresh concrete.

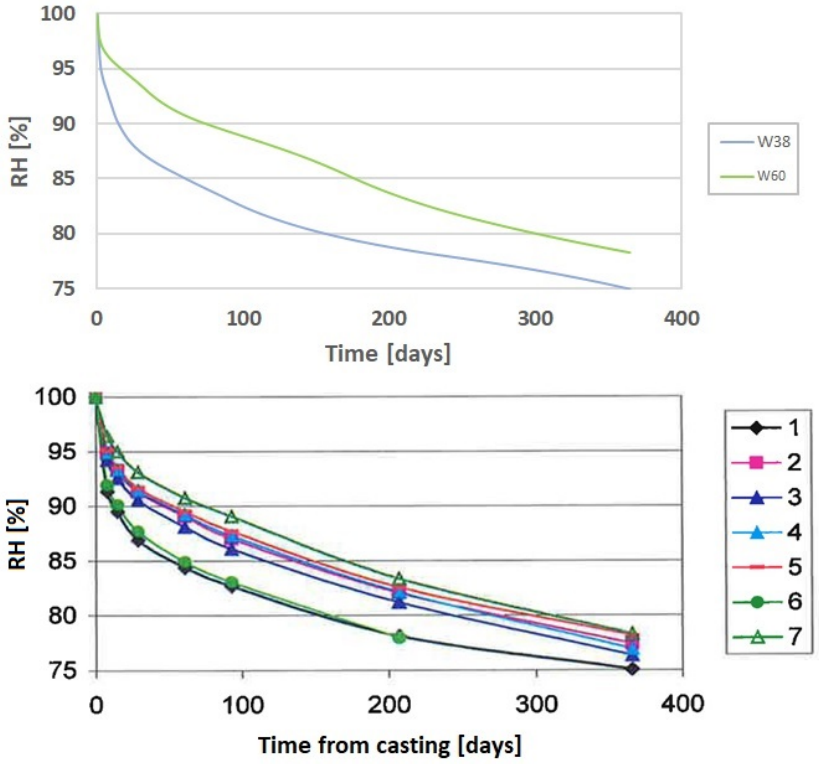

Figure 4.13: Drying performance comparison between experiment-based materials (top) and materials from Mjörnell's research (bottom). 6 = 0.38 w/c ratio; 7 = 0.6 w/c ratio.

4.2.2 Curing and Drying Conditions

The condition during curing and drying of fresh concrete has to be controlled to a certain temperature to achieve the targeted concrete quality and time of drying. This affects the temperature and relative humidity of CLT and has a potential impact on mould growth. The period of casting concrete also has an important influence on the drying time of fresh concrete. The temperature and relative humidity changes constantly depending on the seasons, which was why summer and winter conditions were taken into consideration in the simulations as the relative humidity and temperature vary the most between these two seasons. With these considerations, the climatic conditions used for the simulations were determined and shown in Table 4.2.

Table 4.2: Climate file used for simulations.

Name	Start Date	Curing T (°C) for the first 28 days	Drying T (°C) for the 29th day onward
Summer A	June 1st	Outdoor	Outdoor
Summer B	June 1st	13	Outdoor
Summer C	June 1st	13	23
Winter A	January 1st	Outdoor	Outdoor
Winter B	January 1st	13	Outdoor
Winter C	January 1st	13	23

Summer A and Winter A were used as a reference case where the slab was dried fully in Gothenburg's outdoor temperature and relative humidity conditions from start to finish, without the use of heaters. Summer B and Winter B had been set to a temperature of 13°C for the first 28 days. This followed the requirement for ideal concrete curing temperature mentioned on Section 2.4.1. Summer C and Winter C controlled both curing and drying condition, heated to 23°C from the 29th day onward, to simulate the concrete being heated at room temperature.

The relative humidity of all the B and C climate files were modified from extracting Gothenburg's outdoor climate data in the program. Heating or cooling has an impact on the relative humidity of air. It changes the air temperature, which consequently changes the saturation vapour content, but not the actual vapour content in the air. Based on Equation 2.1, a change of saturation vapour content (v_s) changes the relative humidity (RH) if the air vapour content (v) stays the same. With this, the relative humidity on Gothenburg's climate file had to be converted to accommodate the temperature changes from heating or cooling for the indoor heated climate files. This conversion was done with a simplification by rounding up the temperature to the nearest 1, as the difference of saturation vapour content between 0.1 and 0.9 °C is not significant. An example of this conversion is shown on Equation 4.1 with the example climate data shown on Table 4.3.

Table 4.3: Example of climate data conversion from outdoor condition to heated indoor condition.

Climate file	T (°C)	Rounded T (°C)	Saturation vapour content (g/m^3)	RH (%)
Gothenburg	4.2	4	6.37	85
Heated	13	13	11.35	RH_{13}

$$\begin{aligned} v &= RH_4 \cdot v_{s4} = \frac{85}{100} \cdot 6.37 = 5.4\ g/m^3 \\ RH_{13} &= \frac{v}{v_{s13}} \cdot 100 = \frac{5.4}{11.35} \cdot 100 = 47.55\ \% \end{aligned} \tag{4.1}$$

This conversion of Gothenburg's climate data was done for the whole year for every hour. With this conversion, climate data Summer C and Winter C had different relative humidity, even though the temperature is the same. The complete climate data can be seen in Appendix A.

4.2.3 Regional Climates

In addition to Gothenburg's climate condition, the regional climate for three other cities was simulated to see the mould growth activity across the areas in Sweden. The four cities chosen were Kiruna, Lund, Stockholm and Gothenburg, to represents the climate condition in the north, south, east coast and west coast, respectively, during summer and winter.

4.2.4 Initial Concrete Condition

The initial condition of concrete has a critical effect on moisture safety of timber. It takes several months for fresh concrete to dry to a certain relative humidity level which is considered to be safe regarding mould growth, while precast concrete is already hardened with lower relative humidity. A comparison between cast-in-situ and precast concrete was studied in order to be able to understand the risk for different initial conditions of concrete. Since the initial relative humidity of precast concrete varies depending on the desired delivered condition, different values for the initial relative humidity were chosen to be analyzed, which were 80%, 90%, 95% and 100%. Precast with a high relative humidity of 100% in this study was purely theoretical as it is unlikely to occur in constructions. The material properties for precast were taken directly from the program for hardened concrete with w/c ratio of 0.5 from the Fraunhofer-IBP material database, as discussed in Section 4.2.1.

4.2.5 Existence of Vapour Retarder

The main purpose of this research was to determine if casting fresh concrete directly on top of CLT floor would cause any moisture related problem in the timber. The addition of vapour retarder between the concrete and CLT may provide a better protection for the CLT, thus it was of interest to investigate this alternative. The location of vapour retarder can be seen in Figure 4.14.

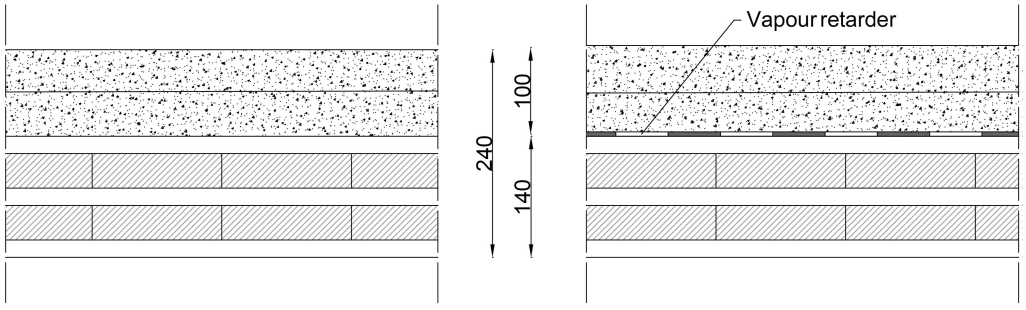

Figure 4.14: Floor drawings without and with vapour retarder.

The most common vapour retarders used for a construction have Sd values of lower than 10 m, therefore the vapour retarder used in the simulations had an Sd value of 10 m. It was also of interest to simulate using a vapour retarder with a higher Sd value (100 m) to study the influence of vapour retarders in the floor section. Sd value describes the thickness of stagnant air that has the equivalent vapour resistance as a certain material. For example, the resistance of a material with an Sd value of 10 m is equivalent to the resistance of 10 m of stagnant air.

4.2.6 Influence of Building Envelope

Other than floor details, the other type of section that are of interest to analyze in this research was a floor to wall connection detail. The influence of outdoor temperature and relative humidity through the building envelope can potentially affect the drying behaviour of the floor. Two types of floor to wall section were analyzed in this research. Both sectional details were the designed building envelope from Section 3.4, with one detail lacking a vapour retarder within the wall compared to the other.

4.3 Modelling Simplifications

Some simplifications had to be made to the floor section due to one of the limitation of the program. These simplifications were to remove the shear connectors and the shrinkage reinforcement and model it as plain timber and concrete as shown in Figure 4.15. As mentioned in Section 4.1.1.8, the program is unable to model non-porous materials, although the steel shear connectors in this floor section does not play a significant factor in the heat and moisture transfer, due to their mesh-shaped profile and small size percentage in comparison to the whole floor section.

From preliminary simulations with the inclusion of steel shear connectors, the results showed that the program did not perform well with the transition from the steel to the surrounding material. Regarding relative humidity, the addition of steel did not affect the results significantly, but temperature-wise it differed by some degree. The addition of steel had made the concrete and CLT around it slower in terms of temperature change and the closer the material was to the steel, the greater this effect was. At a point in the CLT located directly under the steel, it took around 26 days for it to change temperature from 20°C (initial temperature) to 13°C (curing temperature). In comparison, it took 8 days for the same temperature change in the same monitoring point for the simulation case without the added steel shear connectors. Therefore, it was decided to exclude the steel shear connectors in the simulation.

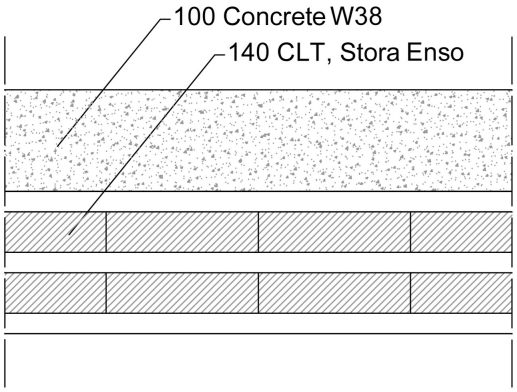

Figure 4.15: Simplified floor section for the simulations.

Simplifications were also made for the designed floor to wall connection in order to have a more time efficient model for the simulation. All of the steel parts were removed from the model for the same reasons explained previously. The external panel and nail studs were also removed from the wall to reduce the needed time for simulations. These were done simultaneously with removing exposure to driving rain and solar radiation from the outdoor climate. These simplifications were assumed to give the same result as a model that included cladding that is exposed to driving rain and solar radiation. The simplified wall connection can be seen in Figure 4.16. It could be noticed that the rubber list in Figure 3.7 are replaced with vapour retarders. This was due to the unavailability of a rubber material in the program. Vapour retarders were considered as an adequate substitute as it has similar properties to rubber with regards to moisture transport. Although vapour retarders have a higher thermal conductivity than rubber list, the overall contribution on the thermal behavior in the construction is neglectable due to its small thickness.

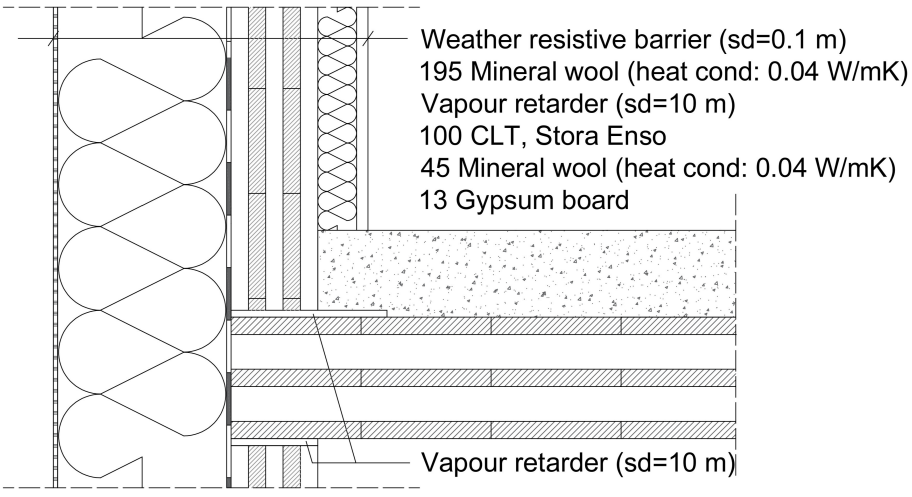

Figure 4.16: Simplified floor to wall section for the simulations.

4.4 Input Data for The Base Model

A description of the simulation steps for the base model is presented in this section. The base model referred to the simplest model made for the simulation, which included neither building envelope nor vapour retarder, concrete with 0.38 w/c ratio, saturated initial condition and Summer A drying condition.

4.4.1 Geometry and Grid

The CLT layer had a thickness of 140 mm with a length of 1000 mm and the concrete layer had a thickness of 100 mm with the same length. An example of the geometry is shown in Figure 4.17. The type of grid used for the models was coarse in Y direction and manually set to 1 in X direction. The number of elements in both materials in X and Y directions can be seen in Figure 4.18.

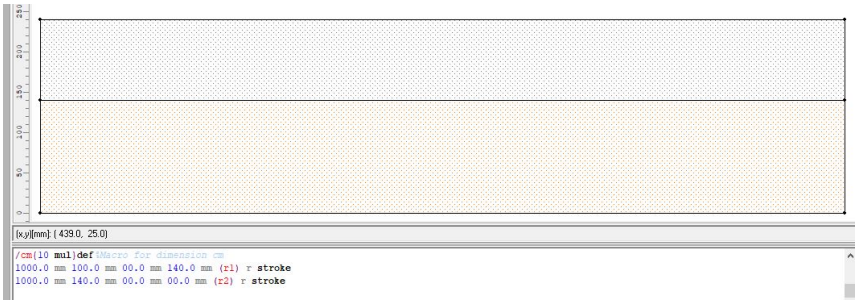

Figure 4.17: Geometry of the simulated models.

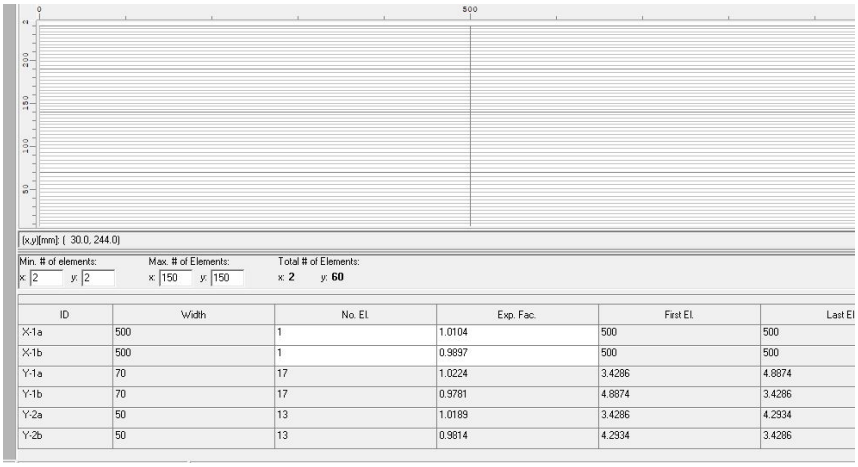

Figure 4.18: Grid of the simulated models.

4.4.2 Material Properties

The simulations material for CLT used the material properties provided by Stora Enso on their website (Stora Enso, 2013). The properties were tested by the Fraunhofer Institute and included in the material database of the program, which are

shown in Table 4.4 and Figure 4.19 to 4.22. As for concrete, the material used was W38 which was concrete with 0.38 w/c ratio discussed in Section 4.2.1.

It can be noticed that in Figure 4.21 the material has zero liquid transport coefficient. It was assumed that this was not measured by the material properties provider. However, liquid water transport was not a significant factor in this study as previous research had found that the glue layers in the CLT limits the movement of liquid, except for the top and bottom CLT layer where they are not covered by glue. Preliminary simulations were done with using plain spruce material from the Fraunhofer-IBP database as the top CLT layer and Stora Enso CLT for the other four layers. The results were not significantly different compared to simulation with Stora Enso CLT as the whole floor section. It can be assumed that this was due to the low liquid water transport coefficient of spruce in the tangential direction. For these reasons, the whole floor was modeled as Stora Enso CLT.

Table 4.4: CLT material properties used for the simulation.

Properties	**Stora Enso CLT**	**Units**
Bulk density	410	kg/m^3
Porosity	0.74	m^3/m^3
Specific heat capacity, dry	1300	J/kgK

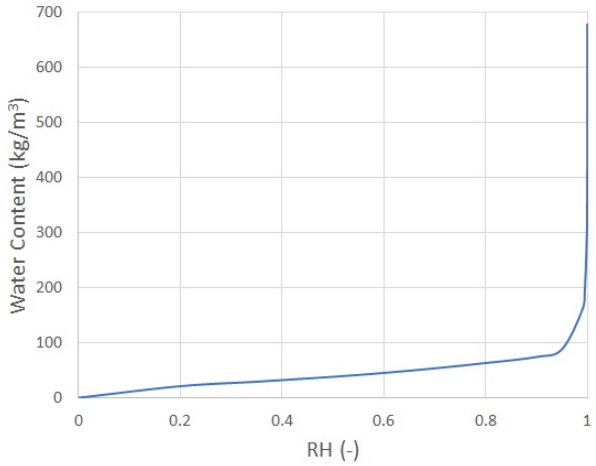

Figure 4.19: Moisture storage of Stora Enso CLT.

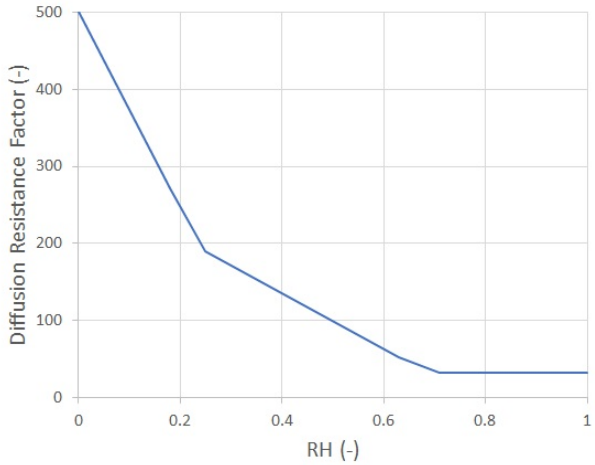

Figure 4.20: Vapour diffusion of Stora Enso CLT.

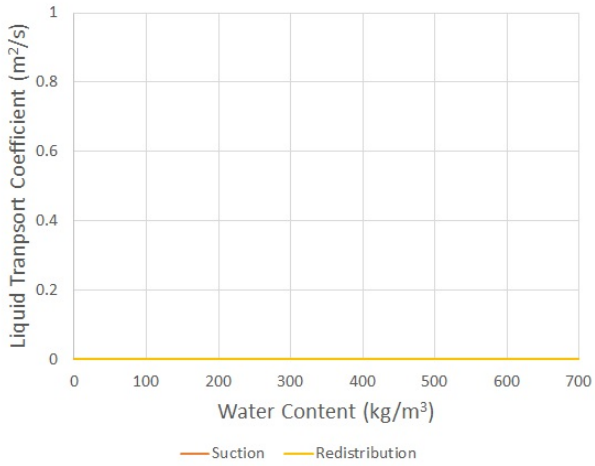

Figure 4.21: Liquid transport coefficient of Stora Enso CLT.

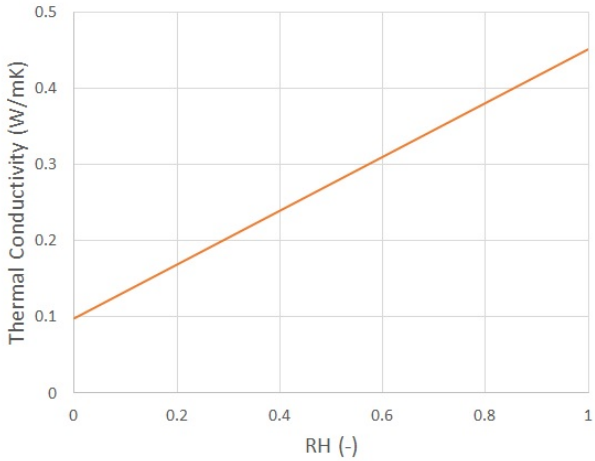

Figure 4.22: Thermal conductivity of Stora Enso CLT.

4.4.3 Initial Conditions

The initial temperature for concrete and CLT was assumed to be 20°C. The initial relative humidity for cast-in-situ concrete was 100%. The highest acceptable moisture ratio for the CLT at delivery is 16%, in which it was suitable to assume the initial relative humidity for CLT to be 80%. Figure 4.23 shows the initial temperature and relative humidity for CLT and cast-in-situ concrete.

Heat and moisture

Identifier	Temp. [°C]	W. [kg/m^3]	R.H. [-]
Concrete, w/c=0.38 SBUF Experiment :: Con	20	128	1
CLT - Stora Enso :: CLT - Stora Enso	20	63	0.8

Figure 4.23: Initial conditions of the simulated models.

4.4.4 Climate Data and Boundary Conditions

The climate file used in the simulations were discussed in Section 4.2.2. For the base model, the climate file used was Summer A, which was the default outdoor Gothenburg climate provided in the software. This climate file was set at the top and bottom surfaces, while the left and right boundaries of the model were set to adiabatic. The blue boundaries in Figure 4.24 are adiabatic and green boundaries are the Summer A climate file.

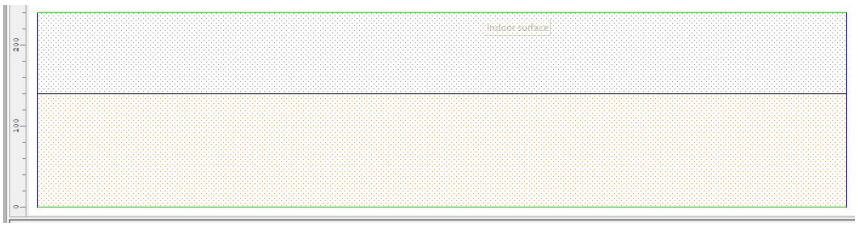

Figure 4.24: Boundary condition of the simulated models.

4.4.5 Heat Source

Casting freshly mixed concrete on top of CLT causes heat generation due to the hydration process of concrete, and this heat of hydration is modelled as a heat source in the program. The heat source data used in the model was the heat flow data provided by Sedaghat in his experiment, mentioned previously in section 2.4.4. The heat flow data was in mW/g unit and it had to be converted into applicable units for the software, which is in W/m. This was done by extracting the values of heat flow (Q) from Graph 2.14 and multiplying them with the cement content (w_{cement}), height (h_{concrete}) and width (b_{concrete}) of the modelled concrete floor. An example of this heat flow conversion at the 28^{th} hour can be seen in Equation 4.2 which gives the correct units (W/m) to be used for the modelling. Figure 4.25 shows the converted heat flow in a period of 168 hours. It can be observed that the heat flow started to decrease gradually after 48 hours until it converges towards zero by the end of the experiment.

$$
\begin{aligned}
\dot{Q_{28\text{h}}} &= Q_{28\text{h}} \cdot w_{\text{cement}} \cdot h_{\text{concrete}} \cdot b_{\text{floor}} \\
Q_{28\text{h}} &= 1\ mW/g \\
w_{\text{cement}} &= 360\ \cdot 10^3 g/m^3 \\
h_{\text{concrete}} &= 0.1\ m \\
b_{\text{concrete}} &= 1\ m \\
\dot{Q_{28\text{h}}} &= 36\ W/m
\end{aligned}
\tag{4.2}
$$

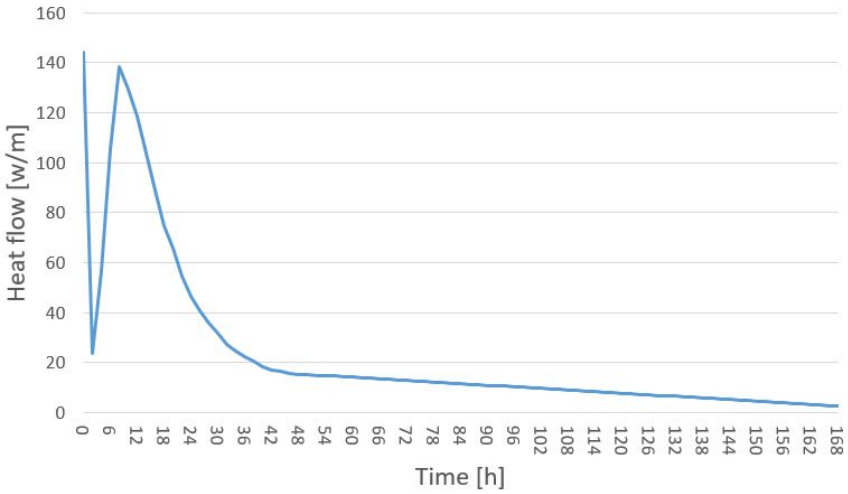

Figure 4.25: Converted heat flow of cement paste.

The duration of Sedaghat's experiment was one week, 168 hours, but the heat source data had to be inserted for one year in the software to avoid the cyclical effect of the heat source data. The heat flow data was extrapolated from 168 hours to one year period with the assumption that the heat flow decreases continuously towards zero. The red area in Figure 4.26 shows the generated heat source from concrete with the dimensions given in the figure.

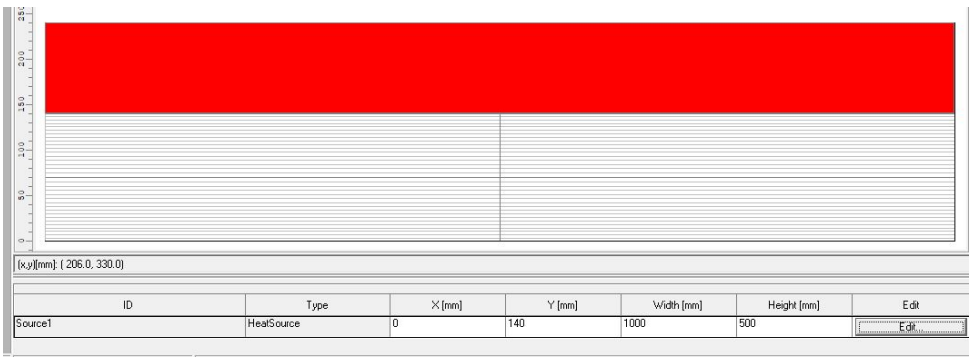

Figure 4.26: Heat source of the simulated models.

4.4.6 Computational Parameters

Figure 4.27 shows the computational parameters set for the simulation. Most of the settings were left to the default option. The model was set for 1 year (8760 hours) period of simulation. This was due to the fact that the experiment-based materials were made to mimic the drying behaviour of fresh concrete based on a 1-year experiment explained in Section 4.2.1. Any simulation beyond that point would be invalid as the behaviour of concrete was unknown. Moreover, in reality, the building could soon be used after the floor dries. By that point in time, the indoor climate condition is no longer the same as during curing or drying, which is why it was not reasonable to simulate for longer periods.

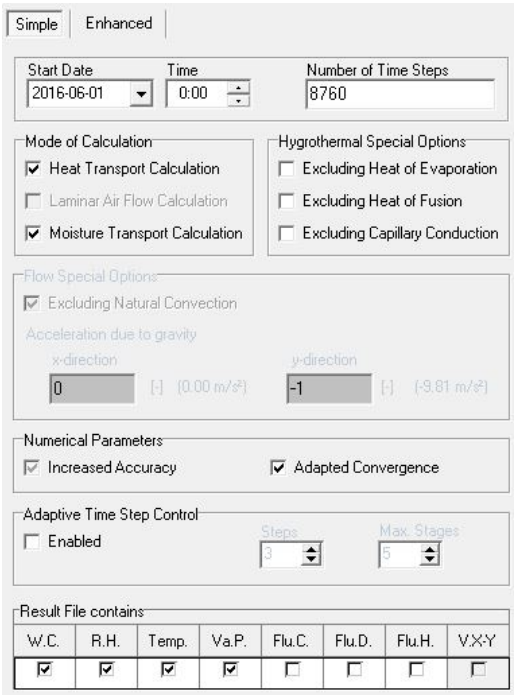

Figure 4.27: Computational parameters of the simulated models.

4.5 Finnish Mould Growth Model MATLAB Script

The mould growth model has different sensitivity classes and mould decline factors depending on the material, as mentioned in Section 4.1.2. These determines the inclination and declination rate of mould growth, as well as the maximum mould growth index possible. Inorganic material such as glass is defined as resistant in the sensitivity class and considered to have a strong decline in the mould decline factors. For planed or shaved wood, the mould sensitivity class is sensitive and the mould decline factor is moderate decline. Along with these classifications, the hourly temperature and relative humidity results from the model is processed to show a mould growth index graph using the mould growth model MATLAB script.

5

Results and Discussion

In this Chapter, the results from WUFI 2D and the Finnish mould growth model are presented and followed by discussions. The monitoring points of the simulations for each variable are shown in Figure 5.1. Point F1 was used to compare the drying behavior between the experiment-based fresh concrete and the default hardened concrete from the software. The highest MGI was suspected to be in the top CLT layer (F2) where the CLT met the wet concrete. If that monitoring point showed mould growth, it was important to also check the moisture condition on the second CLT layer which was point F3. Point F4 was the farthest from the concrete, if that point showed any signs of mould growth, then every other point in the CLT would be subjected to mould growth as well.

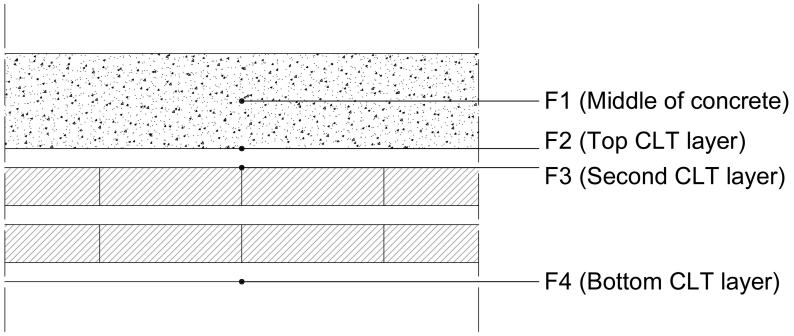

Figure 5.1: Monitoring point of the floor simulations

For simulation cases with the addition of building envelope, the monitoring points are described in Figure 5.2. Point BE3 should have a similar behavior to point F2 due to its location, which was relatively far from the building envelope. Point BE2 was a joint connection which has a high moisture transport rate and therefore it was of interest to show the MGI for this point. Point BE1 was used to check the moisture safety of the CLT wall that was in contact with the fresh concrete.

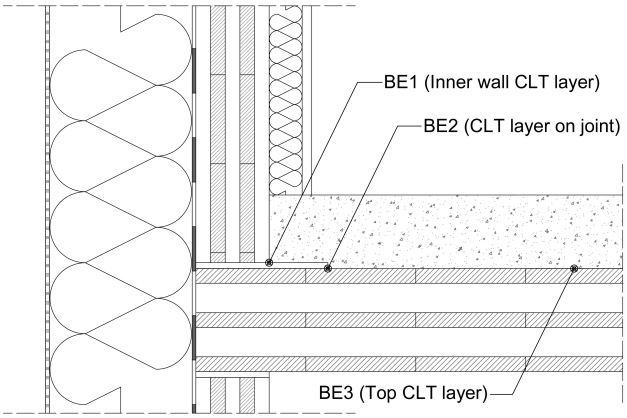

Figure 5.2: Monitoring point of the floor to wall simulations

5.1 Base Model

Figure 5.3 shows the relative humidity decline of air at point F1 (middle of the concrete). The concrete in the base model needed approximately 4 months to reach a relative humidity of 82%. It can also be noticed that the relative humidity started to follow the outdoor relative humidity after reaching 82%. The reason behind this behaviour was that the vapour diffusion resistance factor of W38 concrete was very low at high relative humidity with the modification, which made it very vapour open in humidity range of above 80%. This made the material easily influenced by the outdoor conditions.

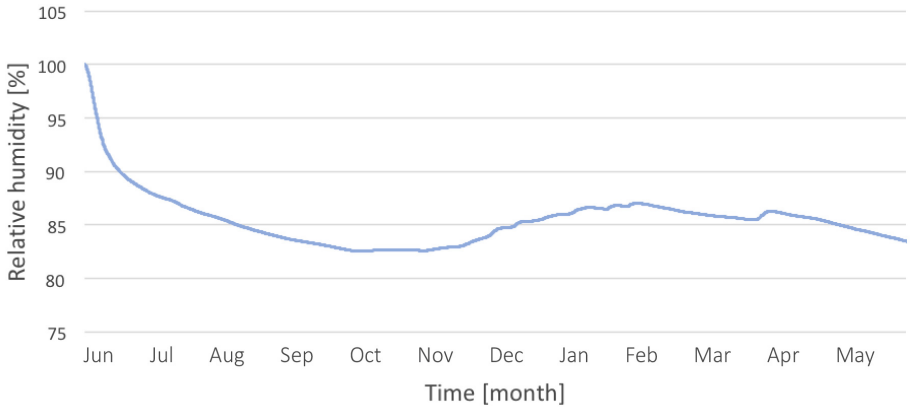

Figure 5.3: Relative humidity for W38 at point F1.

Figure 5.4 shows the mould growth index (MGI) at points F2, F3 and F4 for the base model. The results showed that the highest MGI at the investigated points were at point F2 and it had an MGI of slightly above 1.2. All the examined points, including F2, had MGIs of much lower than 3, thus they were considered to be moisture safe as the risk for mould growth were below the safety limit.

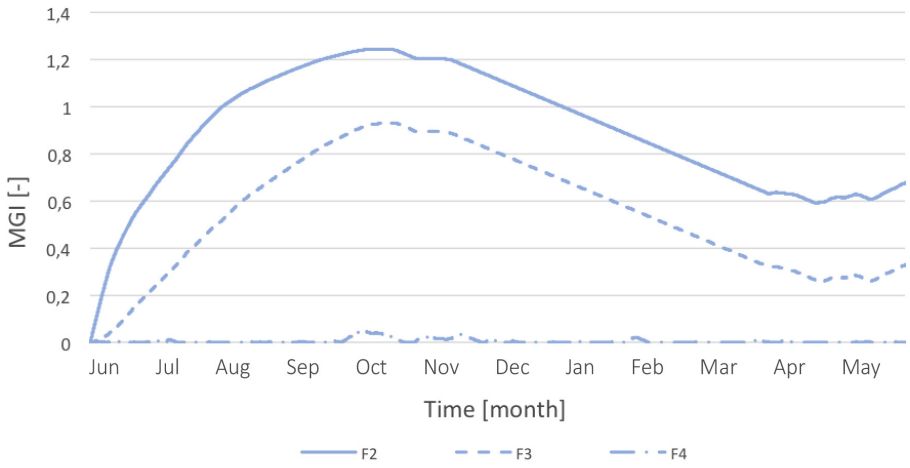

Figure 5.4: MGI at different points for the base model.

5.2 Water-Cement Ratio of Concrete

Figure 5.5 shows the relative humidity of the air inside the drying concrete located at point F1 with different w/c ratios. The climate data used for the simulations was Summer A, in accordance with the base model. The properties of W38 and W60 were based on (Mjörnell, 2003), which reflected the drying behaviour of fresh concrete with w/c ratios of 0.38 and 0.6 respectively. H50 was taken from the Fraunhofer-IBP material database which reflected the behaviour of hardened concrete with w/c ratio of 0.5. The results showed that the relative humidity of H50 was still above 90% after one year, while W38 and W60 reached 90% in approximately 16 and 54 days, respectively.

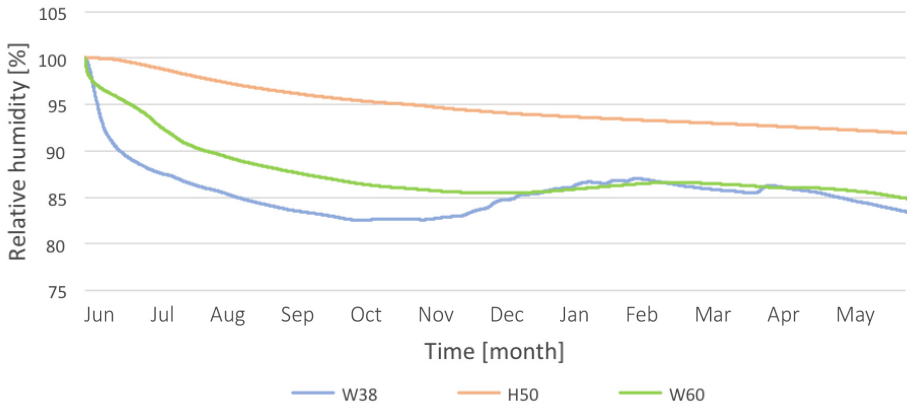

Figure 5.5: Relative humidity decline at point F1.

It can be observed that the W38 curve started to follow the outdoor relative humidity after 5 months and the same applies to the W60 curve, but in a smaller scale. The reason behind this behaviour was the low vapour diffusion resistance factor at high relative humidity as mentioned in Section 5.1. The vapour diffusion

resistance factor of the H50 curve was constantly high, which made the decline of relative humidity less rapid than the other two materials and took a longer time to dry.

In reality, the relative humidity decline of fresh concrete should be somewhere in between the drying behaviour of hardened concrete and fresh concrete shown in Figure 5.5. Fresh concrete gradually hardens and less water is consumed along the hydration process of cement over the course of its drying period. Evaporation and vapour diffusion govern the drying mechanism of the concrete afterwards. This means that the initial relative humidity decline of fresh concrete should look similar to W38 or W60, where all three drying mechanism works to its fullest simultaneously. The rate of cement hydration slows down as concrete hardens, and evaporation as well as vapour diffusion dominates the drying process. At this stage, the concrete should have a similar relative humidity decline to H50 where the variation is less volatile. This indicates that the resulting MGI for fresh concrete in reality could also be between the experiment-based material (W38 and W60) and the default hardened concrete (H50) discussed in the following sections.

5.3 Curing and Drying Conditions

Figures 5.6 and 5.7 show mould growth index at point F2 (top CLT layer) for W38 and W60, respectively. The simulations were done for the 6 climate files which were described previously. Results for both w/c ratios showed that the Summer A climate file gave the highest MGI, although there were still below 3 in both cases which meant that the CLT was moisture safe. The MGI for Summer C started to decline rapidly after approximately half a year for W38, while the mould index for W60 with the same climate file declined constantly after approximately 8 months. This was reasonable with the assumption that heating would help with drying of concrete and lowered the relative humidity in the CLT. Winter B and Winter C gave worse initial performance than Winter A, as the use of heater gave a more suitable temperature for mould growth during the initial winter period.

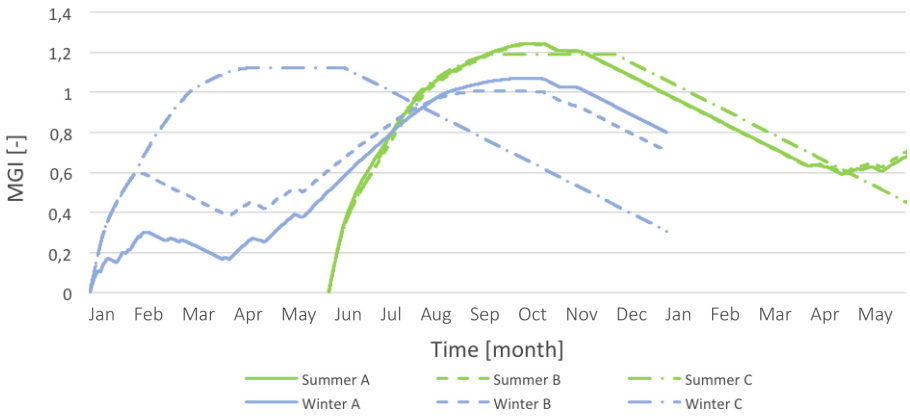

Figure 5.6: MGI at point F2 for W38 concrete.

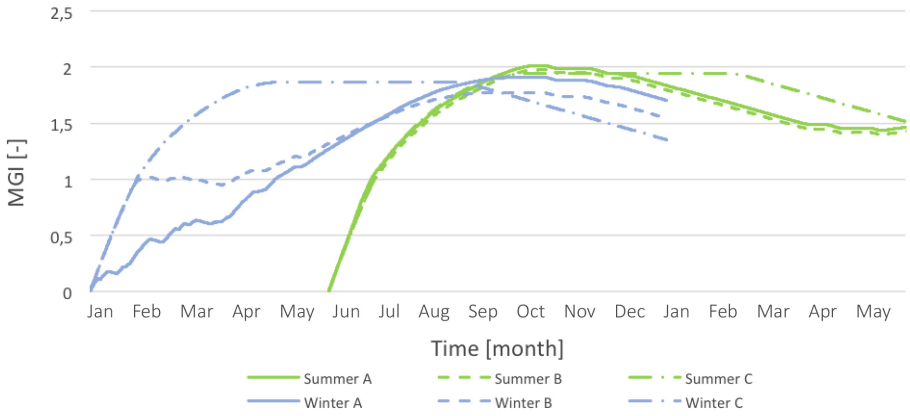

Figure 5.7: MGI at point F2 for W60 concrete.

For all climate files, the MGI started to incline as it reached summer as it provided suitable temperatures for mould growth. Afterwards, as the temperature fell during winter, the MGI decreased as well, even though the outdoor relative humidity were higher during the winter period. It can also be observed that the MGI at winter climate for W38 declined for a short period (between February and April) and inclined afterwards as the summer approached. The reasoning was that within the same winter season, with the same temperature range, the relative humidity in CLT started to decrease as the concrete dried. However, this was not the case for W60 as it contained more water which needed longer time to dry and decrease the relative humidity significantly in the CLT.

Figure 5.8 shows the MGI for 6 climate files at point F2 for H50 concrete. It can be noticed in the figure that the MGI were relatively high for all the climate files as they reached 3.5 in around half a year. An MGI of 3.5 means that new spores are produced and mould cover approximately 30% of the surface. The MGI showed similar behaviour to the previous w/c ratios, as the mould growth index increased during summer. However, the winter climate had the highest MGI in this case, instead of summer. The reason was that an initial mould growth had already existed for winter climate when it reached summer time, in which it gave a better chance for higher MGI than if it started from zero, which was the case for the summer climate. Although the same phenomenon occurred for W38 and W60 when they reached summer, the winter climate did not give the highest MGI because the materials were more vapour open, which made the relative humidity in materials low when summer time approached. This can be confirmed by following the relative humidity variation in Figure 5.9. W38 and W60 reached their maximum relative humidity in a period of 12 days, while H50 needed 82 days to reach its maximum relative humidity. Maximum relative humidity for W38, W60 and H50 were 95.9%, 96.4% and 95.7%, respectively. At the start of summer time (June) the relative humidity of W38 and W60 had already declined to 85.2% and 88.3% respectively, while H50 still had a high relative humidity of 94.7%.

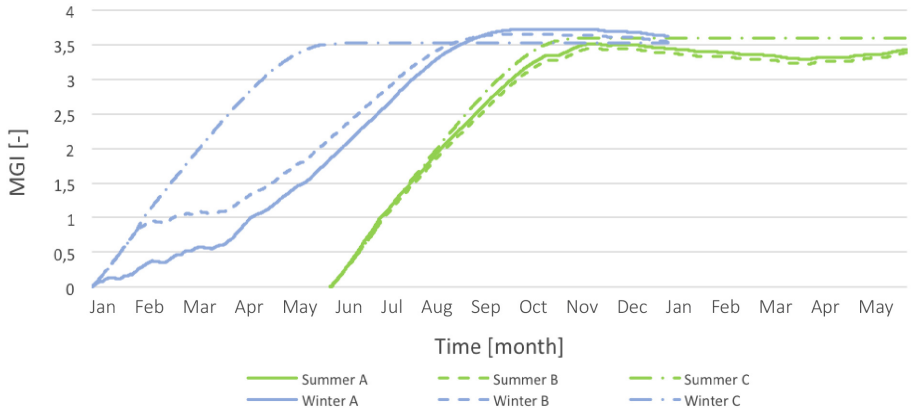

Figure 5.8: MGI at point F2 for H50 concrete.

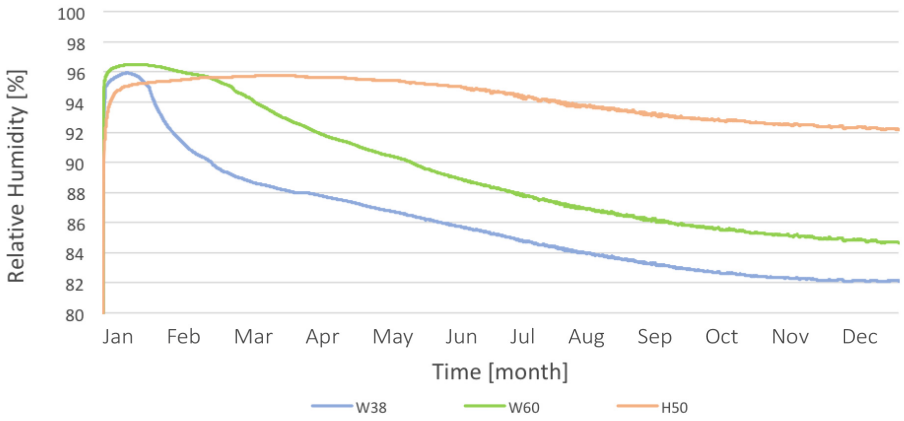

Figure 5.9: Relative humidity decline at point F2 with Winter A.

As mentioned in Section 2.4.5, concrete is a highly alkaline material and it could compromise the adhesive's bonding system and affect the rate of mould growth as mould needs a suitable pH range to grow rapidly. However, the results showed that the relative humidity at point F2 did not reach 100% for both the fresh and hardened concrete, which meant that there would not be any liquid water transport in the CLT, only vapour transport. Therefore, the effect of pH on both the CLT and the adhesive was considered to be negligible because pH transfers through liquids, but not through vapours.

The results for the different w/c ratios also showed large variations of mould growth index. This was due to the difference of nature between fresh and hardened concrete. All of the previous results showed that outdoor Gothenburg condition (Winter A and Summer A) gave the worst performance for the construction with regards to mould growth. The use of heating in climate files B and C had hindered mould growth activity to some extent. Therefore, the climate file used for further analysis was Summer A which gave the worst result for the experiment-based materials, unless it was stated otherwise.

The simulation results with the Summer A climate data were further analyzed at points F2, F3 and F4 of the CLT, which can be seen in Figure 5.10. The results showed that at point F4 for all w/c ratios was moisture safe and had an MGI of nearly zero. Point F3 for W38, W60 and H50 were also moisture safe, although the

MGI of the hardened concrete seemed to be increasing at the end of the first year. In all cases, the MGI at point F3 was lower than F2, which was expected.

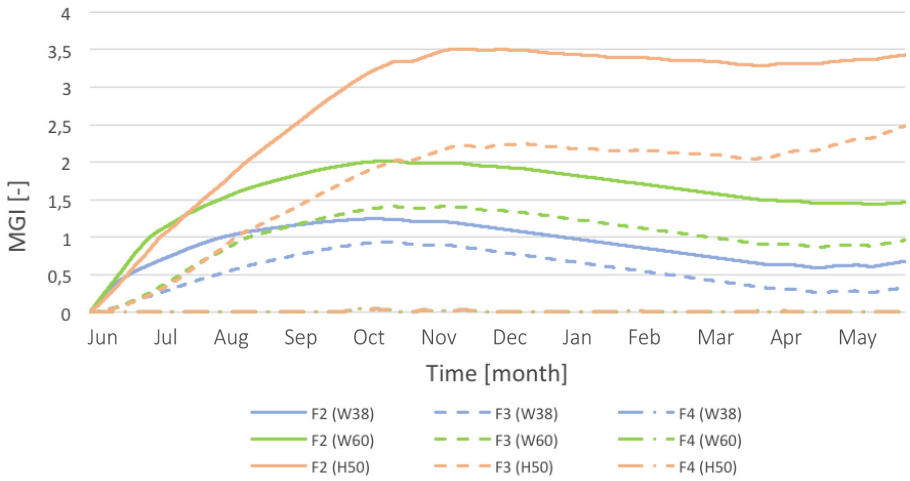

Figure 5.10: MGI at different CLT layers for different w/c ratios.

5.4 Regional Climates

Figures 5.11, 5.12 and 5.13 show the MGI at point F2 of the CLT at different regional climates. The climate file used was each region's summer and winter outdoor conditions. The results showed that the more south the location was, the higher risk of mould growth there was in the construction. The combination of temperature and relative humidity of each region was the reason behind these results. Kiruna showed the lowest MGI as it had the lowest temperature, which was not suitable for mould growth. Stockholm had the highest relative humidity out of all regions but the temperature was lower and less suitable than Gothenburg or Lund, hence it showed less MGI. Gothenburg and Lund had a similar temperature through the year, but Lund had a higher relative humidity, which is why the mould growth index was the highest.

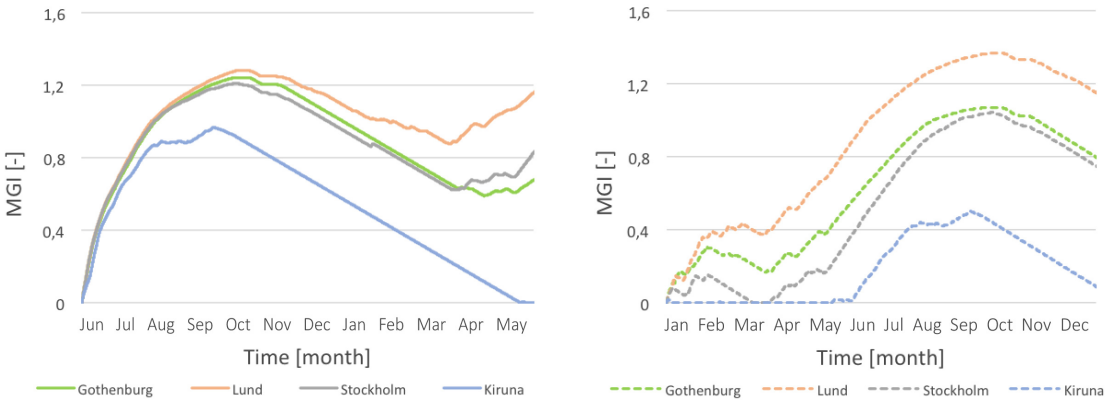

(a) Summer **(b)** Winter

Figure 5.11: MGI at point F2 for W38 concrete in different regions.

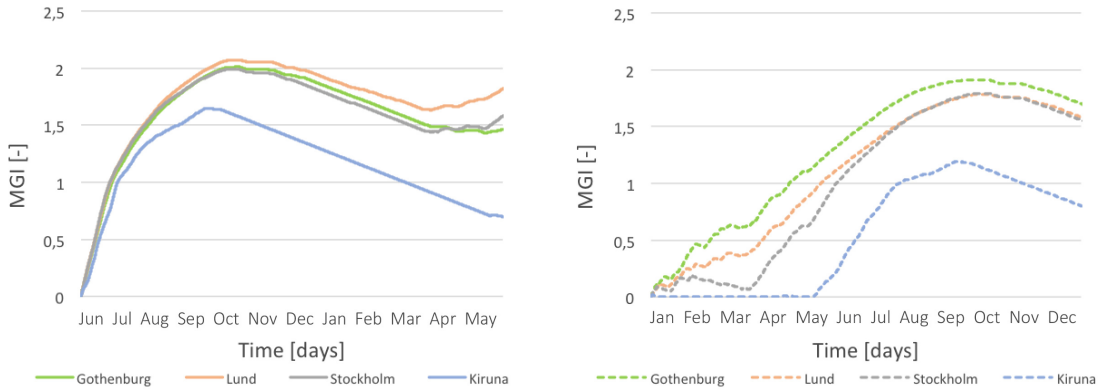

(a) Summer **(b)** Winter

Figure 5.12: MGI at point F2 for W60 concrete in different regions.

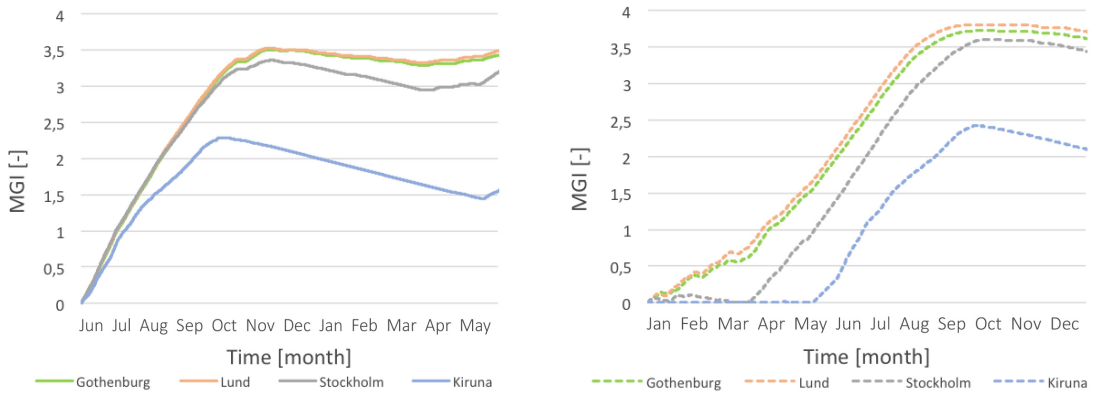

(a) Summer **(b)** Winter

Figure 5.13: MGI at point F2 for H50 concrete in different regions.

5.5 Initial Concrete Condition

Figure 5.14 shows the mould growth index at point F2 for H50 concrete with different initial relative humidity. This simulates the use of precast concrete as an alternative of fresh concrete in the composite floor. The lowest chosen relative humidity for the precast concrete in this research was 80%, and with that level of concrete humidity, there was no risk of mould located in all layers. Concrete with relative humidity of 90% and 95% were also tested and compared with the previous result using 100% relative humidity condition. The MGI shows that the construction was moisture safe for up to 95% RH, resulting in a maximum MGI of less than 2. All the results with different initial relative humidity showed that the MGI started to incline by the end of the simulation period. This is due to higher temperature during summer which increase the MGI.

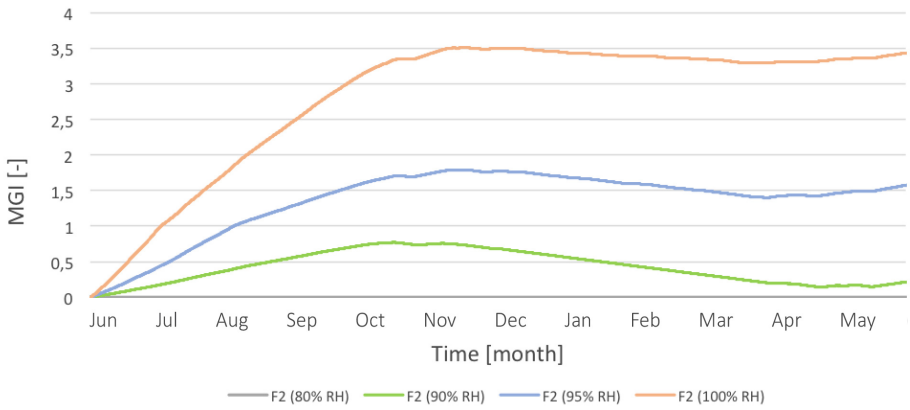

Figure 5.14: MGI at point F2 for H50 concrete with different initial RH.

5.6 Existence of Vapour Retarder

Figure 5.15 shows the MGI at point F2 with concrete W38, W60 and H50. The simulations were done with the addition of vapour retarder with Sd values of 10 m and 100 m. The results were compared thereafter with the case without a vapour retarder. The results showed that the vapour retarder could reduce the mould growth index significantly, negating the risk of mould growth. H50 concrete, which constantly showed the worst performance out of all water-cement ratios was greatly improved with the added vapour retarder. The MGI were below 0.5 for both vapour retarder with Sd 10 m and 100 m and the higher the Sd value, the lower was the mould index.

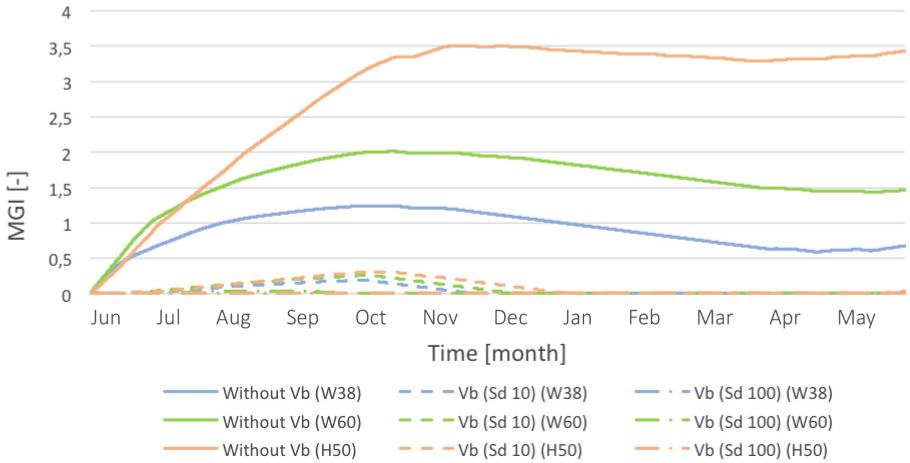

Figure 5.15: MGI at point F2 for different w/c ratios and vapour retarder properties (Vr).

5.7 Influence of Building Envelope

Figures 5.16, 5.17 and 5.18, show the mould growth index at points BE1, BE2, BE3 and F2 for concrete W38, W60 and H50 with the influence of building envelope. The previous results of the model without building envelope are also shown for comparisons. The climate file used at the exterior part of the building envelope was Summer A, and Summer C was used for the interior side, which was the wall, and top and bottom side of the floor. The reasoning for this was, with the use of heater on the summer C climate file and with no added indoor moisture load from people and people related activities, the relative humidity is much lower than the outdoor condition. With this difference of relative humidity, it would trigger the movement of moisture from higher outdoor humidity to lower indoor humidity, which was of interest to see compared to having the same climate condition over all boundaries.

The results showed that by comparing the MGI at point BE3 and F2, the presence of wall would not make any noticeable difference regarding MGI in the top CLT layer. However, at point BE2 near the joint had a lower MGI than BE3. This could be due to the existence of rubber in the joint which acted as a vapour retarder and reduced the relative humidity in that area of the construction. The MGI at point BE1 was relatively similar to BE3 as both are fully exposed to the wet concrete. It was also noticeable that the mould growth index in BE1 started to decrease sooner than BE3 and this could be because of the difference of surface area between the CLT floor and the CLT wall that were exposed to the concrete. The CLT wall had a lower surface area that was in contact with the wet concrete than the CLT floor, which made the relative humidity on point BE1 decline faster and had lower MGI as it can spread the moisture to the other parts of the wall that is not in direct contact with concrete.

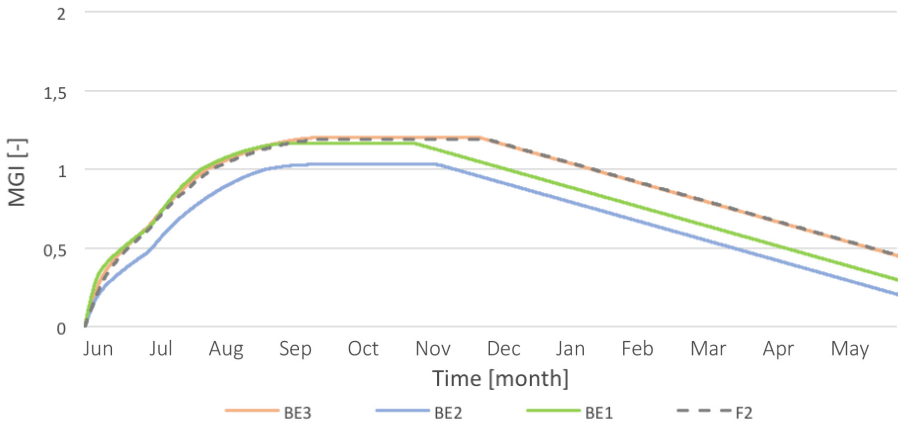

Figure 5.16: MGI at different monitoring points for W38 concrete with influence of building envelope.

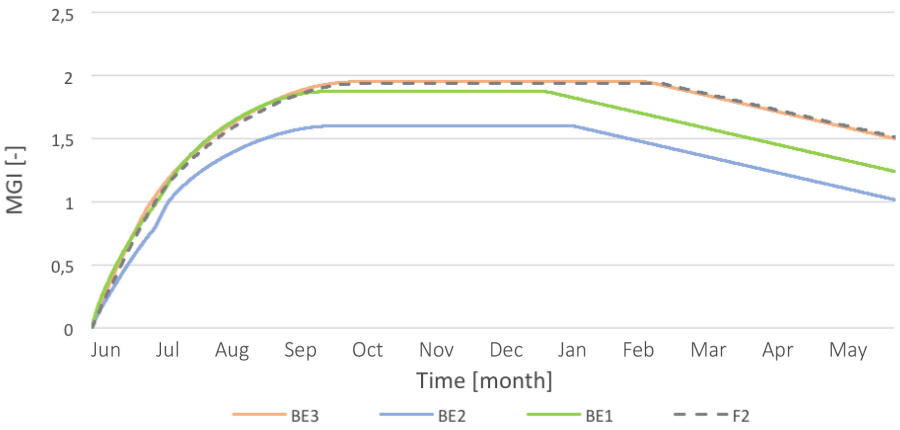

Figure 5.17: MGI at different monitoring points for W60 concrete with influence of building envelope.

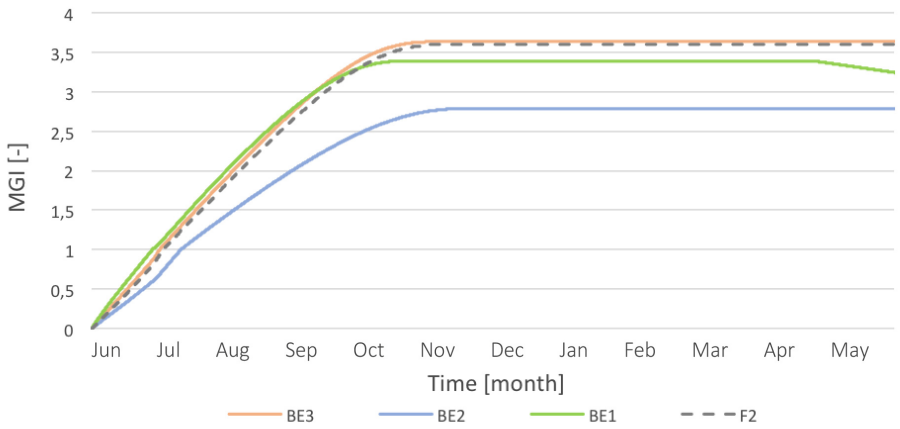

Figure 5.18: MGI at different monitoring points for H50 concrete with influence of building envelope.

Figures 5.19, 5.20 and 5.21 show a comparison of mould growth with and without the presence of vapour retarder in the wall, at the same monitoring points. It was of interest to remove the vapour retarder from the wall structure to enable moisture movements between the concrete and the outdoor climate through the wall. For point BE3, the results showed that the mould growth was not affected by the removal of the vapour retarder as the monitoring point was located relatively far from the wall. For point BE2, the change had an effect on the MGI where it declined faster by a small amount. Meanwhile, the resulting MGI in point BE1 declined faster without vapour retarder in the wall. The absence of vapour retarder had helped the structure that was close to the wall to dry out faster through moisture movement towards the outdoor. Moisture moves from high humidity to low humidity, and the floor construction had the highest humidity of all from the saturated fresh concrete. Removing the vapour retarder had helped the structure to dry towards both vertical and horizontal direction.

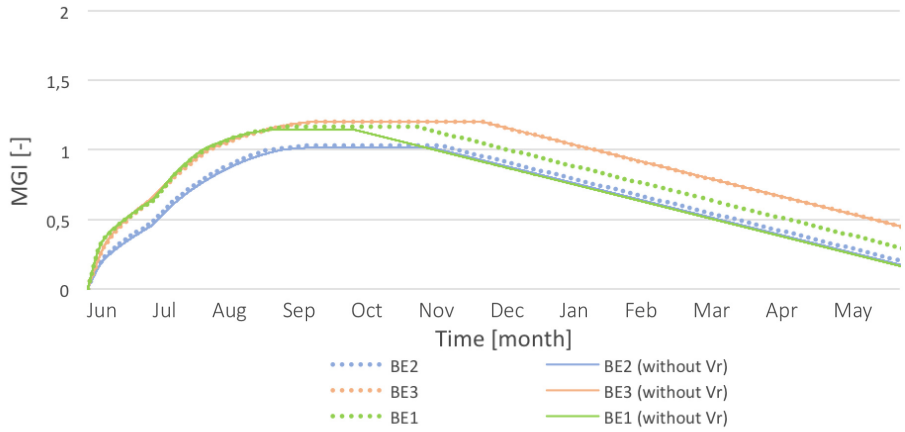

Figure 5.19: MGI at different monitoring points for W38 concrete with and without vapour retarder in the wall.

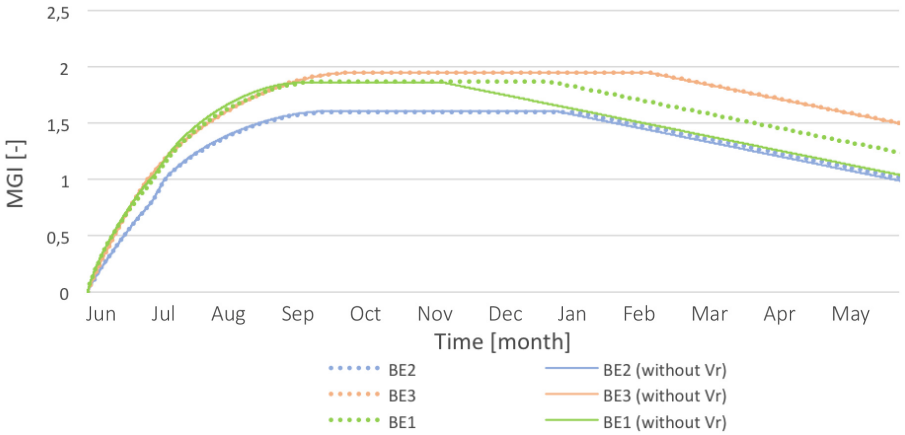

Figure 5.20: MGI at different monitoring points for W60 concrete with and without vapour retarder in the wall.

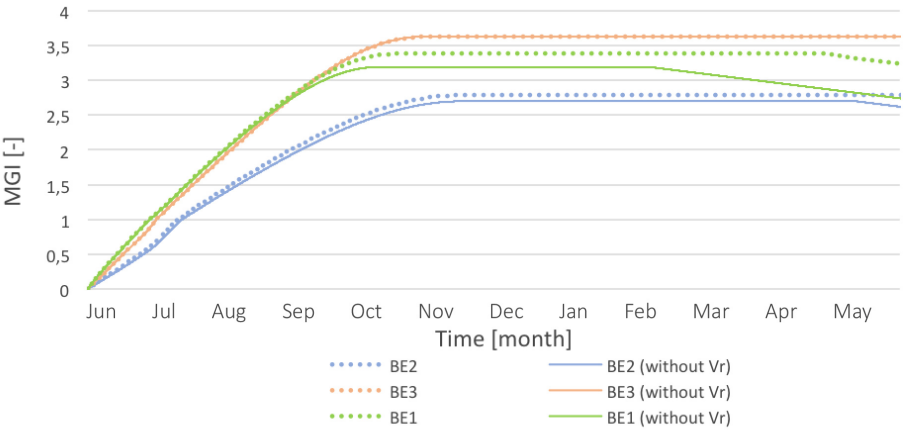

Figure 5.21: MGI at different monitoring points for H50 concrete with and without vapour retarder in the wall.

6
Conclusion and Recommendations

The main purpose of this research was to evaluate CLT-concrete composite slab with regards to moisture-related problems in the CLT due to the exposure to fresh concrete. This was done by simulating various floor details, properties and conditions for the composite slab in a transient heat and moisture transfer simulation software and evaluated with a mould growth model. Concrete with different water to cement ratios were investigated in this research and the material properties of the fresh concrete had to be modified due to the limitations of the program. The duration of the simulations in this study were one year because the drying behaviour of the fresh concrete was based on a one year experiment. The results of this research were solely from computational simulations and were not validated with experiments, therefore the presented results were not to be fully depended without any further investigations.

6.1 Conclusion

The experiment-based fresh concrete material with 0.38 and 0.6 w/c ratios had significant differences in results compared to the default hardened concrete with 0.5 w/c ratio from the program's material database. The results of the analysis showed that the studied CLT-concrete composite floor sections with concrete of either 0.38 or 0.6 w/c ratios were safe from possible moisture damages under all the simulated variables. Analyses using the 0.5 w/c ratio showed risks of potential mould growth and some cases reached an MGI of above 3.5. With properties of hardened/precast concrete of the 0.5 w/c ratio, simulations with fully saturated condition did not achieve results under the safety limit under the defined variables. Lowering the relative humidity to 95% and below showed some improvement in the results, as the mould growth index were within the allowable range. Adding a vapour retarder between the concrete and CLT also reduced the mould growth substantially, but the details between the vapour retarder and the shear connectors and the possible changes in interaction rate were not further investigated in this research. Regarding the high alkalinity of concrete for all the studied concrete types, the results showed that the moisture transport in the CLT occurred only by vapour and not by liquid, thus the effect of concrete's alkalinity was neglectable.

The use of heater during curing or drying period had a mixed impact on the different climate conditions regarding the rate of mould growth in the construction. The use

of heaters could help the mould growth to rise faster than without heaters when the heating did not help the concrete to dry significantly faster, as it only gave a more suitable temperature for mould to grow. Temperature was equally as important to the rate of mould growth as relative humidity. High humidity without suitable temperature conditions resulted in a lower MGI, which was evidently shown with using different regional climates. Stockholm had a higher relative humidity than Gothenburg, but the temperature was lower and less suitable, which made its MGI lower than Gothenburg. Kiruna showed the lowest MGI of all as it had the lowest temperature out of all the region.

Analyses from the floor to wall section showed that the addition of wall made no significant impact on the moisture behaviour on the CLT floor. The CLT segment of the wall that was in direct contact with concrete showed almost the same mould growth levels as the top CLT layer of the floor, although it dried faster due to the smaller area of exposure to the wet concrete. Removal of the vapour retarder within the wall construction had made the drying faster to some extent, by allowing moisture movement in the horizontal direction towards the outdoor.

6.2 Recommendations for Future Research

The material properties of the fresh concrete with water-cement ratios of 0.38 and 0.6 used in this study were based on one previous research. To replicate the drying behaviour of other concrete w/c ratios, it could be done by using TorkaS or the SBUF method. However, these two methods showed some diversity from real experiments, with TorkaS showing a relatively closer result. To have an accurate drying behaviour, it would be best to base any w/c ratio simulations of concrete from experiment results.

The cement type used in this research was ordinary Portland cement without fillers. However, the use of new types of cement, such as Bascement, is growing in the construction industry. Bascement contains fly ash and is considered to be a possible replacement for Portland cement as it has a lower CO_2 emissions, better workability, and needs a lower amount of water and admixtures. Despite these benefits, it takes a longer time for this cement type to dry, causing a higher risk for moisture problems in the CLT if it is used in composite slabs. It would be of interest to study the combination of CLT and concrete with Bascement as it is considered to be more environmentally friendly than ordinary Portland cement.

Although the simulation results showed that both fresh concrete were well below the safety limit, in reality the MGI could be higher. This comes from the limitation of the program in modelling fresh concrete. Fresh concrete dries out through the hydration process of cement, and evaporation as well as vapour diffusion of the free water inside. The hydration process gradually slows down as concrete hardens. The program could not model this hydration process, where the water inside the concrete is self-consumed, therefore the drying mechanism in the model is constant

throughout the period. As concrete hardens, the drying behaviour should gradually be similar to hardened concrete, which is less moisture-sensitive. This means the relative humidity decline of fresh concrete in reality could be somewhere in between the results of the experiment-based fresh concrete and the default hardened concrete used in the simulation. Other than fresh concrete, the program has several other limitations related to this study. The potential liquid transport through gravity force was neglected in this study due to the inability of the program to include this factor in the simulation. The steel shear connectors were also neglected in the simulations due to unreliable outcomes in using non-porous materials. Based on these limitations, this study can be further developed by conducting some experiments to validate the results of the simulations.

Further simulations should also consider the stages of construction to better represents the building assembly of an actual project. In reality, the indoor climate conditions would change after the building envelope becomes air-tight, which could be done well before the one year period. The climate surrounding the floor section would no longer be purely outdoor conditions as it is affected when it passes through the air-tight envelope. Afterwards, the climate inside the building is further affected by the HVAC system after it starts to function, and when people and people-related activities begin. This construction timeline needs to be considered in future simulations with the use of different time steps to accommodate the change in boundary conditions of the composite floor along the course of construction.

Bibliography

Alsayegh, G. (2012) *Hygrothermal Properties of Cross Laminated Timber and Moisture Response of Wood at High Relative Humidity*. Ottawa: Carleton University. (Department of Civil and Environmental Engineering. Master thesis).

Bathon, L., Clouston, P. and Schreyer, A. (2005) Shear and Bending Performance of a Novel Wood–Concrete Composite System. *Journal of Structural Engineering*, vol. 131, nr 9, ss. 1404 - 1412. DOI: 10.1061/(ASCE)0733-9445(2005)131:9(1404).

Begum, M., Hocking, A.D. and Miskelly, D. (2009) Inactivation of food spoiled fungi by ultra violet (UVC) irradiation. *International Journal of Food Microbiology*, vol. 129, ss. 74-77. DOI: 10.1016/j.ijfoodmicro.2008.11.020.

Bomberg, M. and Brown, W. (1993) Building Envelope: Heat, Air and Moisture Interactions. *Journal of Building Physics*, vol. 16, nr 4, ss. 306-311. DOI: 10.1177/109719639301600402.

Boverket (2008) *Bullerskydd i bostäder och lokaler*. Karlskrona: Elanders Sverige AB. ISBN: 978-91-86045-41-8.

Burström, P. G. (2007) *Byggnadsmaterial: uppbyggnad, tillverkning och egenskaper*. Second edition. Lund: Studentlitteratur. ISBN: 978-91-44-02738-8.

Cŏté, W. A. (1963) Structural Factors Affecting The Permeability of Wood. *Journal of polymer science. Part C, Polymer symposia*, vol. 2, nr 1, ss. 231-242. DOI: 10.1002/polc.5070020122.

Ewing, A. (2003) *En liten bok om mögel*. Stockholm: Skansen byggnadsvård. ISBN: 91-974597-0-4.

Fallqvist, K., et al. (2007) *Utredning Byggnadsklassificering Boverkets Byggregler, avsnitt 5 Brandskydd*. Brandkonsulten AB and Bengt Dahlgren AB.

Fallqvist, K., Klippberg, A. and Björkman, B. (2016) *Brandskydd i Boverkets byggregler : BBR 23*. Stockholm: Brandskyddsföreningen. ISBN: 9789171444400

Forest Products Laboratory (2010) *Moisture Relations and Physical Properties of Wood*. In *Wood Handbook - Wood as an Engineering Material*. Centennial

Edition, red. S.V. Glass, and S.L. Zelinka, ss 4-1 - 4-19. Madison: Department of Agriculture, Forest Service, and Forest Products Laboratory.

FPInnovations and Binational Softwood Lumber Council (2013) *CLT handbook: cross-laminated timber*. U.S. edition. Washington: USDA Forest Service Binational Wood Council. ISBN: 978-0-86488-553-1.

Grant, C., et al. (1989) The moisture requirements of moulds isolated from domestic dwellings. *International Biodeterioration*, vol. 25, nr 4, ss. 259-284. DOI: 10.1016/0265-3036(89)90002-X.

Grubb, J.A., Hemant, S.L. and Ashok, M.K. (2007) Testing pH of concrete. *Concrete International*, vol. 29, nr 4, ss. 78-83.

Hagberg, K. (2007) *Klara ljudkraven i BBR*. `http://www.ingemansson.se/assets/Uploads/BBRByggnadsakustik-PPHandoutsKH.pdf`. (15 February 2018).

Hagentoft, C. E. (2001) *Introduction to building physics*. Lund: Studentlitteratur. ISBN: 91-44-01896-7.

Hansson, M. (2010) *Nedbrytning av trä i markkontakt*. Lund: Lund University. (Department of Structural Engineering. Master thesis).

Hassan, O.A.B. and Anderstedt, R. (2017) Estimation of drying time of fresh concrete slabs: a comparative study. *Journal of Engineering, Design and Technology*, vol. 15, nr 2, ss. 134-148. DOI: 10.1108/JEDT-02-2016-0011.

Hocking, A.D. (1993) Responses of Xerophilic Fungi to Changes in Water Activity. In: *Stress Tolerance of Fungi*, red. D. H. Jennings, ss. 233-256. New York: Marcel Dekker Inc.

Hukka A. and Viitanen, H. (1999) A mathematical model of mould growth on wooden material. *Wood Science and Technology*, vol. 33. nr 6 , ss. 475-485. DOI: 10.1007/s002260050131.

Kosmatka, S. H., Kerkhoff, B. and Panarese, W. C. (2008) *Design and Control of Concrete Mixtures*. Fourteenth edition. Illinois: Library of Congress Cataloging-in-Publication Data. ISBN: 0-89312-217-3.

Kumaran, M. (1996) *Heat, Air and Moisture Transfer Through New and Retrofitted Insulated Envelope Parts, Final report Volume 3, Task 3: Material properties*. Leuven: Laboratorium Bouwfysica. Departement Burgerlijke Bouwkunde. ISBN: 90-75741-01-4.

Künzel, H.M. (1995) *Simultaneous Heat and Moisture Transport in Building Components: One-and two-dimensional calculation using simple parameters*.

Stuttgart: Fraunhofer IRB Verlag Suttgart. (Fraunhofer Institute of Building Physics. ISBN: 3-8167-4103-7).

Laticrete International Inc. (2017) *Drying of Concrete: TDS 183*. https://laticrete.com/~/media/support-and-downloads/technical-datasheets/tds183.ashx?la=en (19 January 2018).

Lukaszewska, E. (2009) *Development of Prefabricated Timber-Concrete Composite Floors*. Luleå: Luleå University of Technology. (Department of Civil, Mining and Environmental Engineering. Division of Structural Engineering. PhD thesis).

Merz, K. (2018) *Timber-Concrete Composite floor system (TCC)*. https://www.svenskttra.se/siteassets/6-om-oss/events/2018/trahybridsem/merz.pdf. (14 February 2018).

Mjörnell, K. (2003) *Uttorkning av byggfukt i självkompakterande betong*. Göteborg: SBUF, Report 10041.

MMK Holz-Beton-Fertigteile GmbH (2015) *XC Das Holz-Beton-Verbundelement*. https://www.holzbetonverbund.at/produkt-downloads/. (13 February 2018).

Moisture Meters (2015) Why Flooring Professionals Must Always Test For Excessive Moisture And Alkalinity. *Wood Moisture Solutions*. https://www.moisturemeters.com/why-flooring-professionals-must-always-test-for-excessive-moisture-and-alkalinity/. (8 February 2018).

Nilsson, L. O. (2004) *Fuktpåverkan på material: kritiska fuktnivåer*. Stockholm: Formas: Svenska byggbranschens utvecklingsfond (SBUF). ISBN: 91-540-5951-8.

Nilsson, L. O. (2015) *Byggvägledning. 9, Fukt : en handbok i anslutning till Boverkets byggregler*. Stockholm : Svensk byggtjänst. ISBN: 9789173337168.

Perré, P. (2007) Fluid migration in wood. In: Perré, P. (ed) *Fundamentals of Wood Drying*. Nancy: Arbolor, cop. ISBN: 9782907086127 290708612X.

Portland Cement Association (1997) Portland Cement, Concrete, and Heat of Hydration. *Concrete Thecnology Today*, vol. 18, nr 2, ss. 1-8.

Powerblanket (2017) *Concrete Curing Temperature Makes a Difference*. https://www.powerblanket.com/concrete-curing-temperature-makes-difference/. (12 March 2018).

Raji, S., et al. (2009) Thermophysical characterization of a laminated solid-wood pine wall. *Construction and Building Materials*, vol. 23, nr 10, ss. 3189–3195, DOI: 10.1016/j.conbuildmat.2009.06.015.

Raquel De Sousa Monteiro, S. (2015) *Load Distribution on Timber-Concrete Composite Floors*. Coimbra: University of Coimbra. (Department of Civil Engineering. PhD thesis).

Sandin, K. (1997) *Introduktion till fuktmekaniken*. Stockholm: SBUF and Svensk byggtjänst. ISBN: 91-540-5800-7.

SBUF (1995) *Lathund för betongtorkning*. SBUF Informerar. nr 95:14, SBUF, Box 7835, 10398, Stockholm.

Scalet, T. (2015) *Cross Laminated Timber as Sustainable Construction Technology for the Future*. Helsinki: Helsinki Metropolia University of Applied Sciences. (Department of Civil Engineering. Bachelor thesis).

Sedaghat, A. (2016) *Cement Heat of Hydration and Thermal Control*. Tampa: University of South Florida. (Department of Civil and Environmental Engineering. PhD thesis).

Siau, J. F. (1995) *Wood: influence of moisture on physical properties*. Blacksburg: Dept. of Wood Science and Forest Products, Virginia Polytechnic Institute and State University. ISBN: 0-9622181-0-3.

Stora Enso (2013) *Admission of CLT into WUFI extends design opportunities*. `http://www.clt.info/en/media-downloads/wufi/`. (16 April 2018).

Svenskt Trä (2003) *Värmeegenskaper*. `https://www.traguiden.se/om-tra/materialet-tra/traets-egenskaper-och-kvalitet/termiska-egenskaper1/varmeegenskaper/`. (22 January 2018).

Svenskt Trä (2016) *Dimensionering av träkonstruk - Del 1*. Second edition. Stockholm: Skogsindustrierna. ISBN: 978-91-981922-6-1.

Svenskt Trä (2017a) *KL-trähandbok*. Stockholm: Skogsindustrierna. ISBN: 978-91-981922-5-4.

Svenskt Trä (2017b) *Fuktinnehåll och sorptionskurvor*. `https://www.traguiden.se/om-tra/byggfysik/fukt/fukt/fuktinnehall-och-sorptionskurvor/?previousState=1`. (16 February 2018).

Svenskt Trä (2017c) *Ånggenomsläpplighet*. `https://www.traguiden.se/om-tra/byggfysik/fukt/fukt/anggenomslapplighet/`. (27 February 2018).

Swedish Standard Institute. SS 25268:2007. *Acoustics - Sound classification of spaces in buildings - Institutional premises, rooms for education, preschools and leisure-time centres, rooms for office work and hotels*. Second edition. Stockholm:

SIS Förlag AB.

Swedish Standards Institute. SS-EN 1991-1-1:2002. *Eurocode 1: Actions on structures – Part 1-1: General actions – Densities, self-weight, imposed loads for buildings*. Stockholm: SIS Förlag AB.

Swedish Standards Institute. SS-EN 1991-1-1:2004. *Eurocode 5: Design of timber structures – Part 1-1: General – Common rules and rules for buildings*. Stockholm: SIS Förlag AB.

Tanaka, T., et al. (2015) Air permeability of sugi (Cryptomeria japonica) wood in the three directions. *Maderas. Ciencia y tecnología*, vol. 17, nr 1, ss. 17-28, DOI: 10.4067/S0718-221X2015005000002.

Tarmian, A. and Perré, P. (2009) Air permeability in longitudinal and radial directions of compression wood of Picea abies L. and tension wood of Fagus sylvatica L. *Holzforschung*, vol. 63, nr 3, ss. 352-356, DOI: 10.1515/HF.2009.048.

TenWolde A. (2011) A Review of ASHRAE Standard 160—Criteria for Moisture Control Design Analysis in Buildings. *Journal of Testing and Evaluation*, vol. 39, nr 1, ss. 77-81, DOI: 10.1520/JTE102896.

TiComTec GmbH (2017) *Technisches Dossier HBV-Systems 2017*. `http://ticomtec.de/wp-content/uploads/2017/09/Technisches_Dossier_HBV-Systems_2017.pdf`. (13 February 2018).

Viitanen, H. (1994) Factors affecting the development of biodeterioration in wooden constructions. *Journal of materials and structures*, vol. 27, nr 8, ss. 483–493. DOI: 10.1007/BF02473453.

Viitanen, H. (1996) *Factors affecting the development of mould and brown rot decay in wooden material and wooden structures: effect of humidity, temperature and exposure time*. Uppsala. Swedish University of Agricultural Sciences. (Department of Forest Products. PhD thesis).

Viitanen, H. and Ojanen, T. (2007) *Improved Model to Predict Mold Growth in Building Materials*. ASHRAE.

Viitanen, H. and Ritschkoff, A.C. (1991) *Mould growth in pine and spruce sapwood in relation to air humidity and temperature*. Uppsala: Swedish University of Agricultural Sciences. ISBN: 9157645221.

Wheeler, K.A., Hurdman, B.F. and Pitt, J.I. (1990) Influence of pH on the growth of some toxigenic species of Aspergillus, Penicillium and Fusarium. *International Journal of Food Microbiology*, vol. 12, ss. 141-150, DOI:

10.1016/0168-1605(91)90063-U.

Wu, Y. (2007) *Experimental study of hygrothermal properties for building materials*. Montreal: Concordia University. (Department of Building, Civil and Environmental Engineering. Master thesis).

Yeoh, D.E.C. (2010) *Behavior and design of timber-concrete composite floor system*. Christchurch: University of Canterbury. (Department of Civil and Natural Resources Engineering. PhD thesis).

Zabel, R. and Morrell, J. (1992) *Wood microbiology: decay and its prevention*. London: Academic Press. ISBN: 978-0-12-775210-5.

A

Climate Data

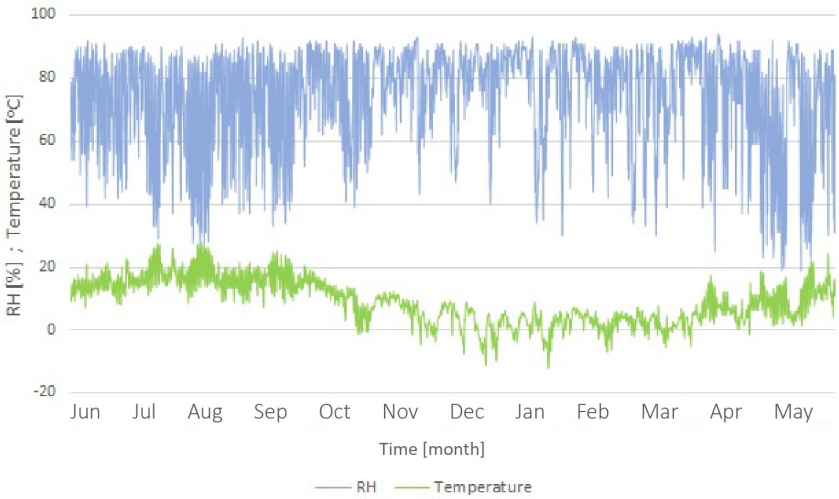

Figure A.1: Summer A climate file

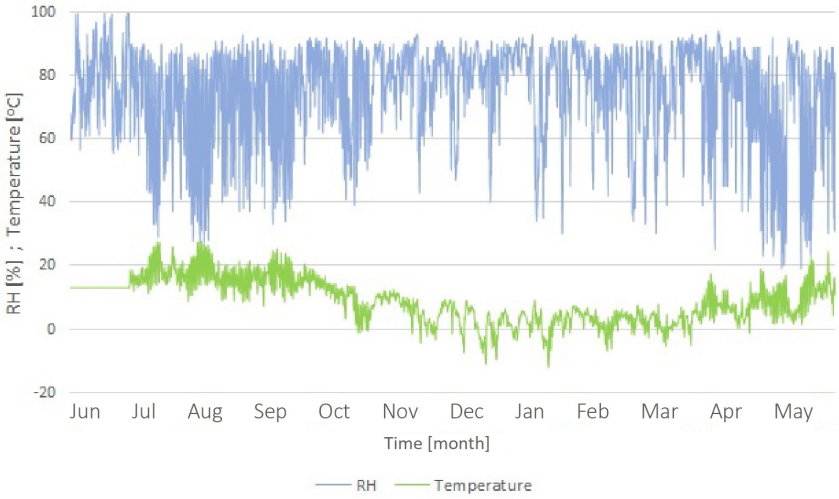

Figure A.2: Summer B climate file

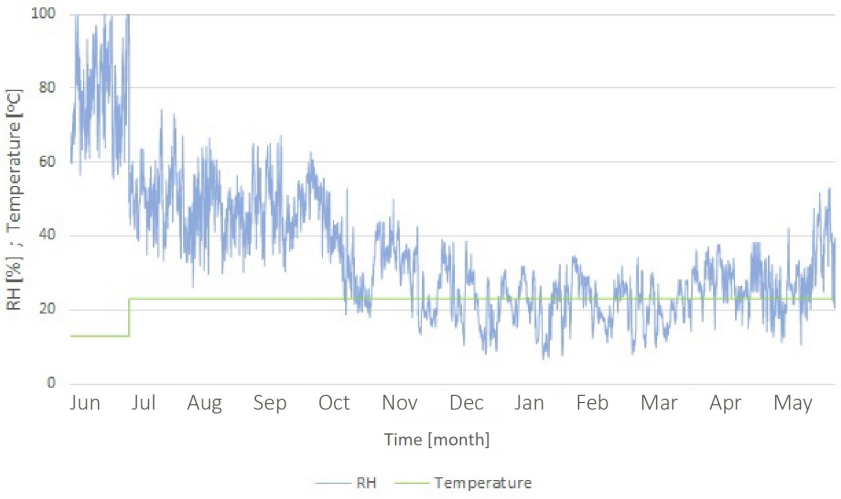

Figure A.3: Summer C climate file

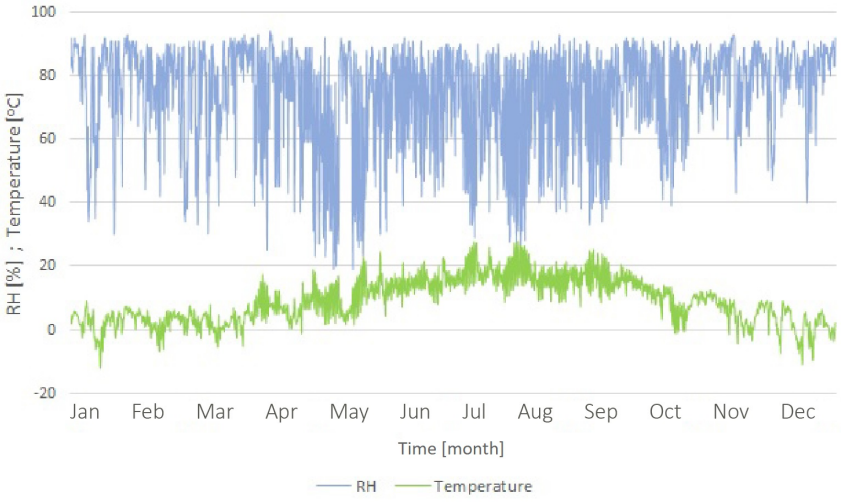

Figure A.4: Winter A climate file

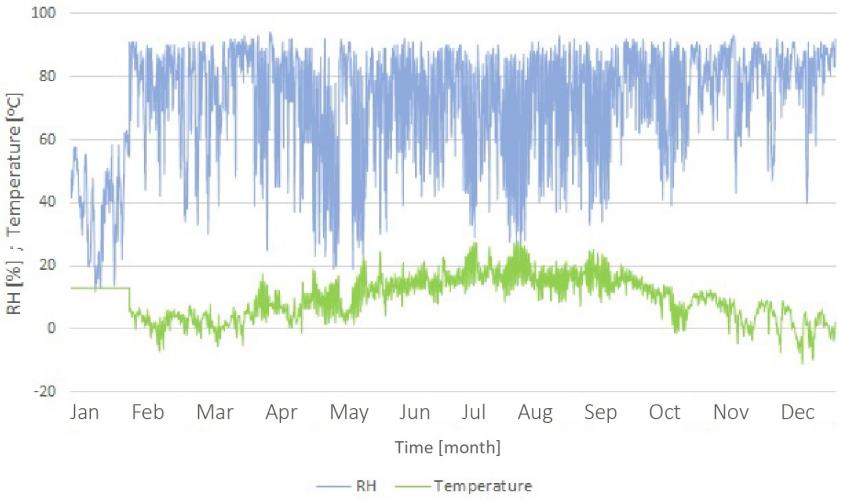

Figure A.5: Winter B climate file

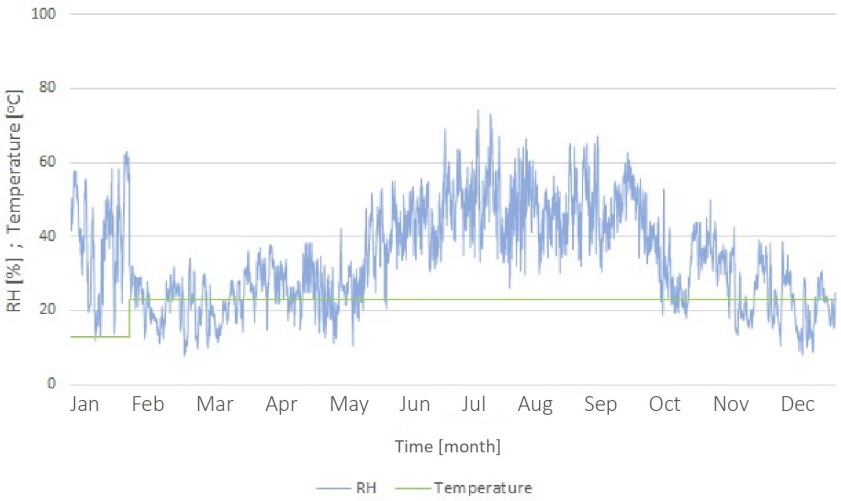

Figure A.6: Winter C climate file